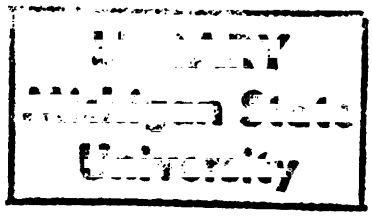

This is to certify that the

thesis entitled
THERMODYNAMIC AND KINETIC ASPECTS OF HUMAN ERYTHROCYTE HEMOLYSIS IN HYPERTONIC SOLUTION OVER TEMPERATURE RANGE OF -10 TO 25 C

presented by

Amir M. Fallahi

has been accepted towards fulfillment
of the requirements for

Ph.D degree in Mechanical Eng.

John J. McGrath

Prof. John J. McGrath
Major professor

Date Feb 6,1986

THERMODYNAMIC AND KINETIC ASPECTS OF HUMAN ERYTHROCYTE HEMOLYSIS IN HYPERTONIC SOLUTION OVER TEMPERATURE RANGE OF -10 TO 25°C.

By

Amir M. Fallahi

A DISSERTATION

Submitted to

Michigan State University

In partial fullfillment of the requirments

for the degree of

DOCTOR OF PHILOSOPHY

Department of Mechanical Engineering

1986

ABSTRACT

THERMODYNAMIC AND KINETIC ASPECTS OF

HUMAN ERYTHROCYTE HEMOLYSIS IN

HYPERTONIC SOLUTION OVER TEMPERATURE

RANGE OF -10 TO 25 C

By

AMIR M. FALLAHI

Thermodynamic and kinetic analysis of biomembranes subject to thermal and chemical perturbations is applied using the human red blood cell as a model system. Since chemical and thermal effects occur simultaneously during the freezing and thawing of living cells, a complete data base in the form of the hemolysis kinetics as a function of solute concentration and temperature is generated for the human red blood cell. To decouple the chemical and the thermal effects an improved stop-flow system equipped with temperature control has been designed and developed to measure the destruction dynamics of the red blood cell. The stop-flow technique provides very rapid mixing and therefore the damage dynamics for short times (order of seconds) is obtained. This technique represents a definite advantage as compared to the standard technique for hemolyis measurement (inferred by static measurement of the hemoglobin absorption) with characteristic times on the order of several minutes. Specifically, the hemolysis kinetics for the human red blood cell population induced by un-buffered sodium chloride solution s between 2m and 4m are

presented for temperatures between -5 and 25°C. The rate of the destructive hemolysis reaction is characteristically very rapid at short times compared to that at relatively long times for all temperatures and concentrations. The appearance of measurable damage in the stop flow device is delayed for sub-ambient temperatures. The characteristic time (delay time) is on the order of 3.5 minutes for 2m concentration, about 1 minute for the 2.5m concentration and several seconds for higher concentrations. Compared to room temperature, the damage process at sub-ambient temperatures proceeds at higher rates for relatively long times. That is, the transition from the initial rapid rates to the final slow rates are smoother and delayed. The largest effect of the reduced temperature in survival is observed when the isothermal temperature is dropped from 25 to 10°C. Further decreases in temperature have comparatively less significant effect. The hemolysis process is treated as a chemical reaction of the blood cell sample and hypertonic sodium chloride solution. The temperature and the sodium chloride concentration dependence of the hemolysis kinetics is interpreted in terms of the 1st and 2nd order rate laws for short exposure times. The thermodynamic activation parameters associated with these kinetics have been analysed. On the basis of these results, it is postulated that dissolution of one or more membrane components is responsible for cell injury due to the exposure to hypertonic sodium chloride. A theoretical argument in support of the dissolution theory is given.

To my

parents, Javad and Afkham ..

wife, Sima ...

and

sons, Kianoosh and Kiamarz

ACKNOWLEDGEMENT

I would like to thank the members of my dissertation committee Professor McGrath, Professor Tien, Professor Anderson and Professor Atreya for their guidance throughout this effort.

A special thanks is due to my thesis advisor, John McGrath, whose enthusiasm and dedication to research inspired his students including the author of the present work. His commitment to science and his fantastic personality created the most pleasant research and learning environment.

My deepest appreciation must go to my parents and my wife whose love, encouragement, and understanding helped me overcome the most difficult situations throughout these many years.

TABLE OF CONTENT

LIST OF TABLES

LIST OF FIGURES

LIST OF FIGURES

CHAPTER I

INTRODUCTION

In recent years the surgical technique of organ transplantation has been an area of very active experimentation in medicine. New surgical techniques have been developed and organ transplantations of heart, liver, and kidney have become the most promising hope for extending human life. Success of such a transplant relies heavily upon the availability as well as the viability of organs at the time of need. To overcome the time factor an effective preservation technique needs to be developed. One of the most promising preservation techniques at the present time is offered by low temperature technology. Today through cryopreservation techniques several classes of "simple" biomaterials such as blood, spermatozoa, cornea, skin, and embryos are reversibly preserved for periods as long as 30 years [1-5]. However, for the more complex biomaterials such as organs no successful cryopreservation technique has been developed.

In order to extend the scope of cryopreservation to more complex systems such as the heart or liver a detailed understanding of the cellular behavior at low temperatures is

required. Fundamental thermodynamic analysis in conjunction with kinetic theory of the reactions and processes involved in a cryopreservation protocol could provide the basis for the development of cellular behavior in response to low temperatures. The purpose of this work is aimed at providing a better understanding of the damage sustained by living cells as a result of changes which occur in the cellular environment during the process of freeze-preservation. Specific environmental changes of interest are the effects of high solute concentration (a chemical effect) and low temperature exposure (a thermal effect).

When the liquid phase of water is excluded from the cell suspension through the formation of ice, there results an increase in the extracellular solute concentration. This increase in the extracellular solute concentration creates an osmotic pressure which acts as a driving force for the flow of water out of the cell. The chemical effect and the strong temperature dependence of many life processes constitute two major mechanisms in cell freezing. According to Mazur's classic two-factor hypothesis for freezing injury the slowly frozen cells are damaged on the one hand by their relatively long exposure to high solute concentrations. This is the so-called "solution effect". Furthermore, rapidly frozen cells are damaged as a result of intracellular ice formation [6]. The chemical and thermal factors are then necessarily inter-related in a given freezing and thawing

protocol. That is, The chemical and thermal variables are coupled during a freezing and thawing process.

Therefore a complete, decoupled, and quantitative understanding of cell injury caused by thermal and chemical effects is essential for developing a thermodynamic model describing a freeze-thaw protocol. A decoupled study of the thermal and chemical effects responsible for the cell damage during freezing should yield an important understanding of the degree and extent of injury caused by each perturbation mode. Cryopreservation is a thermodynamic process where kinetics play an important role since it is known that the survival of biological systems is usually sensitive to cooling and warning rates [7]. Studies of the cell response to the thermal and chemical perturbations can therefore generate kinetic information about the cell injury. Thermodynamic analysis of kinetic information generated by such studies provides data for the development of a thermodynamic model for the cell injury mechanism(s). Therefore, the main objective of this work was to study independently the effects of thermal and chemical perturbations on the kinetics of red blood cell hemolysis. Specifically it was intended to determine the kinetics of damage to the human red blood cell system induced by sodium chloride solutions of different concentrations at different temperatures.

Even though hemolysis of erythrocytes has been the subject of extensive studies associated with low temperature preservation [8-11], the area of study proposed here has received little attention. In this work the kinetics of hemolysis of the human red blood cell in the form of rate information is obtained. Damage histories of cells subject to "chemical shock" is quantified at different temperatures. Specifically, the damage induced by sodium chloride solutions between the concentrations of 1 molal and 4 molal is studied as a function of time for temperatures between-5C and 25C (the rational for these ranges of concentration and temperature is given in chapter IV).

To analyze the cell injury process, a thermodynamic approach will be taken. The reaction rate theory of Eyring will be employed to reduce the rate data to obtain thermodynamic activation parameters such as enthalpy, entropy, and Gibbs free energy for the hemolysis process. The role of these parameters in the stability of the cellular system relative to the proposed injury mechanism will be investigated. Such an application of the principles of thermodynamics in conjunction with kinetic theory of reactions will result in an important classification of thermal-chemical effects on cell damage modes.

This research is expected to have a significant impact on the area of low temperature preservation. An improved understanding

of the effects of simultaneous thermal and chemical changes accompanying freezing should help to improve cryopreservation protocols for a wider class of biological systems including tissues and organs. A better understanding of the alterations experienced by biological systems in terms of thermodynamic and reaction rate theory has the potential to provide a better conceptual framework for further research from the theoretical standpoint. Furthermore, simulations and predictions of cellular behavior in arbitary environments based upon quantitative models may be possible in the future.

Even though the model cell system for this study was limited to the human red blood cell, it is hoped that the experimental techniques and theoretical methods used here as well as the overall understanding gained by this research could be generalized to a larger class of biological systems.

A. Background

Living systems contain a substantial amount of liquid water and it is apparently necessary for a minimum amount of liquid water to be present in most living systems to insure viability. Therefore most biological systems exhibit "normal" behavior only at temperatures above 0C. It has been known for centuries that

the deterioration process of biomaterials could be severely slowed down or even stopped at low temperatures. This effect of low temperatures in the reduction of metabolic activities of biological systems has been employed in modern industrial scale food stuffs preservations for many years [12-14].

The potential of freezing preservation as a promising clinical technique for long term preservation of biomaterials was not realized until the 20th century. The fact that living organisms are in general disasterously injured when exposed to subzero temperatures was probably the most important factor limiting succesful cryopreservation. The first successful freezing preservation of biological systems occurred in 1949, when Polge, Smith, and Parks [15] reported the first successful freezing technique. Their work was primarily concerned with the preservation of human and fowl spermatozoa. Since then the field of cryobiology has been an area of very active experimentation. This has resulted in the development of clinical scale reversible low temperature preservation techniques for several biological systems including the human erythrocyte, cornea, skin, and embryos [1,3,4,5].

Due primarily to its clinical value, the human red blood cell has received some of the most intensive considerations. This has in turn resulted in the development of very successful

cryopreservation protocols enabling blood banking for long periods of time [16-18]. The large biophysical data base available for the human red cell also makes this system a very attractive model system.

The general uncontrolled effect of cooling of "living" organisms to subzero centigrade temperatures results in injury and consequently "death" of such systems. A review of the cryopreservation techniques in cryobiology reveals that two of the most important factors controlling the fate of the biological system are the cooling rate during freezing and the warming rate upon thawing [7,19-24]. It is also known that the storage time and storage temperature play very important roles in the success of a freeze-thaw process. It should be pointed out here that the presence of some cryophylactic agent, sometimes referred to loosely as antifreeze agent or simply antifreeze, is essential for the success of a cryopreservation technique. The most commonly used cryophylactic agents are glycerol and dimethylsulfoxide (DMSO) [5,7,17, 23,25]. The presence of a cryophylactic agent will greatly complicate the analytical as well as experimental analysis. It will also reduce the hemolysis reaction rate considerably making it difficult to study the damage mechanism. Therefore, in the present work in order to simplify the system under study as well as emphasizing the damage to learn more about the cause, the effect of such agents will not be considered.

Among the controlling factors mentioned earlier, the effect of cooling rate has received the most attention. This is partly due to the fact that if the system is severely damaged during the freezing stage of the process, consideration of the effect of other factors becomes unnecessary. Figure 1.1 shows representative survival percentages of different cells as a function of cooling rate [23]. In spite of the fact that optimal cooling rates differ from cell to cell (ranging from 0.3 C/min for lymphocytes to 3000 C/min for human erythrocytes) the cell survival curves have similar general shapes. The results presented in Figure 1.1 reveal that increasing the cooling rate of frozen cells is only beneficial up to a point and once this point is reached further increase of cooling rate will have a negative effect on the survival. This has suggested to some researchers the existence of two competing mechanisms responsible for detemining cell survival [6,26].

Cooling the cells more slowly than at the optimal rate results in the injury thought to be due to the complex alterations of the cellular environment due to the presence of extracellular ice. These physiochemical alterations are collectively referred to as "solution effects" and include changes in the concentration of solutes, dehydration of the cell, changes in the pH of the solution, and subsequent decrease of the cell volume [8,9,27]. As the cooling rate is increased the survival increases which is

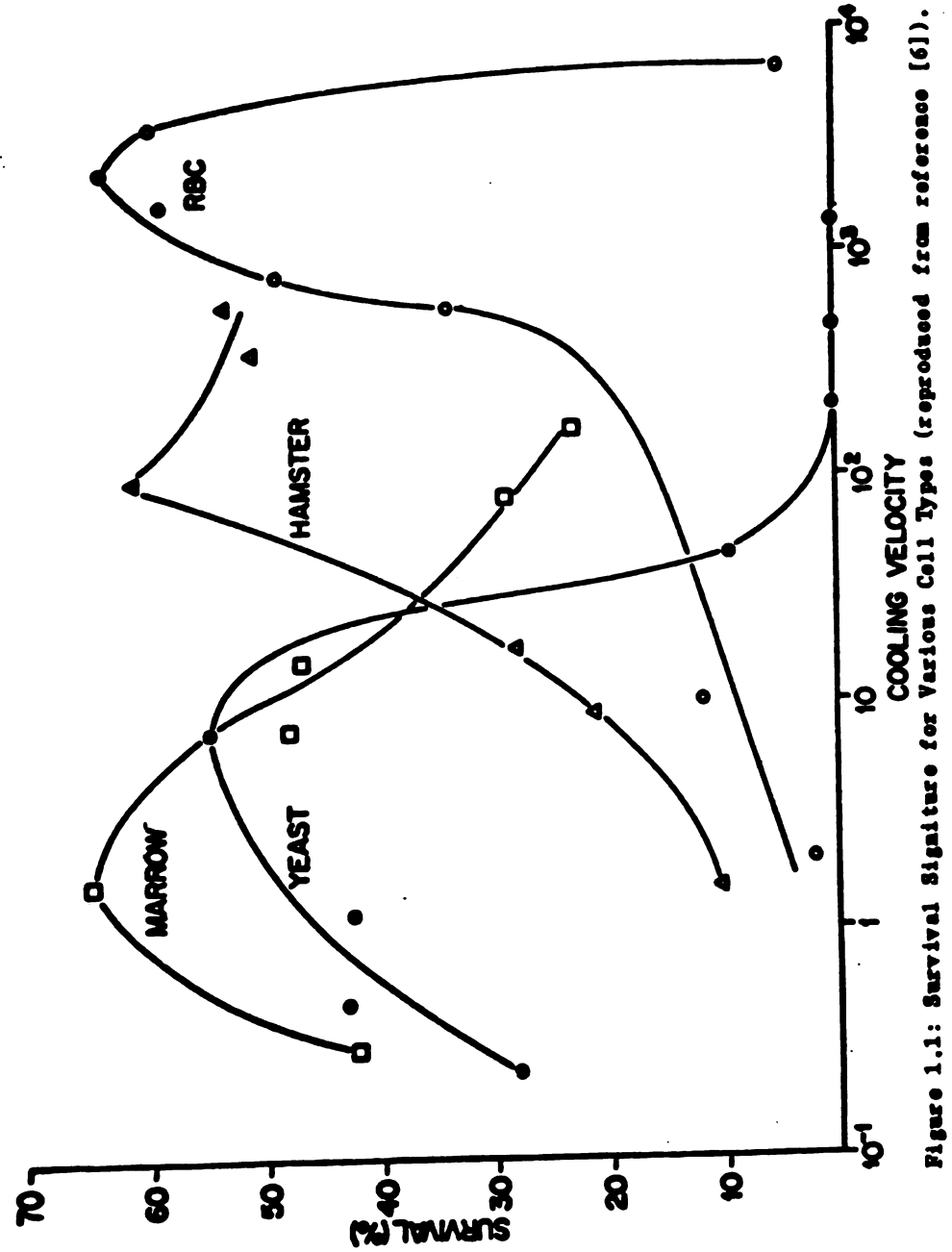

Figure 1.1: Survival Signature for Various Cell Types (reproduced from reference [6]).

interpreted to mean that the increased cooling rate reduces the solution effects. However, the survival is diminished when biological systems are cooled at supraoptimal rates. The damaging effect of supraoptimal cooling rates has been clearly demonstrated, both experimentaly and theoretically, to be due to the intracellular ice formation during freezing [24,29-35]. That is one cannot increase the cooling rate beyond the rates at which lethal intracellular ice will form and survival will be diminished. The action of these two competing factors is manifested in the survival signature of the cells (Figure 1.1).

Studies of warming rate have revealed that the effect of the warming rate is directly coupled with the cooling rate. For fast cooling rate the survival is achieved at fast warming rates and similarly better results are obtained at slow warming rates when the cooling rate is slow [7,8,23,32]. Storage time for systems stored at any temperature other than zero absolute temperature will have a negatie effect i.e. the survival rate is improved as the storage temperature is lowered [33,34]. Storage time effect studies on survival rates reveal that at temperatures below -60C these effects are minimal and that the survival of cell systems seems to be a strong function of storage temperature in the range of -5C to -60C [7,25,33,34].

B. Modes of Freezing Damage

The generally accepted theory of freezing damage is due to Mazur [6,26], where he proposes a two-factor model of freezing damage. Mazur's two-factor theory represents a convincing argument in which an attempt is made to describe the low temperature effects in biological systems subject to slow and rapid cooling. Before discussing the freezing damage in detail it is necessary to define several terms commonly used in such a discussion, namely such terms as "slow" and "rapid" freezing.

The concept of slow and fast freezing is generally defined in light of intracellular crystal nucleation or in terms of dehydration of the cell. Freezing velocity is considered to be "slow" when only extracellular crystalization occurs. When the freezing process results in intracellular crystal formation the cooling rate is considered to be "rapid". It should be noted that these terms are relative, so that rapid for a given cell type may be slow for another. In a freezing process regardless of cooling velocity the water transport across the semipermeable cell membrane is directly linked with the survival of the system under study. A simple model system presented in Figure 1.2 describes the water transport events associated with cell freezing. The system is considered as two compartments seperated by a spherical semi-permeable membrane resulting in an intracellular and an

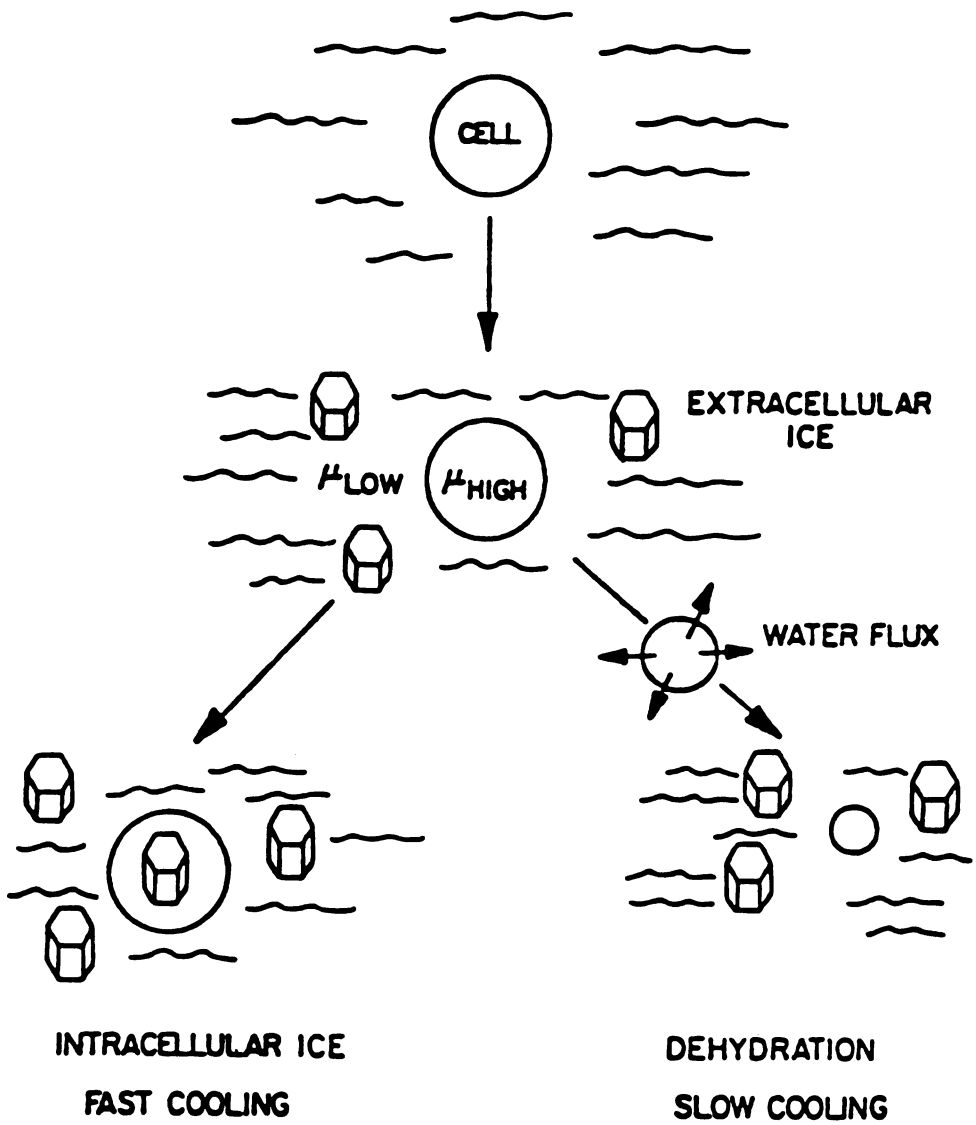

Figure 1.2: A Method for a Supercooled Cell to Achieve Equilibrium (reproduced from reference [31]).

extracellular compartment. At equilibrium the chemical potential for solutes able to diffuse are equal in the intracellular and extracellular solutions. The formation of ice in the extracellular solution results in a lowered chemical potential of water outside the cell with respect to the water inside. A new equilibrium can be reached by either transport of water out of the cell or intracellular ice formation. This matter will receive further attention in conjunction with discussion of red blood cell hemolysis in Chapter 3.

According to Mazur's two-factor hypothesis, when cells are frozen slowly the damage is associated with relatively long exposure to the physio-chemical alterations of the cell system produced by crystalization of liquid water (the so called "solution effects" discussed earlier). When cells are frozen with rapid cooling rates the formation of intracellular ice is the major factor responsible for damage. The implicit assumption here is that the cells are thawed at optimal warming rates. A qualitative argument accounting for Mazur's theory based on the model system given in Figure 1.2 follows.

During a freezing process as discussed earlier the temperature reduction of the cell suspending media results in crystalization of extracellulat water. During the early stages of freezing the membrane acts as a barrier to ice formation within

the cell. As the extracellular liquid water is transformed to solid water by ice formation a solute concentration gradient is developed across the supercooled cell such that the system (the cell) is removed from it physiochemical equilibrium state. But since the cell membrane is permeable to water a new equilibrium state can be established by way of the flow of water out of the cell. If the formation of intracellular ice is to be avoided there should be sufficient time for the cell to loss its free water to avoid supercooling. This means if the cooling process is slow enough the cell will not freeze internally or at least large amounts of water will not solidify. At such slow cooling rates then, the cell will be exposed to high concentrations of solute for a relatively long period of time and the subsequent solution effects can result in injury. The slow cooling rate is characterized by the dominance of mass transfer (water flux across the cell membrane) over the heat transfer process. Now if the cooling rate is rapid, intracellular supercooling occurs in a short time. The cell is unable to lose a considerable portion of its water content and it becomes increasingly probable that the intracellular water will freeze. Specifically, at fast cooling rates the heat transfer process characteristically dominates the mass transfer process so that the intracellular water has little time to leave the cell and the abundance of water in the cell predisposes the interacellular ice nucleation to occur.

Based on the above argument it is evident that the following cell parameters characterize the optimal cooling rate for survival:

(i) the permeability of the cell to water

(ii) the amount of cellular free water

(iii) the surface area to volume ratio.

As pointed out earlier and is evident from the preceeding argument the mechanisms of freezing injury are very involved and complicated phenomena which are yet to be resolved. However, at the present time there exists substantial evidence suggesting that the alteration of the plasma membrane could be a major if not the only, mechanism responsible for freezing damage [45,46]. At this point having discussed the problems involved in cryopreservation and having emphasized freezing as the major cause of injury, a few words are in order to classify the mechanism of injury.

The formation of ice in the freezing process, intracellular or extracellular, could definitely introduce considerable stress and therefore mechanical damage to the cell at the membrane site as well as at the internal level. The damage to the cell could occur either during the freezing or when the system is thawed. However, the hemolysis phenomenon due to freezing of red blood cells in isotonic saline solution is, in some cases duplicated by

the hemolysis due to hypertonicity of the extracellular solution in the absence of freezing [8]. Furthermore freeze-induced changes of spinach thylakoids has been observed to be similar to those observed by transferring thylakoids from an isontonic to hypotonic [37] or hypertonic media [38]. That is the nature of thermal shock damage is similar to osmotic shock damage.

Several biological membrane systems have been studied with respect to the biochemical and structural alterations of the membrane induced by freezing or osmotic stress in the absence of freezing [35-42]. The object of such studies is the phenomenon of cell damage due to extracellular perturbations which has been postulated to be a result of membrane alterations. The notion that freezing injury is due to injury to the plasma membrane was first proposed by Maximov in 1921 [43]. The important role of the plasma membrane in the function of the cell, and the fact that the amount of damage incurred by the presence of external ice is considerably lower than the level of damage introduced by intracellular ice formation are in direct agreement with this notion. The direct involvement of the membrane constituents in the phenomena of cell damage due to osmotic or thermal shock has been observed [8,44]. It has also been shown that intact red blood cells or ghost cells exposed to hypertonic salt conditions resulted in solubilization and release of membrane proteins and phospholipids [10,11]. Perhaps the most intringing are

observations made by Araki [45] and Araki et al [46], where they found that red blood cells exposed to osmotic stress at or below 0C lose their membrane lipids and proteins by virtue of releasing cholesterol-enriched microvesicles. A similar observation has been made on rat hepatocyte cells recovered from freezing [47].

In his studies related to the effect of hypertonic treatment of membrane structures at low temperatures, Araki showed that such treatments result in the release of microvesicles. He showed that the lipid and protein content of the microvesicles were different from the red cell membrane. He was also able to show that the ratio of cholesterol:phospholipid (C:P) in microvesicles was dependent upon the temperature of the treatment. The lower the temperature of the treatment, the higher the (C:P) ratio [45]. Araki et al further found that the total protein content of the microvesicles decreases with decreasing temperature [46]. These observations suggest a temperature and tonicity dependent preferential segregation of membrane constituents due to osmotic stress and low temperature exposure. The molecular segregation and mechanism of vesicle formation induced at low temperatures are not clearly understood. Nevertheless, occurance of such processes suggest a significant temperture and tonicity dependence of the membrane protein-phospholipid interaction and consequently a membrane dominated injury mechanism.

Grunze et al in their studies observed molecular segregation of the red blood cell membrane at room temperature due to treatment with long-chain alcohols [48]. Such treatment results in development of rod-shaped projections. The rods can be separated from the cell without significant hemolysis. Preferential lipid segregation in the membrane was observed where protein content of the cells and the rods remained the same.

Despite the abundance of studies concerning the red cell shapes due to environmental pertubations, the question of "what is responsible for the red cell shape in general and shape changes in particular:is it the bilayer or the spectrin-actin network?" has been a controversial issue. In the study of hypertonic cryohemolysis (the erythrocyte hemolysis in a hypertonic environment when the temperature is lowered to below about 12C is called "hypertonic cryohemolysis" [49-51]). Green et al have presented evidence for the possible indirect effect of the hypertonic environment on the spectrin-actin cytoskeletal system [44]. These investigators suggest that the membrane lipid interaction with the cytoskeleton may be responsible for injury. This notion is in line with results suggested by several studies where the red cell membrane shapes are due to alterations in the cytoskeletal network [52-55]. On the other hand, Lange et al concluded from their studies on the shape of the red cell membrane that the membrane bilayer and not the cytoskeletal proteins is

responsible for ghost cell crenation [42]. They believe that osmotically induced redistribution of lipids between the two leaflets of the membrane bilayer preceeds and results in the ghost creanation.

Concerning what constitutes freezing or hypertonic exposure injury at the cellular and molecular level, it is believed that the loss of membrane material plays an important role [47,48]. This notion is strongly supported by Araki's findings from his work on the red blood cell that the low temperature induces lipid and protein segregation in the membrane and as a result of hypertonic exposure at sub-zero temperatures the membrane material is lost in the form of microvesicles [45,46]. Furthermore Steponkus and co-workers based on studies on spinach protoplast propose that freezing damage is due to loss of membrane material [47,48,79]. Specifically, they propose a hypothesis of exchange of material between the plane of the membrane and a reservior of membrane material induced by an increased tension imposed in the membrane during freezing.

The arguments given here suggest that freezing or hypertonically induced stresses result in tension or increased pressure in the plane of the cell membrane. This is concomittant with a significant redistribution and loss of membrane constituents and consequently of the surface area and cell volume.

Therefore the notion that the membrane is the site of damage or at least that major damage is at the membrane site is a well justified assumption. All the evidence and theories put forward emphasize that in order to resolve the uncertainties of the damage processes and mechanisms, a complete understanding of the nature of forces and molecular interactions at the molecular level is required . Due to the biological nature of the problem it has been extremely difficult to arrive at such an in depth insight at the molecular level. This, however, does not mean one should await such an advancement and ban exploring different and in some cases simpler approaches. No theoretical approach could account for all the parameters of such a complex system, and direct experimental measurements should always be considered the most reliable method to check the theoretical findings.

One such approach is provided by thermodynamics. Thermodynamics in connection with biological systems has been a relatively forgotten tool in many cases even though it offers quantitative as well as qualitative methods of analysis. The process of cryopreservation is in fact a thermodynamic process. The ultimate goal of such a process is to arrive at cryopreservation protocols such that the system under consideration is returned to its initial thermodynamic state, that is the task involved here is to design a cyclic thermodynamic process for the cell. Therefore methods of analysis of such

process should be based on fundamentals of thermodynamics. Thermodynamic is a quantitative subject and it can be employed to enhance our quantitative understandings of structure and function of living system. For example, regarding the membrane system, equation of state information based on principles and fundamentals of thermodynamics can in principle be derived by direct measurements. Furthermore, concerning the development of Physics of the membrane interactions and knowledge of ultrastructure of such systems, characterization and quantitative classification of thermodynamic parameters such as entropy, enthalpy, and energy is required. For example, the entropy and enthalpy changes associated with the hemolysis interaction form a valuable basis for the interpretation of the thermodynamic parameters concerning the molecular organization of the cell membrane as related to environmental parameters.

A classical thermodynamic method of analysis is concerned with equilibrium states, i.e., it yields static information. However, as discussed earlier, the survival and degree of injury as a result of freezing and thawing is very sensitive to cooling and warming rates involved in such a process. Therefore to classify the injureous characteristics of such a dynamic process, kinetic information is needed. That is to study the hemolysis interaction, a kinetic reaction rate theory is required to complement the thermodynamic analysis. The present effort deals

with the hypertonically induced osmotic hemolysis kinetics of human red blood cels at different temperatures. Specifically the osmotic shock aspect of the so-called "solution effect" freezing injury is considered. The data obtained here is in the form of damage histories obtained when human red blood cells are subject to step changes in extracellular concentration at various isothermal set points. As discussed earlier Lovelock showed that injury due to freezing of red cells could be duplicated by exposure to hypertonic sodium chloride if the cells were returned to the isotonic state [26]. He also concluded that hypertonic exposure alone is not in itself damaging enough to explain the total amount of injury observed when red blood cells are frozen and thawed.

In light of Lovelock's findings the erythrocyte hemolysis has been re-examined here for the following reasons. It is well known in cryobiology that frozen and thawed cell recovery can be very sensitive to the rate of freezing and thawing. It is therefore important to study the damage process on a rate basis in order to correlate the extent of damage with the exposure time at various temperatures and concentrations. Data of this form are not available in the literature. Also, hypertonic sodium chloride induced hemolysis has never been interpreted in terms of the Eyring rate equation. This has been done for the present results to suggest the mechanism by which osmotic shock causes an

instability in the human erythrocyte membrane, thereby leading to hemolysis. As will be seen the mechanism suggested by thermodynamic activation properties derived from the Eyring equation is consistent with the membrane dissolution theory offered by Lovelock [57].

Chapter II

MEMBRANE STRUCTURE, FUNCTION AND MODEL MEMBRANE SYSTEMS

In order to pursue the cell freezing problem and acquire an understanding of factors or processes effecting the extent of the subsequent cell injury, one naturally must acquire some primary knowledge of the cell and cell membrane structure and function as well as the properties of the constituent elements comprising such structures. Furthermore, study of the nature of the interactions and forces between membrane constituents which are responsible for the formation and stability of such systems is essential for interpreting the cellular response to external perturbations.

In this chapter, the cell function will be discussed first. Secondly, since the cell membrane plays a significant role with respect to a successful freezing protocol among other things, membrane structure, function and composition will be discussed in detail. Third, general properties of the membrane are discussed in reference to the effects of the external perturbation imposed on the cell. Fourth, the self-assembly of the lipid and protein

molecules into a membrane structure in an aqueous medium and the roles played by the intermolecular forces in connection with such a process is discussed. Finally, membrane models will be considered.

A. The Cell Function

The living cell is the fundamental unit of structure in biology. It is the basic unit making up an organism of greater complexity. Two basic types of cells have been characterized: prokaryotes and eukaryotes. Prokaryotic cells are characteristically small and posses minimal interacellular structure. Specifically they do not possess nuclei, nuclear membrane or chromosomes. On the other hand, eukaryotic cells are much larger and contain numerous interacellular organelles in particular nuclei and chromosomes [29]. Many relatively large organisms may posess a single cell (the protists). The unity principle in biology is arrived at due to striking similarities among the structure and functional organization of cells in organisms. Regardless of the complexity of the cellular structure of an organism, it is essential for the survival of the cell, as an individual and as a species, that each cell carries out its basic functions. These functions include:

1)Acquisition of nutrients and energy sources.

2)Disposal of unusable and toxic materials.

3)Reproduction

4)Locomotion

5)Interaction with the environment

To carry out the forementioned functions every cell must regulate between its internal activities and the environment.

An outstanding characteristic of the cell is that the relationship between the intracellular activities and the extracellular environment is regulated by an encapsulating envelope. The interior of the cell is made up of needed components and organelles of widely differing structure, chemical composition and functional behavior. Within the cell the activities may occur either in a relatively undifferentiated internal milieu or in a series of functionally distinct, but coordinated, regions which are themselves seperated by an envelope. The integrity of these components and consequently by the cell's internal machinery necessarily depend on the encapsulating envelopes.

B. Membrane Structure and Function

The cell envelope, called the plasma membrane also known as the cytoplasmic membrane or cell-surface membrane, encapsulates the cytoplasm and defines the boundaries of the cell while creating internal components in which essential functions are carried out. This may exist alone or be part of a more complex cell-surface structure.

No single structure for the membrane can be described. Its complexity varies considerably, and can take on a number of forms according to the physiological functional role of the cell [60]. A single cell can also have several different areas of plasma membrane with different morphology and function [60].

Biological membranes at the cell suface and within the cell are of lipoprotein structure, i.e., are mostly composed of lipid and protein molecules Electron microscopy has revealed a characteristic trilamellar feature of the lipoprotein membranes [61]. The micrograph images of these membranes appear as pairs of parallel dense lines separated by a less dense region. This trilamellar feature corresponding to the plasma membrane in different cells is typically 70-150Å in width. In membranes of intracellular organells the thickness is 50-80Å.

1. Chemical Composition of Biological Membranes

Two major constituents of biological membranes are proteins and lipids. Composition of membranes varies from cell to cell but in general the dry weight of the membrane is 40% lipid and 60% protein. The lipid content of the biomembranes range from 20% in bacterial and inner mitochondrial to 80% in myelin plasma membrane of the dry membrane weight [59,60,62,63]. Protein and lipid content of some membranes are compared in Table 2.1, and the overal composition of human erythrocyte membrane is given in Table 2.2.

In addition to lipid and protein the membrane contains water, the most important constituent of any known biological system. Membranes contain about 20% of their total weight as water which is a very active participant in all membrane interactions [64,65].Much information about the water in the membrane has been obtained from calorimetric and nuclear magnetic resonance (NMR) studies [65-68]. These experiments distinguish a water component in the membrane possessing different properties than bulk water. This water is referred to as "bound" water. Another technique which has provided very useful information about the state of water in membranes is x-ray diffraction. (The matter of water in the membrane will be discussed further in Chapter III.) Such

TABLE 2.1

Approximate Protein and Lipid Content
of Several Membrances

Membrane	Protein:Lipid*	Cholesterol:Polar Lipid**
Myelin	0.3	1.00
Liver Plasma Membrane	1.0	0.40
Red Blood Cell	1.0	0.30
Endoplasmic Reticulum	1.0	0.06
Mitochondrial Outer Membrane	1.0	0.06
Mitochondrial Inner Membrane	3.0	0.03
Bacterial Membrane	3.0	0.00

*Weight Ratio **Molar Ratio.

TABLE 2.2

Overall Composition of Human Erythrocyte Membranes

Component	Dry Mass %
Protein	49.2
Lipid (total)	43.6
Phospolipid	32.5
Cholesterol	11.1
Carbohydrate (total)	7.2
Sialic Acids	1.2
Hexosamines	2.0
Neutral Sugars	4.0

studies have confirmed the essential importance of the water content for the integrity and maintenance of the biological membrane structure [59,60,69,70]. From these experiments the water associated with the membranes is broken down as

i) bulk water 90%

ii) bound water 10%

iii) irrotationally bound water 10-20 molecules*

*Irrotationally bound water molecules are known to be located within the protein interior.

2. Physical Properties of Membrane Components

In general membrane components are amphiphatic; i.e., they posess two different natures, polar and nonpolar. The polar nature is due to the fact that they are charged species. These amphiphatic molecules are in active interactions with one another and polar water molecules. From energy considerations the optimal stability of the system is attained when the free energy of the system is minimized. Therefore, the amphiphatic molecules in an aqueous environment, should form a structure such that polar elements comprise one phase and nonpolar elements, the other [71-73]. The structure of an amphipatic molecule is shown schematically in Figure 2.1.

a.Lipids

Characteristic major lipid components of the cell membrane are phosphoglycerides (more commonly referred to as phospholipids). The red blood cell contains four major phospholipids and one major neutral lipid [59,60,74]. The different types of phospholipids differ in size, shape and electric charge of their polar head groups. However, these molecules have a similar overall structure as illustrated in Figure 2.1. They possess two hydrocarbon chains derived from long chain fatty acids. The hydrocarbon chains are normally 14-24 carbons long.

Various types of lipids exist in harmony in the cell membrane. These lipids are asymetrically arranged with respect to the two halves of the bilayer [75,76]. For example, in the erythrocyte membranes, amino phospholipids (i.e., phosphatidylserine and phosphatidylethanolamine) are mostly found to be located in the inner layer, where lipids in the outer half are mainly phosphatidylcholine and sphingomyelin [76]. All phospholipids (at pH7) have a negative charge assiciated with the phosphate group. Phosphatidylcholine and phosphatidylethanolamine (at pH7) are dipolar zwitterions with no net charge, as their head groups have a positive charge. Besides the variations in the head

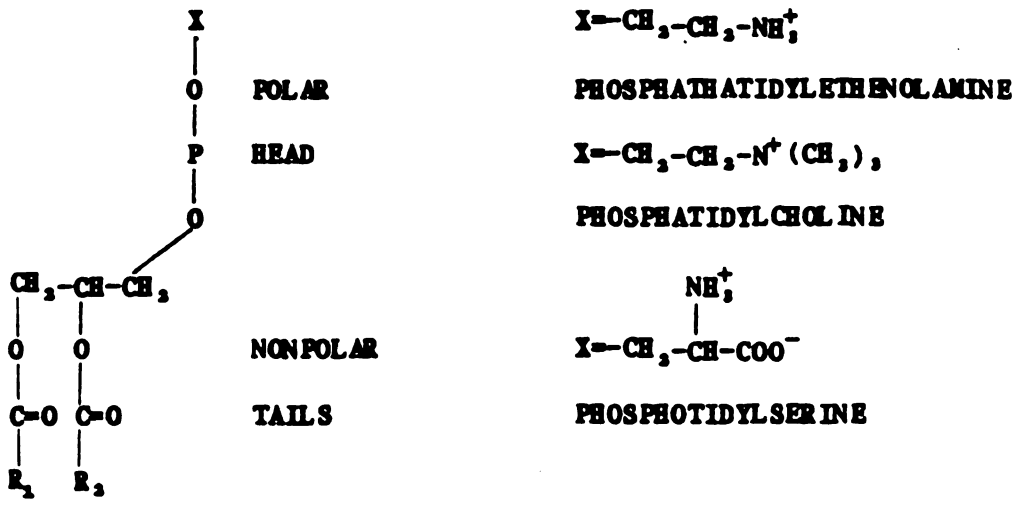

Figure 2.1: Typical Phospholipid Structures. (R_1 and R_2 are Hydrocarbon Chains 14-24 Carbons Long).

group charge and size, the hydrocarbon tails vary in length and degree of saturation. These considerable variations are believed to play a significant role in the functional and structural classification of biological membranes.

To represent lipid molecules, the following shorthand representation is adopted. The polar head groups, are represented by filled circles, whereas the hydrocarbon tails are represented by straight or wavy lines. According to minimum free energy analysis, the hydrophilic region also called the polar head group should be in contact with the aqueous environment [73]. On the other hand, fatty acid chains in order to be stable should be sequestered from contact with the aqueous environment. Now in light of this thermodynamic consideration we shall consider the arrangment of such amphiphatic molecules in an aqueous environment.

The thermodynamic stability criteria can be accomplished by lipid molecules forming a "micelle". A cross sectional diagram of a micelle is shown in Figure 2.2 where it is illustrated that the polar head groups are on the surface in contact with water and the hydrocarbon tails are hidden from the aqueous environment and form an internal hydrophobic phase. In the hydrophobic phase the hydrocarbon tails are mostly in interactions with one another.

Another arrangement fullfilling the stability criteria is formation of a biomolecular sheet structure generally called a "lipid bilayer". Due to its nature such a lipid bilayer in an aqueous medium will form a completely closed structure. A schematic diagram of such a closed vesicular bilayer structure is represented in Figure 2.2. The matter of molecular organization of the membrane lipid will be further discussed later.

b. Proteins

Proteins are responsible for many of the biological activities of the cell membrane [77]. Proteins also play very important role in the structural makeup of the cell membrane [78,79]. For example the red blood cell cytoskeleton protein network is essential for cellular functional and structural integrity [77,79].

Membrane proteins are classified in two categories: intrinsic or integral proteins and extrinsic or peripheral proteins. Extrinsic, also referred to as membrane-associated, proteins are electrostatically loosely bound and are easily separated from the membrane by such treatment as reducing the ionic strength or altering the pH of the suspending medium. However, the intrinsic proteins are deeply embedded in the

membrane and are associated with lipids. Membrane proteins are responsible for most of the dynamic processes carried out by the membrane such as transport, communication, and energy transduction. Some proteins are very mobile, and freely move in the lipid matrix. These proteins include, rhodopsin [80], bacteriorhodopsin [81] and those associated with ion transport. The red cell membrane contains about 40 types of proteins [74].

The stability criteria discussed for lipid molecules is applicable for protein molecules as well. The non-polar amino acid residues of these molecules should be sequestered from contact with the aqueous environment and the ionic and polar regions should be in contact with the aqueous medium.

C. Membrane Properties

1. Chemical Properties

Membrane processes take place through chemical reactions. The constituent molecules of membranes are mostly lipids and proteins, and their specific distribution give the membrane its unique chemical identity. Therefore any kinetic or thermodynamic analysis of the membrane system must take into account the chemical nature of the processes involved. For example, important

properties of the membrane system such as activation energy or the total energy are purely due to chemical reactions in such a system.

Membranes are very selective permeablility barriers. This is due to the existence of specific molecular pumps and gates at the membrane which regulate the selective transport of matter across the biomembrane. Besides regulating the active transport the membrane composition is also important to regulate passive transport. The major constituents of the membranes, lipid and protein molecules, work in a very cooperative manner to give the cell its characteristic transport properties. The relatively small lipid molecules form layers which act as barriers to the flow of polar molecules. On the other hand the larger protein molecules serve as gates, pumps, energy transducer, and enzymes.

Another important aspect of the chemical properties of the cell membrane is that its shape is a strong function of the chemical composition of the environment. In the case of the erythrocyte cell, depending upon the chemical make up of the suspending media the normal biconcave shape goes through several variations, such as, stomatocyte (cup shape), echinocyte (creanated spheres) and a class of shapes commonly referred to as myelin figures [82-84]. While some of these shape transformations are reversible, some are associated with hemolysis [82,85,86].

3. Mechanical Properties

An important consequence of the perturbation of the cell system is the observed shape changes. This implies the existence of mechanical stress and physical forces on the membrane. Any descriptive analysis of the membrane system then must include the mechanical properties of the membrane. Thermodynamically speaking, the ultimate goal is to arrive at the thermodynamic equation of state of the model membrane system. Such an equation could be derived from direct measurements of the mechanical properties such as interfacial membrane tension as a function of temperature and surface density. A classic theoretical development of mechanical behavior of membranes by Evans and Skalak [87] deals with the above topic.

The monolayer system is a much simpler system than the bilayer system and has been studied extensively over the years. For this reason this system has been used to interpret the mechanical and thermodynamic properties of membrane systems. Monolayer surface pressure versus area behavior is studied for numerous lipid molecules which gives the internal equation of state of such a system. However, one can not define a surface pressure for a closed membrane system in the same manner defined for the monolayer system. Furthermore, the surface pressure of a membrane system cannot be directly measured in contrast with the

monolayer system. The definition of the surface pressure could eventually lead to the development of an internal equation of state. Since the surface pressure could be considered as a negative tension, surface pressure and surface tension within the membrane are sometimes referred to as interfacial membrane tension.

The surface pressure is a strong function of temperature and surface density and therfore area changes by definition. On the other hand the surface tension is a weak function of area changes [87]. The red cell membrane for example is very resistant to changes in area. In fact a few percent membrane area increase results in membrane rupture whereas it can be sheared easily. This is due to the fact that the red cell membrane elastic shear modulus is 4 to 5 orders of magnitude smaller than the area compressibility modulus (Bending modules, B, is of order $10^{\mp 13}$ to $10^{\mp 2}$ dyn/cm [87]).

From the thermodynamic point of view the energy expenditure associated with bending a red cell membrane is quite small and negligible compared with membrane tension [88]. (Shear modulus, μ, and compressibility modules, k, are of the order $10^{\mp 2}$ dyn/cm and 10^{2}-10^{3} dyn/cm respectively [87]). However free energy variation caused by local deformations in the outer layer of the membrane with respect to the inner layer could result in

relatively large bending moments (essential for the shape stability). Therefore considerable energy storage in bending may result: such is the case for example for a creanated cell or echinocyte formations.

D. Physical Principles of Membrane Self-Assembly

The formation of lipid structures such as micelles, lipid bilayers, and liposomes is a self-assembly process. This process is due to the structural and functional characteristics of the fundamental units of such systems, namely their amphipathic character. Any physical and thermodynamic understanding and analysis of the biomembrane system requires a fundamental understanding of the intermolecular interactions involved in the self-assembly process. All the theoretical analysis for the red cell in this work will be based upon our model system, namely lipid vesicles or liposome.

1. Nature and Role of Forces

Surface phenomena in general and stability and formation of lipid bilayers in particular are a direct consequence of interatomic and intermolecular forces. For example the existence

of a surface or interfacial tension is due to the unsymmetrical force field at the interface. Molecular orientation at any liquid interface is also a direct consequence of intermolecular forces. The hydrophilic head-groups of lipids in bilayers are subject to strong interactions with each other, with the surrounding aqueous medium, and with nearby bilayers (if such bilayers are near). These interactions and hydrocarbon chain interactions are all interdependent and it is this intimate interdependence which manifests itself in the formation and is responsible for the stability of lipid bilayers. Three important interactions encountered in surface physics will now be considered.

a. Steric Repulsion

A strong repulsive force arises when atoms or molecules are brought in or near contact. Basically, the repulsion effect is a manifestation of the Pauli exclusion principle (that the electron clouds could not overlap each other). Steric interaction depends upon the size of the atoms or molecules and it strongly depends upon the seperation distance of such particles.

For steric interaction various functional forms for the potatial energy of the interaction have been proposed. A classic form is

$$E(r) = \lambda r^{-s} \quad , \quad s \sim 12$$

Where E(r) is the potential energy function and r is the distance between two particles (atoms or molecular groups). Another functional form E(r) is

$$E(r) = b*EXP(\rho/r)$$

This latter form is preferred due to the fact that quantum mechanical arguments suggest that the interaction should be closer to being exponential than an inverse power. This functional form is used when molecules are modeled as hard, impermeable particles, e.g. hard spheres, discs or cylinders [89]. This repulsion is important only at atomic distances (<4Å).

b. Electrostatic Interactions

The potential energy of interaction of two particles with charges q_1 and q_2 which are seperated by distance r, is given by Coulomb's law as

$$E(r) = q_1 q_2/r$$

For two dipoles interacting with the field of the other the

interaction energy is given by

$$E(\mu,\mu) = -2\mu/r^3$$

where μ is the dipole moment. If the dipole were free to move which is the case in the biological system such as with bilayers, the combined effect of the dipole-dipole interaction and thermal agitation should be considered. One such analysis due to Keesom [92] gives

$$E(\mu,\mu)_{ave.} = -2\mu^4/3KTr^6$$

where K is the Boltzman's constant and T is temperature.

In case of complicated charge distribution one needs to also consider possibilities of higher level interactions such as dipole-quadrapole, dipole-octapole, quadrapole-quadrapole, etc. interactions.

The electrostatic interactions play an important role in bilayers as the lipid head groups are charged. The ionic or zwitterionic charges on the polar head groups are subject to mutual interactions while interacting with the dipole moments associated with water molecules. It is known that the extrinsic proteins are bound to membranes via electrostatic and

hydrogen-bond interactions. Furthermore, the aqueous phase usually contains an appreciable amount of charged solute species.

An ionizable membrane surface will preferentially attract the oppositely charged ions and repel like charged ions, creating a region of nonuniform ion concentration. This region is referred to as the electrical double layer or the diffuse double layer. Exact treatment of the actual charge distribution is impossible due to its descrete nature. The Gouy-Chapman theory combined with the specific ion adsorption and uniform charge distribution assumptions [90-91], gives the surface charge density σ and potential ξ of the charged membranes. For the case in which the charge binding sites are negatively charged, the surface charge density is given by

$$\sigma = \sigma_i/(1+KC_e) \qquad [2.1]$$

where σ_i is the initial charge density, K is an association constant, and c_e is the concentration of free cations at the membrane surface.

C. Dispersion Forces (van der Waals Forces)

The origin of dispersion forces lie in the van der Waals

state equation of gases. This force also called the van der Waals attraction force exists between neutral (uncharged) particles (atoms, molecules or group of molecules). The credit for the theoretical understanding is due to the works of Debye, Keesom, and London [92,93]. Debye in 1920 introduced induction or Debye forces and Keesom in 1921 introduced orientation or Keesom forces, which exist due to the permanent dipole moments of the atoms. When these forces are compared with the forces deduced from the van der Waals equation, it is apparent that they do not account for all the existing forces. Furthermore, there exist forces between atoms or molecules possessing no permanent dipole moments such as rare gas molecules H_2, N_2, CH_4, etc. Forces of the type which exist between such neutral atoms or molecules are called Dispersion forces, first introduced by Wang in 1927. An explanation for nature of these forces was set forward by London [92,93], he noted that the neutral atoms and molecules do posses instantaneous dipole moments due to their zero point motion. This motion which is a direct consequence of the uncertainty principle creates a fluctuating dipole at the site of the atom or molecule. London gives the dispersion energy as

$$E(r) = -C/r^6$$

which is obtained through quantum mechanical calculations. Dispersion forces as implied by the above equation are long-range

attractive forces. These forces are always present between two bodies possessing dipole moments. van der Waals forces are made up of dispersion, induction and orientation forces, with the dispersion forces contributing most except in the case of very polar molecules where the orientation energy dominates.

Hydrocarbon tails in the membrane interact mainly through van der Waals and steric forces. The van der Waals forces between the tails favor close packing of the tails.

2.Effect and Range of Forces

The combined effect of all the forces in a given system will be to drive the system to its minimum free energy state. The force involved could be divided into two categories, Long-range and short-range.

In lipid structures, such as liposomes and biomembranes, it is the short-range interfacial forces that play dominant roles. This is a reflection of the "soft" structure of lipid molecules which makes them very susceptable to any shape charges induced by short-range interfacial forces. This is exactly the main reason for biophysical systems being so sensitive to any charges in the ionic strength or pH of the aqueous medium.

In summary, hydrophobic interactions are the major driving force for the formation of lipid structures such as micelles and bilayers. These interactions play an important role in the folding of proteins in aqueous medium. Credit is due to favorable electrostatic and hydrogen-bonding interactions between head groups and water molecules for the spontaneous formation of lipid bilayers in water.

B. Membrane Models

The discussion presented in this chapter has revealed the complexity of the biological membranes both in terms of their properties and behavior. This is reflected in the experimental and analytical difficulties associated with studies of such systems. For example for any thermodynamic analysis the system must be clearly defined. The model systems are desirable and advantageous on the basis that it allows one to design and construct a structure in vitro with precisely known parameters which mimics the real systems behavior in vivo. The control over parameters of the model system is then possible where it may not be accessible with a real membrane system. Study of known processes and properties which are associated with the real system of the model will contribute considerable insight to the basic understanding of the real membrane system. However, one should

always bare in mind that results obtained from such well-defined and controlled model studies must be interpreted in light of the real system.

To account for all the different types of lipids and proteins in the membrane in a membrane model system at this point is not possible. The problem is further complicated as all biological membranes have different components in their inner and outer surfaces and each surface has a different enzymatic activity. However, the major parameters of interest concerning this work appear to be independent of the fine structure of the membrane to a certain degree. For example, single component lipid vesicles which are commonlly referred to as liposomes mimic the low temperature behavior observed in living cells remarkably well and are widely used as a very useful model system [94,95]. The current model for the gross organization of biomembranes is the conceptual view of the fluid mosaic model proposed by Singer and Nicolson (1972). This model basically is a refined version of several earlier models. Gorter and Grendel in 1925 were the first to put forth the lipid bilayer picture as the basic structure of biomembranes [97]. The bilayer picture was accepted and retained by the subsequent models as an integral part of the membrane [98-100]. Development of the black lipid membranes commonly referred to as BLMs was perhaps the most important step in the development of the fluid mosaic model. Muller et al (1962)

developed a method to form a thin membrane of a lipid mixture. BLMs have been extensively studied and have provided significant insight into the way the real membranes behave. However, these studies have concentrated mostly on the permeability and electrical properties. The reader is referred to an excellent reference by H.T.Tien for further details [102]. The essence of this model is that the membrane is a two-dimentional fluid of oriented lipids in which globular proteins are inserted. Proteins if not restricted by special interactions may pass from one side of the lipid matrix to the other. Proteins and lipids are also capable of rotational and lateral diffusion. In fact proteins are found loosely bounded to the inside or outside of the membrane as well as imbedded in the bilayer. This is a reflection of the role played by specific proteins such as transport, communication, and energy transduction. Therefore, proteins localized on the external side of the membrane allow communication with the environment. Accordingly, membrane protein involved in interacellular activities should be located within or on the inner surface. This model does not account for interactions between lipid and proteins, where as, there is experimental evidence indicating significant association of proteins with lipids in the bilayer structure all pointing to existance of mutual interactions between proteins and lipids [103-105]. Proteins classified as "integral" or "intrinsic" interact extensively with the hydrocarbon chains of membrane lipids. Furthermore, proteins

classified as "peripheral" or "extrinsic" are bound to membranes via electrostatic and hydrogen-bond interactions, again emphasising the interdependence of lipid-protein interaction.

CHAPTER III

OSMOTIC BEHAVIOR OF THE CELL

Water is the solvent vital for the structure and function of living organism regardless of their morphological complexity. The functional and structural as well as the morphological properties of the living cell are very sensitive to changes in the water content. The thermodynamic process of self-assembly discussed in the previous chapter is a dramatic example of the role of water in living cells. It is then not surprising that the most important environmental alteration of the cell system is directly associated with the state and amount of water. Here we will discuss the osmotic behavior of the cell in response to freezing and thawing damage as it relates to solvent water in such a system.

Removal of water as ice during freezing processes of cell suspensions results in a decrease in the liquid volume of the system [23]. For a system consisting of a cell suspension the most important consequence of freezing, as it relates to the biochemical and biophysical as well as thermodynamic state of the system, is the accompanying increase in the solute concentration of the system. The removal of water during a freezing process is

therefore manifested in the perturbation of the osmotic equilibrium between the cell and its environment. Once the concentration of the suspending medium is increased above the physiological isotonic level and the cell is exposed to hypertonic conditions the cell will experience dehydration and volumetric reduction. These effects are collectively referred to here as osmotic stress. The osmotic stress and the molecular changes produced by high electrolyte concentrations may either result in an irreversible injury or leave the cell vulnerable to any further alteration of the system. This vulnerability for the cell system undergoing the cryopreservation process could manifest itself in the thawing stage when the cell experiences further osmotic disequilibrium.

It is then clear that the decrease of temperature during freezing and its increase during thawing result in an osmotic stress. This is a reflection of the fact that the damage caused by dehydration and high salt concentration in the absence of low temperature resembles the freezing damage [32]. In fact the major determining factor of the cell survival during suboptimal cooling is believed to be the direct result of the hypertonic exposure and the concomittant pressure gradient build up across the membrane as a consequence of the decrease of temperature [106].

When the chemical equilibrium between the cell and its

environment is altered as a result of freezing, the chemical potential of the water across the membrane will be altered. The living cell osmotically responds to such a perturbation by a change in volume. The osmotic behavior of the cell plays an important role concerning the site and extent of injury experienced by the cell exposed to osmotic stress conditions.

Cells during a cryopreservation process experience concentrations different from isotonic and these concentration differences result in a change in volume [23]. However, it is known that shrinkage of the cell is more injurious than the absolute increase in solute concentration [106-108]. This is directly reflected in a hypothesis proposed by Meryman and Williams which states; freezing injury is due to the alterations to the plasma membrane as a result of stress imposed by cell water loss [109-111]. The relation between cell injury and osmotic shrinkage in general and the relation between cell water content and osmotic pressure of the surrounding medium in particular are primary motivations to study the osmotic properties and behavior of the cell under different conditions. The physiochemical principles responsible for observed osmotic properties as a result of exposure to "severe" environments are not well understood at this point. This makes a thermodynamic analysis of the osmotic properties more appealing as such analysis will be based on well-defined and preceisly controlled parameters such as

temperature and concentration. It should be noted here that the idea of the minimum cell volume is related to the cell injury is losing support (for other hypothesis regarding this matter refer to chapter 2 and 8).

A. Water Associated With the Membrane

The overall concept of the extent of involvement and amount of water in living systems have been recognized for many years. However, questions concerning the state and amount of water associated with membranes remains unresolved. This is an added difficulty to any thermodynamic analysis of the membrane. Such a quantitative study has to deal with this problem at the outset where the system and environment are to be defined.

The observation has been made that the red cell does not behave as an ideal osmometer and that a portion of the cell water does not seem to be affected by the change in the enviromental conditions. This has led to the belief that part of the cell water (called "bound water") is associated with the membrane and has a structure and dynamic properties different than bulk water. This is a direct result of proximity and interaction of water molecules with the protein and lipid molecules residing at the membrane. In fact it is known that the bound water is associated

with the proteins and phospholipids at the membrane. Existence of water with properties different from that of free solution would have great consequences concerning the transport across the membrane and the thermodynamic treatment of membrane system.

Water is a polar molecule which acts as an inert solvent in all living systems. Molecules comprising the biomembrane are not soluble in water (negligible solubility of approximately 10^{-4} molecules for each water molecule [72]) and as was discussed in chapter 2 possess a dual nature as one part is attracted to water (hydrophilic) and the other is expelled from it (hydrophobic). In fact this dual nature is responsible for the self assembly of structures comprised by such molecules. Water has a complex structure where individual molecules are linked to each other by hydrogen bonds which are known to be effected by the introduction of non-polar molecules, due to the hydrophobic effect [73,112]. Frank and Evans measured a negative entropy change when non-polar molecules where transfered into water [73]. The explanation for such energetically favorable process is given as follows. The water molecules at the surface of the cavity created by a non polar solute must be capable of rearranging themselves in order to regenerate the broken hydrogen bonds (in fact, where the enthalpy change is negative they may be slightly stronger than before), but in doing so they create a higher degree of local order than exists in pure liquid water, thereby producing a decrease in entropy

[73]. It has also been shown that the removal of bound water requires high energies (comparable to the binding energy in solid phase) which is a direct manifestation of the negative entropy of formation of such bonds [66,69,113].

Most of our knowledge on the amount and state of water in living systems is due to calorimetric, X-ray, and nuclear magnetic resonance (NMR) studies, where the red cell has been the most widely used biological system for such studies [64,65,68]. These studies have measured the amount of bound water to be 20%-40% (by weight) of the hydrated membrane (25-70 gm H_2O/100 gm dry membranes). According to X-ray diffraction and differential scanning calorimetry studies 20% hydration is required for membrane integrity [64] and phospholipid-cholestrol mixing [68]. This means the water is a major constituent of the biomembrane. The aboundence of water in the membrane system is revealed when the 20%-40% estimate of the water content is translated into the mole fraction. Assuming typical molecular weights of 100,000 for protein and 700 for lipids gives better than (10:1) mole ratio of water in the membrane. Water content of human red blood cell is reported to be .68gm water/gm cells [114].

The NMR studies on the state of membrane bound water suggest a more tightly bound water called irrotationally bound water [69]. This membrane bound water characteristically has a more ice-like

behavior. Heats of binding of the irrotationally bound water has been measured and are similar to or greater than the heats of binding of water in ice [66]. The amount of tightly bound water for the red cell ghost membrane is 4% of the dry weight which is believed to be closely associated with protein molecules [118]. At this point we will briefly discuss the role of membrane associated water in a more general format.

As discussed in the foregoing section, the most important role of water is the consequence of its unique structure which is manifested in the inherent tendency of hydrocarbons to aggregate in the water environment. NMR studies have shown that the dynamic molecular structure of the bound water is modified and is more ice-like. The modified molecular configuration seems to result in an increase in the diffusion across the membrane [115]. This is attributed to the fact that the free energy of bonding between water and water (when bounded to membrane) is very compatible with the free energy of attraction between water and nonelectrolytes in water. According to Horowitz and Fenichel hydrogen bonding by nonelectrolytes in water competes with water-water bonds which results in a local structure disorder and when the molecular structure of water is disrupted diffusion proceeds at faster rate [116]. It has also been pointed out that hydrogen bond formation leads to intramolecular attractions which increase the intramolecular spacing which is manifested in a decrease in the

density of hydrogen bonding molecules [117].

B. Osmotic Pressure

An outstanding characteristic of the cell membrane is the discriminating nature which enables it to maintain many substances at different concentrations across it. This enables the cell to regulate the movement of matter across the membrane i.e., membranes are permeable only to certain substances. When a solution is seperated by such a membrane, if the concentration of the non-permeable solute is different on the two sides, the solvent will tend to be drawn toward the higher concentration. Then what is called the "osmotic pressure" of the solution is the excess pressure which must be applied to the solution in order to prevent the movement of solvent across the membrane. The osmotic pressure is therefore to be regarded as a thermodynamic property of the solution. Therefore in order to define the thermodynamic equilibrium conditions in living cells the first step is to consider and understand the principles and meaning of osmotic pressure in such systems.

The movement of matter across the cell membrane is termed collectively as "transport" or "osmosis". The thermodynamic quantity used to describe the transport phenomenon is the chemical

potential ,μ, which is an intensive system property analogous to temperature and pressure. For equilibrium it is required that the chemical potential of the solvent (water) must be equal on two sides of the semi-permeable membrane. When the solute concentration is increased, for example in the process of freezing, the chemical potential of the solvent is decreased and as a result the solvent is driven from higher chemical potential region across the membrane to re-establish equilibrium.

If the osmotic pressure of the solution of a system at pressure, p, and temperature, T, due to a semipermeable membrane separating two phases (1) and (2) is π, then the osmotic equilibrium condition in term of the solvent (water) is

$$\mu_w^1(T,P+\pi,X_1) = \mu_w^2(T,P,X_2) \qquad [3.1]$$

where X is the mole fraction of the solute. Now μ is defined as

$$\mu(T,P,X) = \mu^\circ(T,P) + RT\ln X \qquad [3.2]$$

where μ° is the chemical potential for pure solvent. Note that in Equation 3.2 ideal solution behavior is assumed. Equation 3.1 could then be written in the form

$$\mu_w^\circ(T,P+\pi) + RT\ln X_1 = \mu_w^\circ(T,P) + RT\ln X_2 \qquad [3.3]$$

The Gibbs-Duhem equation gives

$$-\bar{s}dT + \bar{v}dP - \sum X_i d\mu_i = 0 \qquad [3.4]$$

Where $\bar{s}$ and $\bar{v}$ are the partial molar entropy and volume respectively. Equation 3.4 at constant temperature gives

$$d\mu^{\circ} = \bar{v}_w dP \qquad [3.5]$$

Where $\bar{v}_w$ is the partial molar volume of the solvent in the solution. Integrating Equation 3.5 for a pressure increase equal to π we have

$$\mu_w^{\circ}(T, P+\pi) - \mu_w^{\circ}(T, P) = \int \bar{v}_w dP$$
$$= \bar{v}_w \pi \qquad [3.6]$$

Now assuming incompressible solution Equation 3.3 becomes

$$\bar{v}_w \pi + RT(\ln X_1 - \ln X_2) = 0$$

or

$$\pi \bar{v}_w = -RT \ln(X_1/X_2) \qquad [3.7]$$

Equation 3.7 with the dilute assumption can be simplified as follows

$$n_1 \simeq n_2 \simeq n$$

$$\ln(X_1/X_2) = \ln[n_1/(n-n_2^s)]$$

$$= -\ln(1 - n_2^s/n_1)$$

$$= -n_2^s/n_1$$

where n_2^s is the solute mole number and n_1 is the solvent mole number and $n_2^s << n_1$. Then

$$\pi \bar{v}_w = RTn_2^s/n_1 \qquad [3.8]$$

If we further assume an incompressible solution, that is,

$$n_1 \bar{v}_w \simeq n\bar{v}_w = V_w$$

Where V_w is the total volume of the solvent in the solution, then Equation 3.8 becomes

$$\pi = RTC \qquad [3.9]$$

Where C is the molal concentration (n_2^s/V_w) of the solute in the solution.

Osmotic pressure related to molar concentration of the solute in the analysis of living cells given by Equation 3.9 is called Boyle-Van't Hoff law and is conventionally written in the form

$$\pi(V - b) = \text{Constant.} \qquad [3.10]$$

where V is the cell volume and b is the volume of water unavailable for transport.

C. Osmotic Response of the Cell

Osmosis plays an important role in the function of the cell. When the chemical potential of the water in which the cell is suspended is perturbed, the cell responds by morphological changes concomittant with changes in volume. According to the simple transport model discussed earlier the volume of the cell is proportional to the osmolality difference of the solute across the membrane [109-111]. The most studied model for shape transformations due to extracellular perturbations has been the red blood cell. The red cell membrane is a thin viscoelastic membrane with a biconcave disc geometry in isotonic condition. This geometry is very sensitive to the osmolality of the surrounding medium and is known to go through dramatic shape changes. The osmotic response of the cell has received extensive theoretical and experimental considerations in light of the fact that the structure of the membrane and its mechanical properties could be better understood once the shape determining parameters are explained.

The osmotic response of human erythrocyte to hypotonic solution is especially easy to study. It becomes spherical when placed in hypotonic solution and the biconcave shape is recovered when the medium is made isotonic again. This means that the red cell membrane can be considered to be elastic under certain conditions. Several mathematical solutions for the sphering process of the red blood cell are obtained, where the membrane is treated as an elastic shell [118-120]. These studies show good agreement between the observed cell shapes and calculated ones. The fundamental hypothesis of all such studies has been that the membrane curvature elastic (bending) energy is the mechanical parameter governing the shape. The equilibrium shape for an elastic shell is attained when the bending energy is minimized. Several independent studies have shown that the area of the red cell membrane remains unchanged during the sphering process [121,122].

Concerning the osmotic response of the cell to more severe perturbations such as freezing, it has been proposed that freezing injury is the result of osmotic water loss [107-109]. According to these studies the associated cell volume reductions ultimately lead to cell damage. Specifically, it is believed that the cell injury due to freezing or hypertonic exposure in the absence of low temperature is predominantly related to cell shrinkage beyond a critical minimum volume rather than to an absolute increase in

the solute concentration [107,108]. Williams et al proposed that the cell volume reduction is accompanied by cell surface area depletion. That is the membrane components are lost durig osmotic shrinkage. This leaves the cell vunerable and as a consequence the cell cannot return to its initial volume when transferred to isotonic medium. The membrane then bursts under osmotic stress [108]. The matter of cell damage in reference to human erythrocyte under hypertonic conditions will be discussed in detail in the next section.

To describe the osmotic shrinkage on a quantitative basis and theoretically determine the possible mechanism(s) for area depletion, the following argument is given.

The diffusion of the solute molecules across a unit area of the semi-permeable membrane is described by Fick's first law of diffusion,

$$\partial n/\partial t = -D(\Delta C/\Delta X) \qquad [3.11]$$

where

n = mole number of solute

t = time

D = diffusion coefficient

ΔC = molar concentration difference across the membrane

ΔX = membrane thickness.

Note that to arrive at Equation 3.11 a uniform concentration gradient through the membrane is assumed. To describe the osmotic flow of solvent across a membrane in biophysical studies, Equation 3.11 is commonly written as

$$J = -P\Delta C \qquad [3.12]$$

Where J is the molar flux density and p is the permeability coefficient and is defined as

$$P = D/\Delta X$$

If the volume and area of the cell are designated as V and A respectively, the volume flux is

$$dV/dt = JA\bar{V}_w \qquad [3.13]$$

where V_w is the molar volume of solvent. Thus Equation 3.12 takes the form

$$dV/dt = -V_w AP\Delta C \qquad [3.14]$$

For spherical geometry Equation 3.14 becomes

$$dR/dt = -\bar{V}_w P \Delta C \qquad [3.15]$$

where R is the radius of the sphere. Assuming that the membrane thickness as well as its permeability coefficient and ΔC remain constant during the osmosis, Equation 3.15 integrates to

$$\begin{aligned} R &= (-\bar{V}_w P \Delta C)t \\ &= \text{Constant}^* t \end{aligned} \qquad [3.16]$$

That is the radius of the spherical cell is linearly related to time. Such behavior has been observed by several investigators for lipid vesicles (liposomes) as they shrink in response to high concentration exposure [123,124]. The experimental data of Boroske et al on single bilayer egg-lecithin vesicle showes a good agreement with the above relationship [124]. Equation 3.15 is used to arrive at the permeability coefficient ,p, as the rate of change of radius of vesicle is directly proportional to the negative of the solute concentration gradient across the membrane ΔC, and P is the proportionality constant. The permeability has been measured to be 37-41 μm/s for egg-lecithin vesicles [95,123-125].

Now assuming that the membrane is made up of 2n lipid molecules with effective surface area per molecule of $\bar{A}$ and that the lipids are shared equally between the two layers of the

membrane, the membrane surface area is given as

$$A = n\bar{A}$$

Now as (spherical geometry)

$$dA/dt = 8\pi R(dR/dt)$$

solving for dR/dt we have

$$dR/dt = (dA/dt)/4(\pi A)^{1/2}$$

or

$$= [d(\bar{n}A)/dt]/4(\pi A)^{1/2} \qquad [3.17]$$

Therefore Equation 3.15 becomes

$$dA/dt = -4\bar{V}_w\pi^{1/2}P\Delta CA^{1/2} \qquad [3.18]$$

Integrating Equation 3.18 we have

$$A_o^{1/2} - A_t^{1/2} = -\alpha t \qquad [3.19]$$

where

$$A_o = A(t=0)$$

$$A_t = A(t=t)$$

$$\alpha = 6\bar{V}_w\pi^{1/2}P\Delta C$$

Equation 3.19 for a positive α (i.e. hypertonic condition,

positive ΔC) reflects the reduction of the membrane surface area as a subsequence of shrinkage. Now according to our assumption ($A=n\bar{A}$), the reduction in the area of the system is only possible through two modes; (i) the effective area per molecule $\bar{A}$ is decreased while the number of molecules in the membrane is conserved, (ii) the number of molecules residing in the membrane is reduced while the area per molecule $\bar{A}$ remains constant. The first mode of area reduction results in an increase in the density of molecules within the membrane which will be accompanied by an increase in the intra-membrane pressure. It is reported that in fact freeze-induced dehydrated cells have higher intra-membrane pressure at shrunken state [108, 126,127]. It is believed that the second mode of area reduction is preceeded by the first mode. That is, the intra-membrane pressure increases first but it can not increase indefinitely. Once a certain level is reached the membrane is relaxed through expulsion of molecules from the membrane surface. There exist several experimental reports of observations of such behavior [36,128-130]. These matter will be discussed in detail in a later chapter.

D. Description of Osmotic Hemolysis

Red blood cells suspended in a medium removed from the physiological (isotonic) condition undergo drastic shape changes

which is usually concurrent with changes in surface area and volume. The extent of area and volume changes depend on the tonicity of the suspending medium. Specifically, in case of hypotonic exposure the cell volume is increased while the area remains almost constant [25,26], and in the case of hypertonic exposure the cell volume and the effective surface area are decreased. Regardless of the perturbation mode, if the disturbance is large enough it leads to the hemolysis of the red blood cell (perhaps due to distortion of the membrane). A diagramatic representation of the hemolysis process due to action of a lytic agent is given in Figure 3.1 [86]. Hemolysis is not a simple osmotic phenomenon as it depends on the type of solute as well as the extent of osmotic perturbation [26,34]. Nevertheless, a simple thermodynamic analysis with a simplistic view of the cell osmotic behavior gives a good description for the red cell hemolysis.

During freezing water is excluded from the cell suspension through the formation of ice. The subsequent increase in the extracellular salt concentration creates an osmotic pressure which acts as a driving force for transport of water out of the cell. This chemical effect called "osmotic shock" is intimately coupled with temperature and changes simultaneously with changing temperature during the freezing and thawing cycle.

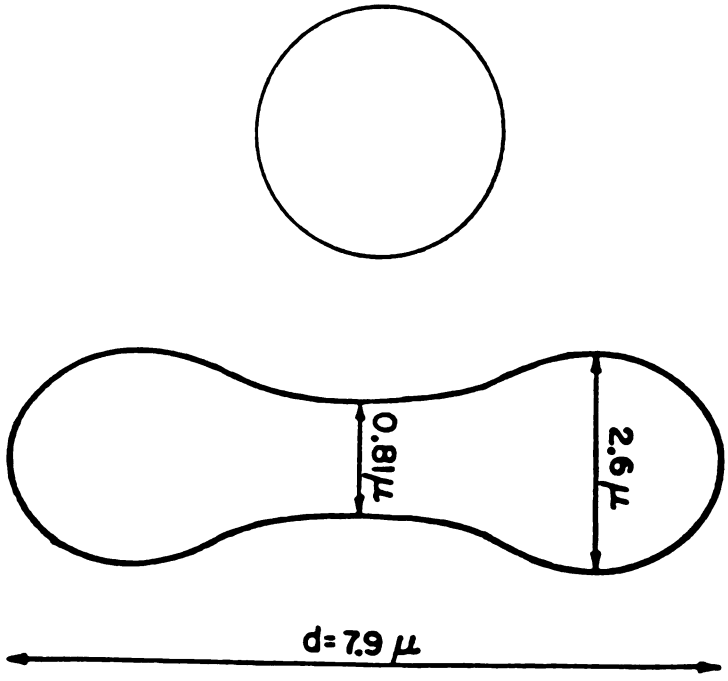

Averaged Dimensions of RBC.

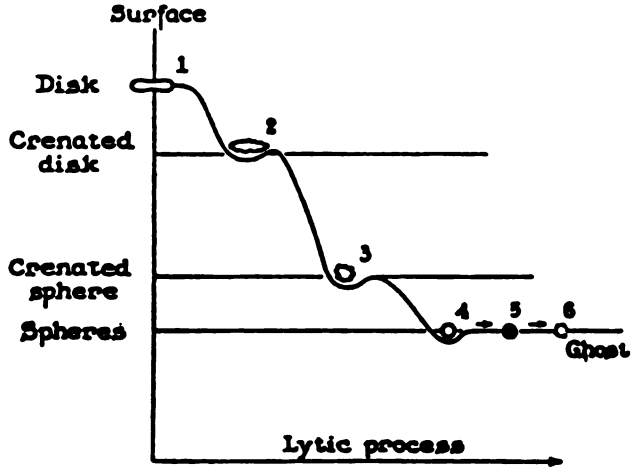

Figure 3.1: Digramatic Representation of the Shape Changes, From Disk to Sphere which Occur During the Action of a Typical Lysin (reproduced from reference [86]).

The chemical potential μ of the ith species in a solution is given by

$$\mu_i = \mu_i^*(T,P) + RT\ln a_i$$

where μ_i^* is the reference chemical potential and is only a function of pressure and temperature for both solute and solvent, and a_i is the activity of the ith species. The cell membrane as mentioned earlier is permeable to water and impermeable to most salts. A model represention of the cell is given in Figure 3.2. As the chemical potential across the cell membrane is removed from equilibrium, for example by freeze-induced dehydration, a chemical potential gradient across the cell membrane will result

$$\Delta\mu_i = RT\Delta(\ln a_i)$$

where

$$\Delta\mu_i = \mu_i^e - \mu_i^i$$
$$\Delta(\ln a_i) = \ln a_i^e - \ln a_i^i$$

This trans-membrane difference in chemical potential results in a water flow across the membrane in order to reach equilibrium ($\Delta\mu_i$=0). If the external solution is made hypertonic, as is the case for freezing, then to reach equilibrium water must flow out of the cell. The loss of water is then reflected in shape changes

and a reduction in cell volume and the cell membrane is forced to shrink on its contents. It is likely that hemolysis occurs when the cell has lost all its free water and under the osmotic pressure due to the trans-membrane chemical potential gradient is forced to release its hemoglobin content. The loss of hemoglobin preceeds by rupture of the cell membrane. If the suspending medium of the cell is made hypotonic as is the case for thawing, the cell volume is increased as the water flows into the cell. Hemolysis occurs when the cell membrane area increase fails to keep up with the increase of the cell volume and ruptures, where hemoglobin is again lost from the cell into the suspending medium.

CHAPTER IV

EXPERIMENTAL SYSTEM

The experimental aspect of this work involves measurement of the hemolysis kinetics of human red blood cell populations at different temperatures due to a step change in the solute concentration of the suspending medium of the red blood cell. To obtain kinetic data a temperature controlled stop flow system is employed which provides rapid mixing. The dynamics of damage are inferred from these measurements.

The hemolysis of a single red cell, provided that sufficient level of perturbation exists, is known to be an all or non event [132]. However, due to a distribution of cellular properties all cells in a sample population do not hemolyse at the same time,i.e., a finite time is associated with the hemolysis dynamics of a cell population. For many years the standard technique for hemolysis measurement of a blood sample involves the static measurement of the hemoglobin absorption [132]. Because of the time required for the sample preparation process (several minutes) this so-called spectrometric technique gives a time average

measure of the hemolysis. Such a static measurement has significance only for a system with a very slow or non-existant dynamics (relatively long-time response). The red cell hemolysis kinetics are very rapid in some cases of interest here and early time data are essential for a complete understanding and modelling of such a kinetic process. To obtain hemolysis kinetic data at reletively short times (seconds) one must apply a technique which provides rapid mixing and a technique to measure the response of the cell in order to produce a complete hemolysis time history.

Since the cellular osmotic response is very fast (about 250msec [133]) the rapid mixing is essential and dictates the accuracy and reproducability of the results. The stop flow technique provides very rapid mixing which has been used to study fast chemical reaction kinetics and cell membrane permeabilities [134,135]. To measure the cell population response to the step change solute perturbations induced by the stop flow technique, the light scattering technique is employed.

In this chapter the experimental apparatus constructed for this work is presented. First, the stop flow system along with the theory of the operation of the experimental system is presented. Second, major components comprising the system are discussed separately.

A. Introduction to the Stop Flow System:

To obtain the kinetics of the human erythrocyte destruction a modified stop flow apparatus equipped with temperature control has been designed and constructed. The stop flow technique allows rapid and controlled alteration of the extracellular medium. In this work it is used to rapidly introduce the red blood cells to a desired level of sodium chloride concentration. By detecting the light transmitted by the cell population the system response is recorded and the hemolysis kinetics are then deduced.

Although the experimental concept seems to be simple at first, due to the biological nature of the problem, extreme care is required at every step of the way in order to minimize and control various factors which can introduce errors. Potential error problems associated with the measurement will be discussed in detail later. The schematic representation of the stop flow system is given in Figure 4.1. The system designed for the present work is a three-part system;

1) a fluid delivery system which consists of a fluid driving system, a mixing chamber, and finally an observation chamber.
2) an optical system which consists of a light source and a light detector (photocell) and an operational amplifier

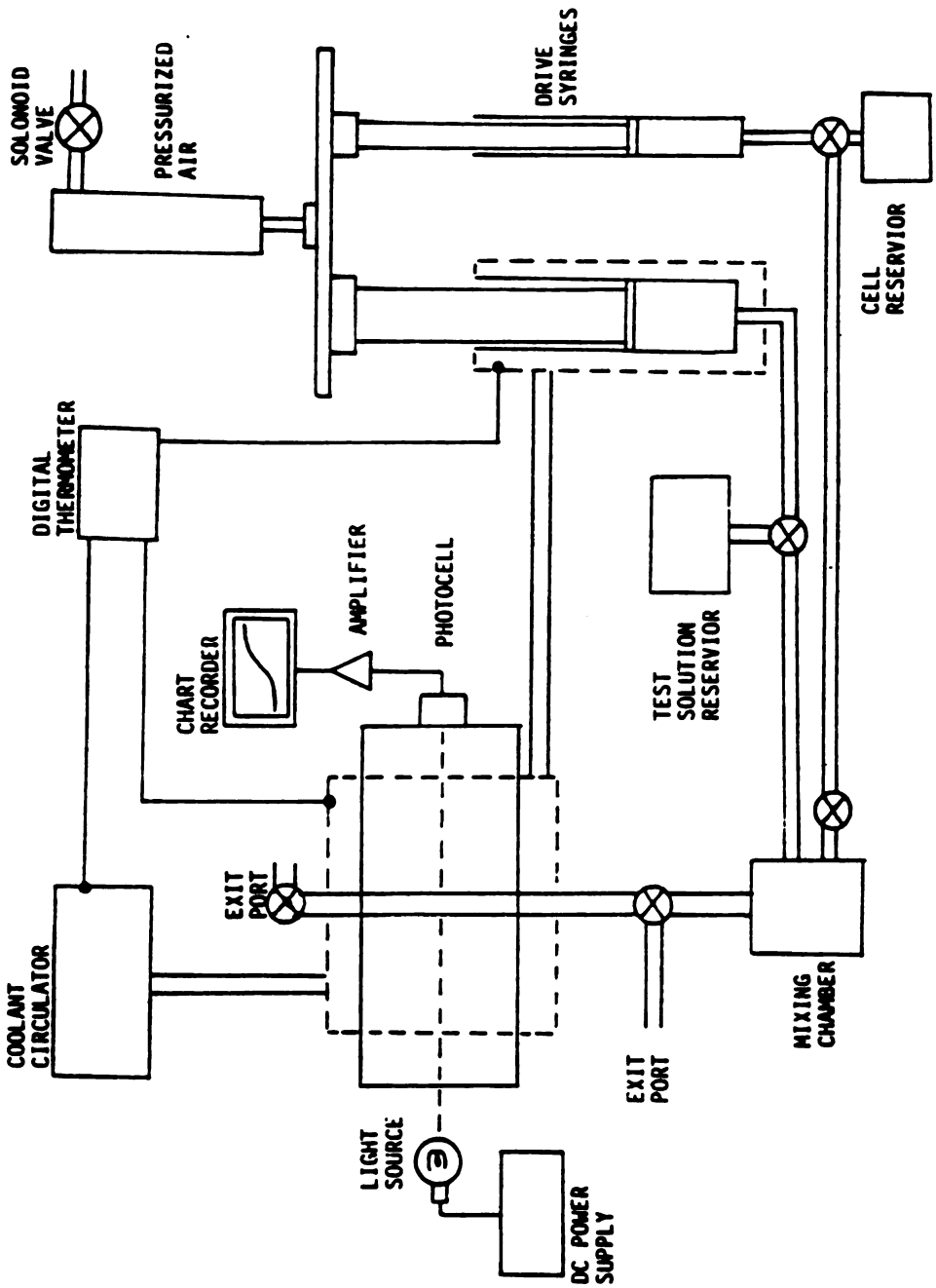

Figure 4.1: Stop Flow Schematic.

circuit.

3) a temperature control system designed to maintain the system at the desired temperatures.

The fluid delivery system delivers the proper ratios of the cell suspension and the desired saline solution to be mixed and delivered into the observation chamber. To insure proper mixing the solutions are passed through a mixing chamber before reaching the observation chamber.

The theory of the operation of the experimental apparatus is described as follows; Intact red cell suspensions scatter and absorb light very effectively which is reflected in the creamy appearance of such a suspension. Once the oxygen-binding protein hemoglobin leaks out of the cell (which for an individual cell is known to be an all or none event, and the cells are so called hemolysed) the cell suspension appears bright red and transmits the light very effectively. Therefore, provided that one can achieve instantaneous mixing of the lytic agent and the red cells without subjecting the cells to a mechanical stress, the transmitted or scattered light intensity once calibrated should provide a measure of the extent of hemoglobin release and consequently the extent of the hemolysis in the population. That is, provided that the light intensity is calibrated as a function of the extent of hemolysis, one can obtain the hemolysis time

history from the light intensity measurements.

At this point we should point out that, as was discussed earlier in chapter 3, the cell responds to a concentration gradient across its membrane osmotically by changing its water content and therefore its volume. In the present work the lytic agent is hypertonic sodium chloride solution, so that when the cell is introduced to such a condition it will lose its water content and subsequently shrink before becoming hemolysed. The reduction in the individual cell volume is concurrent with the reduction of the total cross-sectional area of the light attenuating sites. This at first may seem to result in an increase in the detected light intensity, however, as they shrink the red blood cells become spherical, absorb and scatter the light more effectively than when in the normal state. In fact the amount of the light absorbed by a suspension of cells in the spherical configuration is up to 2.5 times that of the suspension of normal red cells (biconcave shapes). Therefore monitoring the light intensity one observes an initial drop which is a function of the tonicity of the sodium chloride solution. The cell volume effect on the system response will be further discussed in Chapter 5.

B. Major Components

The major components comprising the experimentl apparatus are: the fluid delivery system; the optical system; the mixing system; and the thermal control system. These are described in detail in this section.

1. The Delivery System

The fluid delivery system shown in Figure 4.1 constitutes a major component of the system and consists of:

(i) The reacting solutions reservoir

(ii) Two drive syringes

(iii) A solenoid-activated drive bar connected to the plungers

(iv) The mixing unit

(v) The optical chamber

(vi) Solenoid valves

The drive syringes are connected to the packed red cell reservoir of desired hematocrit level and to the reservoir of reacting sodium chloride solution of known tonicity respectively. The solution reservoirs are housed in a plexiglass block and the syringes are connected to the block through a uni-axial three-way valve.

TOP VIEW

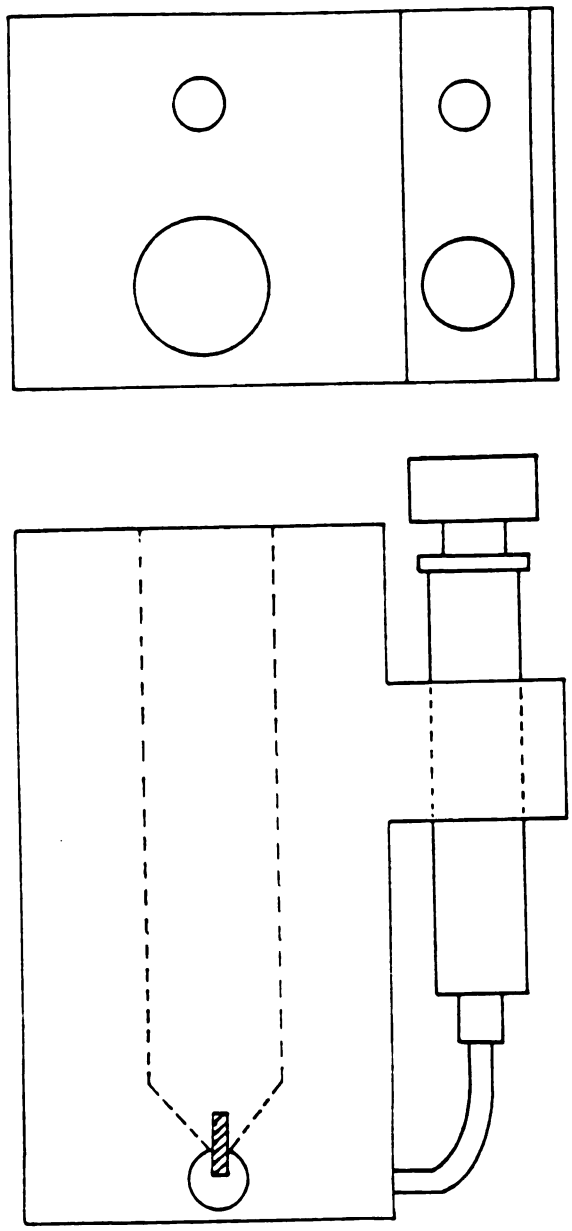

SIDE VIEW

Figure 4.2: Top and Side Views of the Solutions Reservior.

Top and side views of the plexiglass block are presented in Figure 4.2. The drive syringes are 10cc and 1cc Hamilton syringes with Luer tips and the plunger tips are teflon coated to create a biologically-inert environment. The plungers are coupled through a solenoid-activated drive bar which provides equal stroke lengths for both syringes. The subsequent volume ratio of fluid delivered from the two syringes is calculated to be 9.67:1. The drive bar is driven by pressurized air and is usually operated at 30-40 psig which is activated by a solenoid valve. The drive syringes are connected through the three-way valve to a mixing unit with tygon tubing.

The mixing unit is an important part of the stop flow system and plays a significant role in terms of the reproducibility of the data. It is responsible for providing a homogeneous mixture of the test solution and the cells.

The design of the mixing unit is such that it would provide a turbulent flow and therefore effective mixing. A design criteria is that the mixing process must not introduce any mechanical damage or stress to the cells. This criteria in turn dictates the flow characteristics and therefore the driving pressure. To create turbulence and hence enhance the mixing of packed cells and the saline solution, the solutions are introduced into the mixing unit at 90 degrees. The mixing chamber is shown schematically in

Figure 4.3.

The mixed solution after mixing is delivered to the optical chamber which is a vertically held glass column with OD=6mm, and ID=4mm and length of 10cm. The column is held in the vertical position and is made long enough so that the cell sedimentation effects are negligible. That is considering that the red cell sedimentation velocity is on the order of .5cm/hr, it will not effect the measurements with duration periods of 5-10 minutes.

A major source of error concerning the stop flow system is associated with the mechanism of stopping the flow. Once the drive bar is activated it will provide a time dependent force to drive the fluids. The flow velocity may or may not reach a steady value during the delivery period and this may cause significant error in measured hemolysis. This means one needs to use a sophisticated mechanism to stop the flow without creating unwanted transients. In the present system an effective shut-off mechanism is used which insures the instantaneous halt of the mixed fluid in the optical column at zero time with minimal transients. The shut-off mechanism is presented schematically in Figure 4.4.

An on and off trigger is mounted on the drive bar support. The location is chosen such that the drive bar reaches the trigger before it begins the deceleration, assuring a very steady flow at

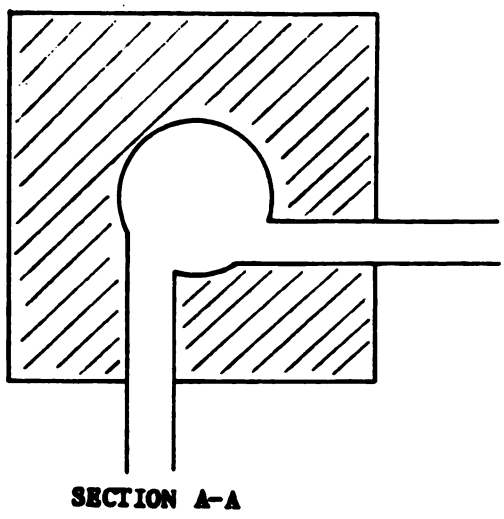

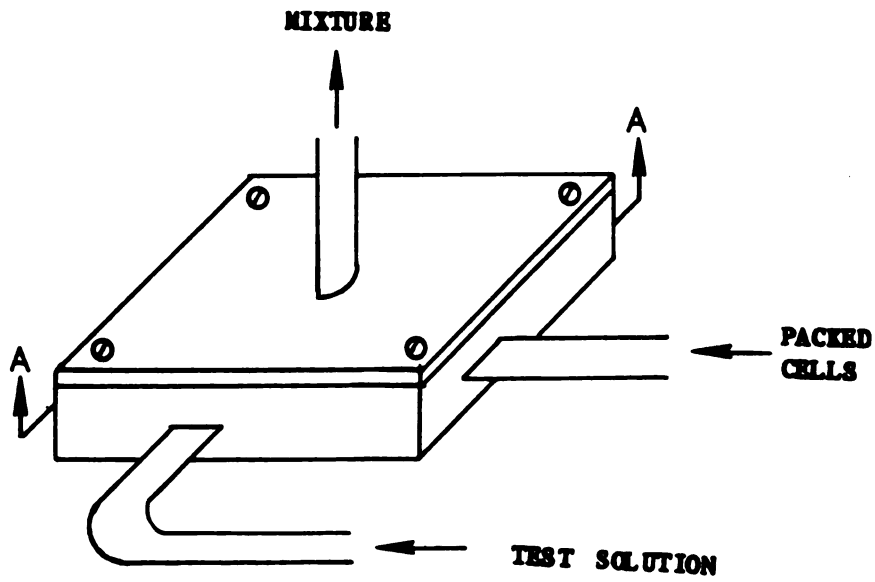

Figure 4.3: Schematic of the Mixing Unit.

the instant of shut-off. The trigger is connected to two solenoid valves positioned at the two ends of the observation column. The two solenoids then shut-off at the same time, thereby bisecting a column of the flow at an instant of time. The mechanism works as folows: The solenoid at the exhaust end of the optical column is a two-port valve while the solenoid at the upstream end, right after the observation chamber, is a three-port valve. The three-way solenoid valve is used to direct the flow from the observation chamber into a collecting beaker which allows the drive bar to come to the resting position without creating a pressure build up due to the trapping the flow in the observation column. Both solenoids are chosen as 12 volt D.C. powered valves to avoid any noise commonly associated with A.C. units.

The synchronized valve shut-off mechanism eliminates problems such as back flow and the pressure build up and the subsequent jet flows associated with other stoppage mechanisms. Besides eliminating the forementioned flow artifacts, it also precisely marks the experimental zero time and enhances the reproducibilty of the delivered mixture ratio.

2. OPTICAL SYSTEM

The optical system is shown in Figure 4.1 and consists of:

(i) The light source

(ii) Voltage regulated D.C. power supply

(iii) Photocell and amplifier circuit

The light source is a 6 volt microscope illuminator tungsten bulb and is powered by a voltage regulated D.C. power supply. To eliminate contact resistance effects associated with ordinary spring loaded electrical contacts, the leads from the power supply are directly soldered to the bulb. A Zeiss universal microscope light housing equipped with a variable diaphragm is used to hold the bulb.

The light is directed through a hole bored in a solid brass cylinder, which is used to hold the observation chamber and also acts as the heat reservoir for the thermal control system. The light after passing through the observation column falls directly incident on the photocell. The photocell voltage output is amplified and is then recorded by a strip chart recorder. The amplified photocell voltage output for the normal saline solution used as a standard is chosen to be 10 volts which is achieved for every experimental run by adjusting the light source intensity level by regulating the power supply voltage. The typical value obtained for the intact cell suspension of about 4% hematocrit at isotonic condition is about 65mv and the output voltage for a totally hemolysed cell suspension is about 5 volts. This means

that for early times the error associated with the drift of the incident intensity from the nominal value is very small (less than .5%). The overall photocell output drift is less than 5% over the period of 2 hours. Considering the 5-10 minutes duration period for each experimental run the photocell output drift is less than 1%. In fact because of the logarithmic behavoir of the photocell response and the normalization procedure the error at later times due to the light intensity drift is also very small.

3. MIXING SYSTEM

The mixing system shown in Figure 4.3 plays a very important role concerning the overall performance of the stop flow system. The mixing chamber is made from clear plexiglass and the test solution inlet is at 90 degrees with respect to the packed cell solution inlet. The flow rate through the mixing unit and therefore the extent of the turbulence created in the unit is a direct function of the driving pressure. This implies that the higher the flow rate, the more effective is the mixing. However, the process of determining the optimal operating flow rate is not so simple. This is due to the compliance of the tygon tubings and the drive mechanism in general and the damaging effect of shear stress on the cells caused by such a turbulent mixing in particular. The shear stresses introduced in the mixing process

could result in an over estimation of the actual damage due to the reacting agent. This matter is discussed in Chapter VI.

4. THERMAL SYSTEM

To obtain the hemolysis kinetics at temperatures different than room temperature, the stop flow system is equipped with a thermal system which consists of:

(i) A heat exchanger unit associated with the test solution
(ii) A heat exchanger unit associated with the observation chamber
(iii) Temperature sensors and coolant circulator

To quantify and account for the effect of the low temperatures on the kinetics of red blood cell hemolysis the intention of this research has been to compare the room temperature responses to those at the subzero temperature experienced by a cell in a cryopreservation process. However, to avoid ice formation in the present experimental system the extent to which the temperature of the system could be lowered is

limited. The lowest temperature which could be achieved without freezing the sample is about -10 degrees centigrade at a sodium concentration of 4m.

Another important factor concerning the design of the thermal control system was that the blood cells should be kept at ambient temperature until they are subject to mixing with the lytic agent. Therefore the syringe and the reservoir containing the packed cells are not included in the temperature control design of the system and are kept at room temperature. The effective mixing ratio for the stop flow system is about 10:1, hence the error introduced due to the temperature discrepancy of the mixing fluids is very small (1 C for about 20 seconds for the lowest temperature considered here). The zero time temperature of the mixture was recorded to be up to 25% higher than the desired temperature, however, the temperature reaches the desired value within 2-4 seconds depending on the final temperature desired.

To cool the test solution a heat exchanger unit was constructed around the syringe containing the test solution. The lines connecting the test solution to the mixing chamber are well insulated to keep all parts of the system with the exception of parts containing packed cells at the desired temperature. To assure that the observation chamber remains at constant temperature throughout the experiment and the fluid delivered to

the column could reach the desired temperature in a short time, the observation column is located inside a solid brass housing.

The brass housing is cooled by passing coolant through copper tubes located on either side of the glass column. This provides a heat reservoir with very large thermal mass and hence a very stable and uniform temperature distribution across the observation chamber. The two heat exchanger units are coupled and the cooling is provided by a coolant circulator.

The temperature of the components of the system are measured by two thermocouples. A thermocouple is located in the observation chamber close to observation site and another is placed at the test syringe wall. The coolant flows through the system for at least 2 hours before each experiment where the temperature of the coolant circulator is adjusted to reach the desired temperature.

CHAPTER V

OPERATIONAL CHARACTERISTICS AND CALIBRATION OF THE STOP-FLOW SYSTEM

The experimental aspect of the present research concerned the design and development of an improved stop-flow system with the potential for measuring destruction dynamics of the red blood cell. The system theory of operation and major components comprising the experimental aparatus were discussed in chapter 4. This chapter is concerned with the operational characteristics and calibration of the experimental system.

First, the general characteristics of the stop-flow system such as the transient response and cell volume effects on the system output will be discussed. Second, the calibration procedures are discussed and the results are presented. Finally, the effect of cell number density on the calibration protocol and measured kinetic data will be discussed.

A. General Characteristics

The experimental aspect of the present work involved the

design and development of a system capable of introducing desired step changes in the concentration of the extracellular medium at controlled temperatures in the range of -10°C to room temperature (about 23°C). Although the original design of the experimental system was straightforward, obtaining quality data proved to be very difficult. Many modifications and refinements of the initial design were required to realize a system with the desired characteristics, such as complete mixing and negligible flow effects, essential for the integrity of the present effort. The problems were effectively dealt with and corrections were made which are discussed in chapter 6. Here we will discuss the general characteristics and response of the refined version of the system used to obtain the reported hemolysis kinetics data.

The system behavior operated at room temperature differed somewhat from that at lower temperatures. The major difference was that it required an initial period of one hour for the system components to reach the isothermal condition at the desired sub-atmospheric temperatures. The compressed-air pressure required to drive the plunger was about 20 psi at -5°C compared to 40 psi required when operated at room temperature. This is due to the difference in the coefficient of thermal expansion of glass and aluminum. The glass syringe expands more than the aluminum plunger, creating smoother and a less tight fit. The warmup time required for the light source and the photocell and operational

amplifier circuit to reach steady state was about 15 minutes. However, the system was allowed one hour to warmup.

The mixing ratio of the blood and test solution delivered to the observation chamber is pressure dependent and the highest blood/test solution ratio was obtained at 30 psi at room temperature. The small syringe (containing the packed cell solution) and the large syringe (containing the test solution) had .455 cm and 1.415 cm radii respectively. Therefore, the theoretical ratio of the test solution volume with respect to packed cell solution volume $(R/r)^2$ is calculated to be 9.67:1. Nevertheless the actual mixture ratio delivered to the observation column was measured to be somewhat less than this. For example for a packed cell solution of 55% hematocrit the delivered hematocrit was 4% at room temperature. The pressure dependence of the delivered hematocrit is presented in Figure 5.1. It should be noted here that the normalized hemolysis kinetic measurements were insensitive to the mixture ratio, i.e. the delivered hematocrit. The percent hemolysis data are obtained at 4% nominal hematocrit and the corresponding photocell is measured to be about 65 mv at isotonic condition.

The light intensity was adjusted to 10 volts for the observation column containing the sodium chloride osmolality equal to that of the test solution before each run. The system output

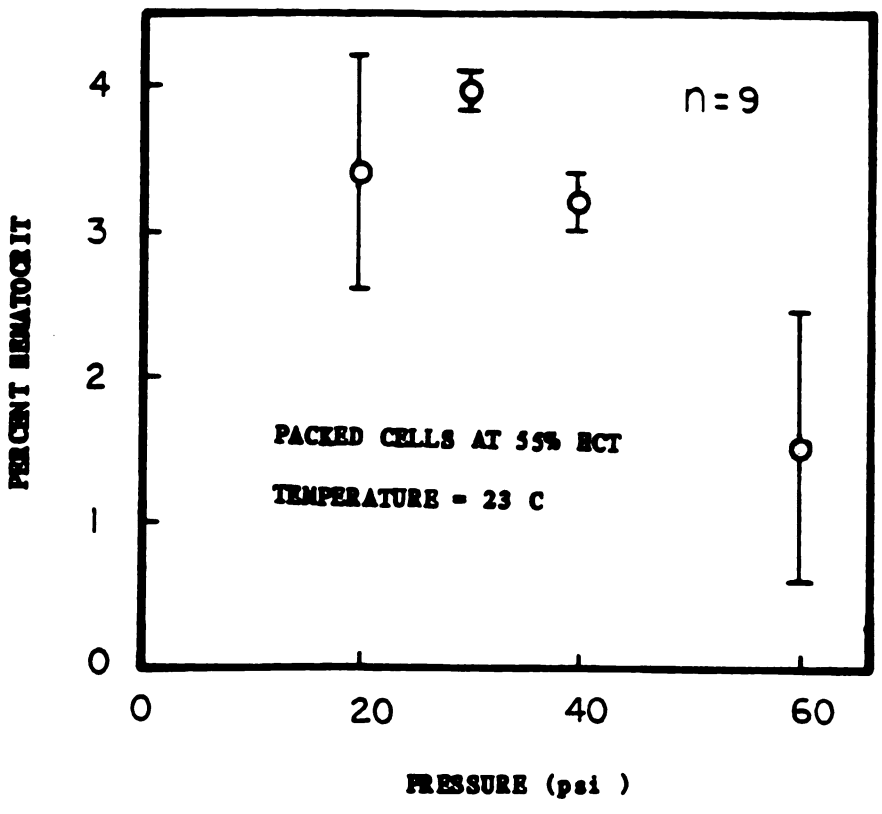

Figure 5.1: Percent Hematocrit Delivered to the Observation Chamber as a Function of Plunger Pressure.

voltages normalized with respect to the isotonic saline solution output for different levels of sodium chloride concentration is plotted in Figure 5.2. The data indicates that the measurements are quite independent of the salt concentration in the observation chamber.

The normalized photocell output behaves very linearly with respect to normalized lamp voltage independent of whether the observation chamber is filled with cells or normal saline solutions. The data is shown in Figure 5.3 which indicates, although the magnitudes of the photocell output are different for the two cases, the normalized voltages are quite the same. This implies that the systems response is independent of the content of the observation column.

1. Initial Transient of Output Signal

The stop-flow system transient response is related directly through the calibration curve to the hemolysis of the blood cell suspension in the observation chamber. In order to relate the photocell voltage output to percent hemolysis the data is normalized with respect to the initial or zero-time response of the system for a given experimental conditions. Specifically the zero-time response corresponds to the condition of 0% hemolysis and the minimum volume state. That is the initial response of

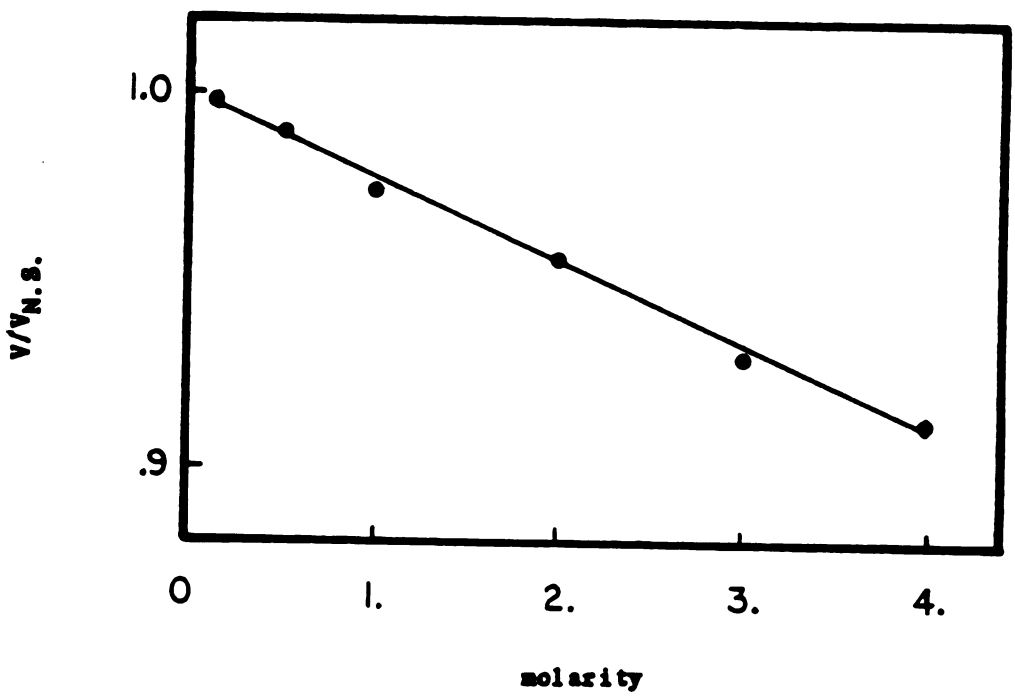

Figure 5.2: Normalized Photocell Voltage as a Function of NaCl Molarity in Absence of Blood ($V_{N.S.}$ = 10.0 V).

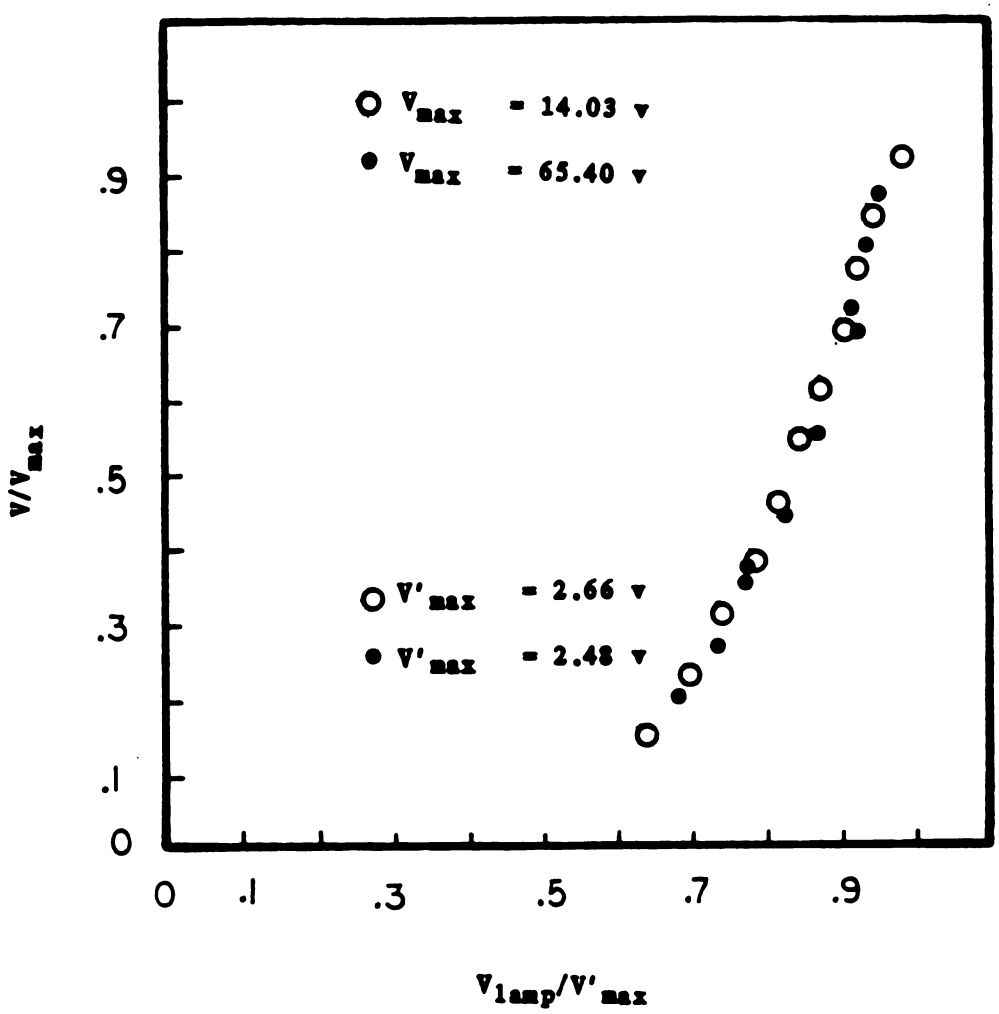

Figure 5.3: Normalized Photocell Output as a Function of Normalized Lamp Voltage for Optical Chamber Filled with, Normal Saline and Blood at 4% Hematocrit .

such a system is a very important factor in concern with the reliability of the normalized data. There exists an unexpected initial transient response associated with every measurement.

The voltage output systematically behaves as shown in Figure 5.4, i.e. the zero-time response is a few percent different from the ideal case. This behavior is likely due to the orientation of the red cells in the direction of the flow as suggested by the results of the following experiments. The initial transient period is associated with some type of flow relaxation. The average relaxation time for 10:1 mixing is measured to be 6.52 seconds on the average, where normal saline solution is mixed with packed cells with resultant hematocrit at 4%. The following experiments were conducted to explain the characteristics of the relaxation period. In order to eliminate other possible sources of problems which might contribute to the observed behavior such as improper mixing, the syringe containing the packed cells is replaced by a syringe identical to the one used for the test solution thereby producing a 1:1 mixing ratio.

i) 16% hematocrit blood is mixed with an equal volume of normal saline solution and the average time required for the photocell output to reach the steady state value is measured to be 7.40 seconds.

ii) 8% hematocrit blood is mixed with equal volume of the

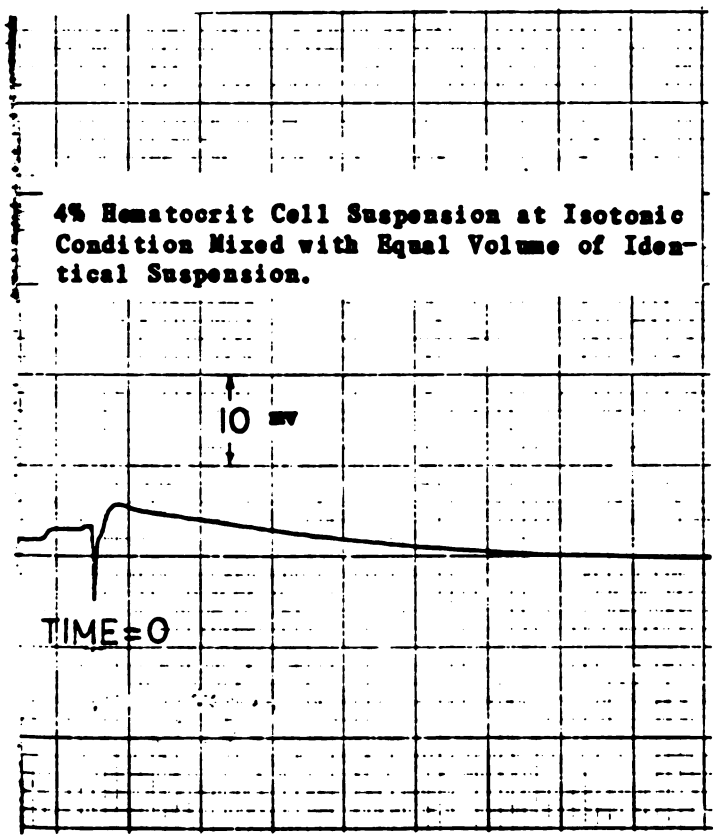

Figure 5.4: The Initial Transient, Effect of Cell Orientation.

identical suspension and the average relaxation time is measured to be 6.33 seconds.

iii) 16% hematocrit blood is mixed with equal volume of 2m saline solution and the average time required for the photocell output to reach the minimum value is measured to be 3.65 seconds.

The results of the above experiments clearly indicate that for the cells suspended in normal saline solution the relaxation time is longer than when suspended in 1m saline solution. The following argument is given in an attempt to explain the observed results above. The cells introduced into the 1 molal saline solution almost instantaneously (in 250msec) reach the minimum volume state and assume spherical geometry hence there is no preferential orientation and consequently a relatively short relaxation period. Where cells suspended in isotonic sodium chloride solution have normal biconcave geometry and therefore could be preferentially oriented and subsequently have a longer relaxation period. Although the initial transients, could not be completely accounted for on the basis of the foregiven argument as there are other possibilities such as incomplete mixing. However, based on the relaxation times obtained for different conditions the major contributing factor is due to the orientation of the cells in the direction of the flow.

2. The Cell Volume Effect-Minimum Volume State

When cells are exposed to tonicity levels of salt different than the physiological isotonic level they experience osmotic stress. The tolerence level of cells to such osmotic stress depends on the amount of stress and the exposure time. Once the tolerable level of perturbation is exceeded the cells are damaged. The cell osmotic characteristics allow transport across the membrane and therefore a volume change preceeds the cell damage. In the case of hypertonic exposure of the red blood cell, a minimum volume state is reached before hemolysis.

When the equilibrium of the cell system is perturbed by imposing a concentration gradient across the membrane, the difference in the chemical potential of water across the cell acts as a driving force for the flow of water across the membrane. The induced flux of water will persist until the cell system reaches a state of osmotic equilibrium with the environment. In this research we are concerned with exposure of the human red blood cells to hypertonic conditions, consequently the induced driving force results in an outward water transport across the plasma membrane. The loss of cell water content results in a decrease of the cell volume referred to as the shrinkage of the cell. The cell shrinkage, when exposed to exceedingly increasing hypertonic

sodium chloride solution; continues up to a concentration of .8 molal. Increasing the salt concentration beyond .8 does not result in further shrinkage and the so called the Minimum Volume State (MVS) is reached. The minimum volume state proceeds the hemolysis under such conditions.

The water transport across the plasma membrane is a very rapid process, and consequently the characteristic time associated with it is very small (~250 msec) compared to hemolysis kinetic characteristic times (~ seconds to minutes) [114,137-139]. That is, relative to the time frame of this work the minimum volume state is realized instantaneously. It should be pointed out here that, the argument given above only holds for a single cell and the cell population seems to reach the minimum volume state in a finite time.

Inferred from the time required for the photocell output voltage to reach its minimum value, the time required for a given cell population to reach the MVS depends on the level of perturbation and ranges between about 1 sec for 4 molal and about 7 seconds for 1 molal salt concentration. The photocell output at MVS is used for normalization of the hemolysis data. To quantify the MVS and therefore obtain the corresponding photocell output, the following experiments were designed and carried out.

Cell suspension of 55% hematocrit was prepared following the standard procedure outlined in chapter 6. The suspension was the exposed to different concentrations of sodium chloride ranging from .075m to 2.5m. The experiments were carried out at room temperature and the usual procedure was followed to obtain the stripchart traces of the photocell output. The photocell output traces were examined and minimum photocell responses corresponding to the quasi-steady state values were tabulated as a function of the extracellular salt solution molality (Table 5.1). The photocell voltage for a cell concentration of 4% hematocrit and known sodium chloride concentrations normalized with respect to the photocell voltage corresponding to 4% hematocrit in normal saline are plotted as a function of the osmolality of the extracellular solution in Figure 5.5.

From Figure 5.5 the minimum volume is achieved for hypertonic Nacl concentration of greater than or equal to about .6m (between 0.5-1.0m). These results verify the earlier finding that the human red cells subject to hypertonic osmotic shock undergo a dramatic volume reduction of about 60% before lysing [114]. These results also suggest that the initial photocell output for Nacl solutions of concentration greater than .6m should be the same for a given cell concentration. The results shown in Figure 5.5 are in excellent agreement with the results obtained by Farrant et al [114] concerning the cell volume estimation based on the amount of

TABLE 5.1

Normalized Photocell Voltage at 4% Hematocrit
as a Function of Nail Molality

Molality	MVS Voltage (v)	$V_{MVS}/V_{N.S.}$
.075	134.53 ± 23.76	1.99 ± .35
.150	67.50	1
.250	42.05 ± 3.17	.62 ± .05
.500	33.12 ± 2.77	.49 ± .04
1.000	29.30 ± 2.23	.43 ± .03
1.500	29.16 ± 2.16	.43 ± .03
2.000	28.55 ± 2.30	.42 ± .03
2.500	28.89 ± 2.25	.43 ± .03

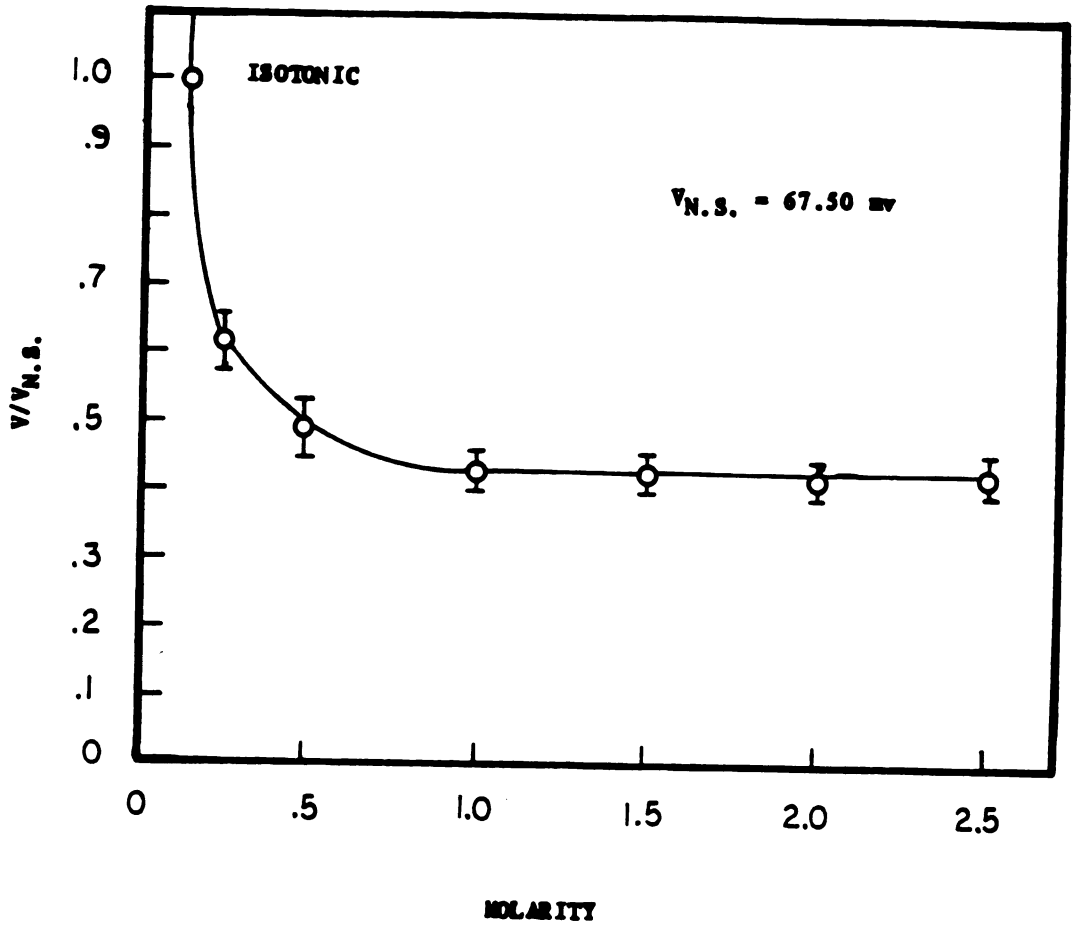

Figure 5.5: Normalized Photocell Voltage as a Function of NaCl molarity (at 4% Hematocrit).

cell water loss due to increased osmolality of the extracellular solution.

B. Calibration of the System

The goal of the present work is to obtain dynamic cell responses due to hypertonic perturbation in the form of hemolysis percent history for the development of a thermodynamic model for the cell destruction. To transfer the kinetic data from the photocell voltage history protocol to the desired form of percent hemolysis as a function of exposure time, calibration of the system is required. That is, a calibration curve is needed to interpret the photocell output voltage in terms of percent induced hemolysis due to a known step changes in the extracellular concentration of Nacl. The rational for the interpretation of the photocell voltage history is as follows.

The incident light is partially absorbed and patially scattered by the red blood cell suspension in the observation column. In fact cells are very effective sites for light attenuation in both the scattering and absorption modes. When cells are perturbed they go through shape changes and if the perturbation level is in excess of that which the cell can sustain it will lyse and lose its hemoglobin content. The damaged cells

become less opaque and more transparent. As the cells in the observation chamber are hemolysed the amount of light that reaches the photocell increases which is directly reflected in an increase in the system voltage output. The increase in the amount of light transmitted can then be recorded and interpreted to infer the time course of the red cell hemolysis kinetics.

To obtain data at a given hematocrit level free of possible errors associated with difference in the initial respose due to discrepancy in the delivered mixing ratio from run to run, we need to monitor the mixing ratio. To infer the percent hematocrit delivered to the observation column and therefore monitor the mixing ratio a calibration protocol in the form of photocell output as a function of percent hematocrit is needed.

1. Calibration of Percent Hemolysis as a Function of Normalized Photocell Voltage

To quantify the photocell output as a function of the percentage of cells lysed, the following procedure was employed. A cell suspension of desired percent hematocrit was prepared following the usual procedure explained for cell handling in chapter 6. A portion of the cell suspension was totally hemolyzed by rapid freezing via submersion in liquid nitrogen and then

thawed by warming under running tab water at 30-40°C. This step was repeated once and then the suspension was checked by the standard clinical cyanmethemoglobin spectrophotometric technique, and 100% hemolysis was verified. The remaining portion of the suspension was also checked by spectrophotometer and was verified to be 100% intact. The optical chamber was filled with isotonic sodium chloride solution and the light intensity level was adjusted for 10v photocell output. The output was verified to be stable for at least 30 minutes. Different levels of hemolysis was then obtained by mixing proper portions of totally hemolyzed and intact suspensions. These suspensions at different known hemolysis levels were then manually injected into the optical chamber and the resulting photocell output were recorded as stripchart traces. A steady state was always reached within 5 seconds. The order of delivered percent hemolysis was always in the same direction, i.e., either increasing or decreasing, and the system was rinsed with normal saline between each run at least twice and the 10v photocell output was verified. The order of the experiment was then reversed,i.e. if for example the percent hemolysis delivered to the chamber was at first from high to low percent of hemolysis, in the second run using the same batch the order was switched and the mixtures were delivered in increasing order of percent hemolysis. An excellent correspondence was observed between two sums.

In order to eliminate uncontrollable parameters involved, such as donor's age or sex and variation in preparation routine, the calibration experiment was repeated many times (22) with different batches of cells over a period of 6 months. The calibration protocols were obtained at 4% and 8% hematocrit and the data are tabulated along with the associated standard deviations in Table 5.2. The photocell voltages normalized with respect to the 0% hemolysis output are plotted versus 1-%H/100 and are presented in Figure 5.6. The least square fit of the data yields

$$V_{test}/V_{0\%H} = 1.014(1-\%H/100)^{**}(-1.42)$$

with

$$r^2 = .9997$$

The %H calibration curve is not a function of temperature and the experiment performed at -5°C produced values within 4% of the ones tabulated in Table 5.2.

The photocell output as discussed earlier is very sensitive to the cell density. The cell density level (% hematocrit) effect is of concern as the %HCT delivered to the observation chamber is a function of several parameters such as driving pressure and packed cell density. This at first may seem to be a source of error, however, the calibration curve at 8% hematocrit was

TABLE 5.2

Calibration of Percent Hemolysis as a Function of Normalized Photocell Voltage

%Hemolysis	Voltage V_{test} (v)	V_{MVS}/V_{NS}	No. of Points
00	64.530	1	18
05	68.015 ± 1.100	1.054 ± .017	12
10	75.455 ± 2.841	1.169 ± .044	18
15	79.784 ± 2.071	1.236 ± .032	12
20	89.813 ± 3.156	1.392 ± .049	18
30	109.772 ± 3.117	1.701 ± .048	18
40	136.733 ± 5.692	2.119 ± .088	18
50	179.935 ± 5.466	2.788 ± .085	20
60	248.188 ± 8.841	3.845 ± .137	18
70	365.388 ± 20.275	5.662 ± .314	17
80	645.481 ± 49.172	10.662 ± .762	13
90	1420.964 ± 165.351	22.020 ± 2.562	16

practically identical with the one obtained at 4% hematocrit. This notion is further supported by the excellent agreement of results obtained here with the calibration protocol reported by Papanek using a completely different experimental set up at 10% hematocrit [137]. This implies that the calibration protocol reported here is a universal one, independent of the system parameters, and that the kinetic data will not be affected by a few percent deviation of the delivered hematocrit from the nominal level of 4%.

The calibration protocol presented in Figure 5.6 is obtained for the unhemolyzed portion of the suspension at isotonic conditions. However, the unhemolyzed cells in a hypertonic condition are at MVS. To account for any differences which may influence the interpretation of the raw data, the following experiment is carried out.

To arrive at calibration protocol at MVS, the cell suspension at 4% hematocrit is adjusted to .6m sodium chloride concentration. This concentration level assures the MVS without introducing measurable, if any, amount of hemolysis for the duration of the experiment. A portion of the cell suspension is totally hemolyzed following the freeze thaw cycle as before. The intact portion was kept isotonic and the Nacl concentration was elevated at .6m right before the injection into the observation chamber. Following the

procedure discussed earlier, a new set of data was obtained. The comparison of the data is made through Figure 5.6, which shows an excellent correspondence.

In summary the calibration has been shown to be independent of hematocrit (over the range 3 to 10%); independent of temperature (over the ranege -5 to 25 °C) and independent of extracellular osmolality (over the range 0.15 to 0.6m). Thus the calibration curve is applied to experiments 1.0 to 4.0m over a temperature range of -10 to 25°C.

2. Calibration of Percent Hematocrit as a Function of Photocell Voltage

The system nominal mixing ratio of 10:1 is not exactly reproduced for every experiment. If the cell density present in the light path in the observation chamber is altered, a different amount of light will reach the photocell and the systems output will be altered. That is the absolute magnitudes of the photocell output for identical experimental runs could be different due to the difference in delivered percent hematocrit. In order to monitor the percent hematocrit delivered to the observation chamber we need to calibrate the photocell output with respect to the percent hematocrit. It should be pointed out here that this

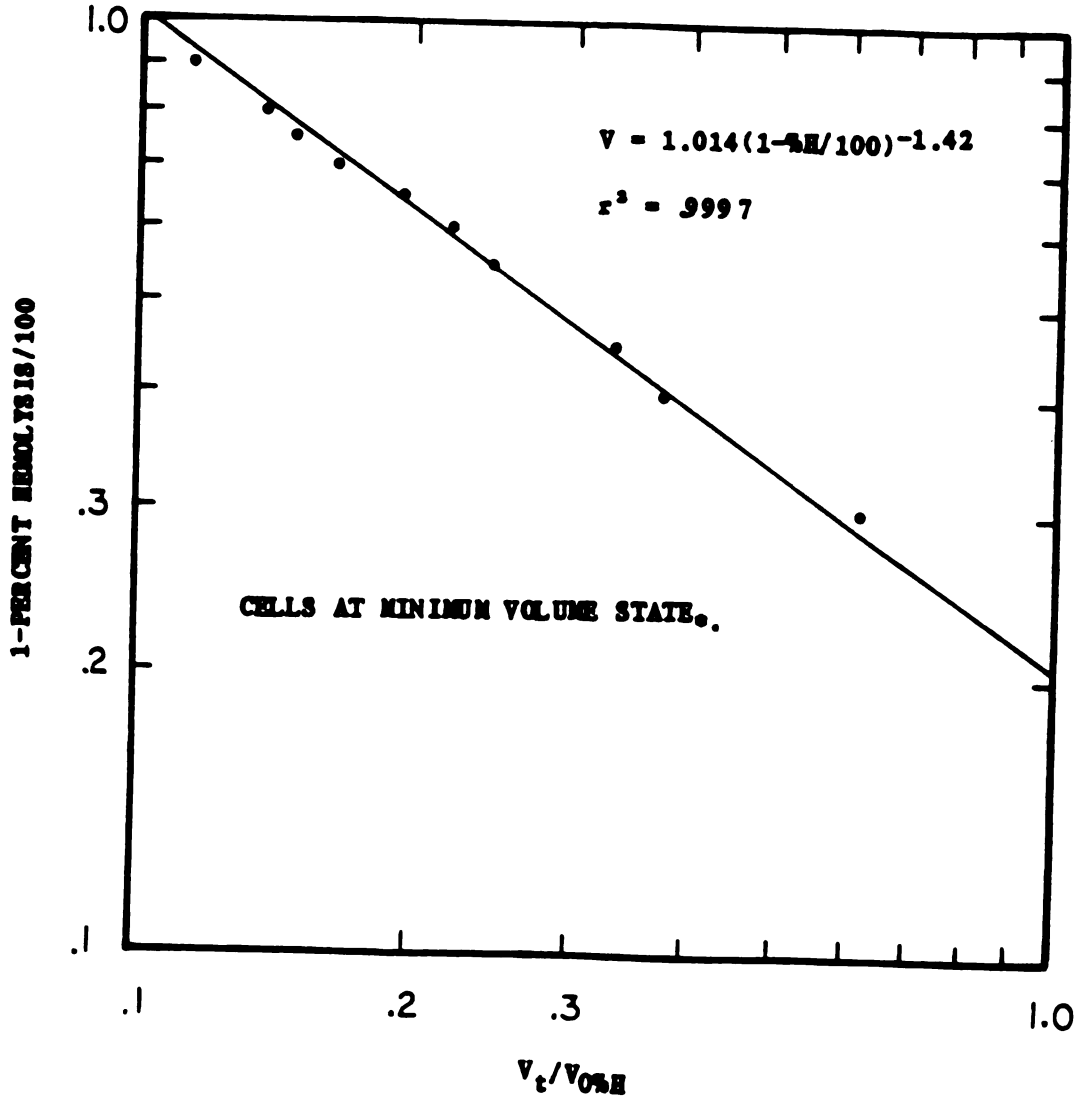

Figure 5.6: Calibration Curve for the Determination of Percent Hemolysis as a Function of Normalized Photocell Voltage.
***The Line Corresponds to the Least Square Fit of Data Obtained for Cells at Isotonic Condition.**

is only a precautionary measure and a few percent variation in the delivered percent hematocrit to the observation chamber is not expected to alter the results. This was accomplished as follows.

A cell suspension of relatively high volume fraction of cells of about 80% was prepared as explained earlier. Proper portions of the packed cell and the isotonic sodium chloride were mixed to obtain desired levels of %HCT. The mixtures were then manually injected into the observation chamber and the voltage output of the system at different cell density levels were recorded. The results are tabulated in Table 5.3 and the normalized photocell voltage with respect to the 10 volts reference for normal saline is plotted as a function of %HCT in Figure 5.7. The range of presented data is 1%-8% HCT as the nominal desired cell number density delivered to the optical chamber was typically 4% for this work. The least square fit of the data yields

$$V = 475.171(\%HCT)^{**}(-1.452)$$

with

$$r^2 = .9995$$

There exists an excellent agreement between the results presented in Figure 5.7 and results obtained by Papanek [137]. The data for the range of 3-10% HCT are in agreement to within 4%.

TABLE 5.3

Calibration of Photocell Voltage as a Function of %HCT

%HCT	V_{Ave} (MV) ± St. Dev.	No. of Pts.
1	459.33 ± 3.49	3
2	178.47 ± 5.51	9
3	98.42 ± 3.98	9
4	64.74 ± 1.84	8
5	45.85 ± 1.88	8
6	35.51 ± 1.48	8
7	27.36 ± 1.77	8
8	22.89 ± 1.75	9
9	19.35 ± 2.23	4
10	16.82 ± 2.10	4

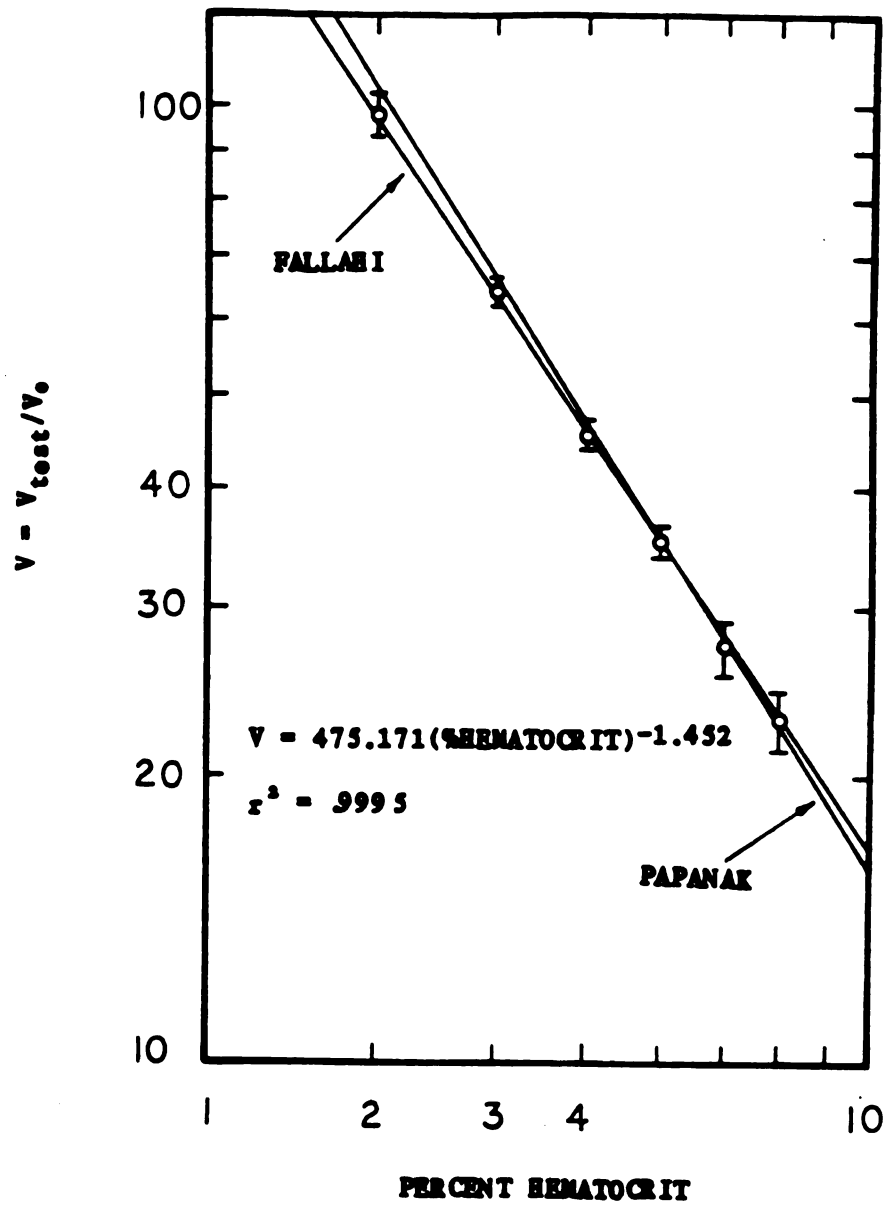

Figure 5.7: Normalized Photocell Voltage as a Function of Hematocrit.

The excellent correspondence of the data obtained independently by two observers using systems with different characteristics suggest the universality of the normalized %HCT calibration protocol.

CHAPTER VI

EXPERIMENTAL PROCEDURE FOR DETERMINING HEMOLYSIS KINETICS

A. Cell Handling and Sample Preparation

Fresh blood collected the same day was obtained courtesy of the Lansing American Red Cross in EDTA tubes. The blood is stored at 4 degrees centigrade until the time of use. Blood not used within 48 hours of collection was not used to obtain hemolysis kinetic data. Blood older than 2 days was used for percent hemolysis calibration protocol and for some control experiments. The blood was first centrifuged at 1104g, while in the EDTA tubes, for 3 minutes and the supernatant fluid was aspirated after the cells had settled. The packed blood was then transferred into larger disposable plastic test tubes and diluted three fold by the addition of normal saline after allowing 30 minutes for the cells to warm up to room temperature. The test tubes were sealed by paraffin paper and gently shaken several times to assure complete suspension of the packed blood. The sample was then centrifuged as before for 5 minutes and the supernatant fluid was aspirated. This procedure (so called "washing") was repeated once more and

the cell count (hematocrit) obtained was measured to be about 80 percent on the average. The hematocrit of the sample is measured through standard clinical procedure. The packed cells were then diluted by the addition of the proper amount of normal saline to obtain a washed cell suspension of 55 percent hematocrit. The choice of 55% is due to the fact that the nominal 4% hematocrit is obtained when a packed cell solution at 55% hematocrit is mixed with the test solution through the stop flow system. The percent hematocrit of the sample was measured after dilution and the deviation from the nominal value of 55% was about 5%. This introduces 0.6% uncertainty in the nominal hematocrit of the mixed suspension delivered to the observation chamber. This compared to the uncertainties of hematocrit associated with the fluid delivery mechanism is extremely small. Washed cells if not used within 4 hours were discarded.

To prepare a totally hemolysed blood suspension, used to obtain a percent hemolysis calibration protocol, blood was washed and prepared as above. The sample was then immersed in liquid nitrogen for 30 minutes to assure deep freezing of the entire blood sample. The sample was then thawed by placing it under running tap water at 30–40 degrees centigrade. This procedure of freeze-thawing was repeated once and total hemolysis of the prepared sample was verified using the spectronic 20 before use.

B. Procedure for the Determination of the Hemolysis Due to Isothermal Hypertonic Step Change of the Extracellular Concentration at Different Temperatures

The experimental procedure for determining hemolysis kinetics of human red blood cells at a given temperature due to different hypertonic concentrations of extracellular electrolyte (sodium chloride) solution will be discussed here.

1. Hemolysis Kinetics at Room Temperature

The voltage supply to the solenoid valves, light source, and the photocell circuit were turned on and the electronics were allowed to warm up for 30 minutes. The drive system and the triggering mechanism were checked and the pressure of the supplied air was adjusted for smmoth drive of the plungers. After flushing the system with normal saline, the observation column was filled with the desired hypertonic sodium chloride solution. The strip chart recorder was turned on and the proper voltage scale was set. The power supplied to the light source was adjusted such that the voltage output was 10 volts with isotonic saline in observation

chamber. This voltage level was verified to be stable to within 2% for at least 30 minutes. The packed blood cell and test solution reserviors were filled with the blood sample prepared at 55% hematocrit and the hypertonic sodium chloride solution of interest respectively. The stop flow system was then primed following the procedure explained in chapter 5, by several injections. The drive mechanism was checked once again for optimum mixing.

Once the system was verified to be operating properly the drive mechanism was triggered and the photocell voltage output was recorded for about 5 minutes. In the meantime while the optical chamber remained undisturbed and isolated from the rest of the system, the drive syringes were reloaded for the next run. Normally 5 to 6 runs for the same conditions were performed to assure reproducibility. Upon completion of datd collecting for a given level of hypertonic saline solution, the reservior and the syringe containing the test solution were emptied and rinsed with the saline solution to be filled next. After flushing the entire system with the hypertonic solution at a concentration different from the previous experiment, the photocell output was adjusted to 10 volts for the new test solution. Following a procedure identical to that mentioned above a new set of strip chart traces corresponding to the sample behavior at the new saline concentration was obtained.

The hypertonic electrolyte concentration was increased by 0.5m each time and the range of concentration from 2m to 4m was covered. The rational for the chosen concentration range is as follows. Although the red cell becomes spherical and reaches minimum volume state, and therfore experiences damaging stress, when exposed to saline concentration as low as .8m, the kinetics at concentrations less than about 1.5m are extremely slow and undetectable on the time scale of the present work. Concerning the upper limit of the concentration range, the maximum attainable sodium chloride concentration is 5.2m. Furthermore at 4m concentration the kinetics are very fast where about 90% hemolysis is induced in the course of the experiment (about 5 minutes).

2. Hemolysis Kinetics at Sub-ambient Temperatures

When hemolysis kinetics at temperatures other than the ambient temperature are desired the experimental procedure for most parts is the same as that explained above. Hence we will only point out the differences between the two cases here. It should be noted that the packed cells are maintained at ambient temperature for the entire course of the experiment and are only exposed to low temperatures beginning at the instant of mixing. Before the electronics are turned on the thermal system consisting of two coupled heat exchangers is hooked up to the coolant

circulator. The coolant flow rate is set at a pre-established level and temperatures at several locations including the observation chamber are monitored. The system is allowed 2 hours to reach the desired equilibrium temperature and then the electronics are turned on.

After each run the syringes are reloaded as before, however at this point the test solution is at a temperature higher than the desired temperature. Hence, the test solution is allowed 15 minutes to reach the desired temperature before another run is attempted.

Once the data are collected for a given temperature at a given concentration , the saline concentration was increased by .5m (procedure explained earlier) while the temperature was kept the same. When all the concentration range was covered the temperature was changed to a new value by appropriately changing the coolant temperature and flow rate if necessary. At this point the system was allowed 1 hour to reach the new temperature before further experiments are carried out. Thermal equilibrium was verified by monitoring temperatures of the test solution and observation chamber.

The temperatures considered for this work were -5,0,5,10, and 25 degrees centigrade. The rational for the chosen temperatures

is as follows. The hemolysis kinetics are found to be quite insensitive to an absolute temperature drop between 25 and 10 degrees centigrade. This behavior has also been observed with respect to hypertonic cryohemolysis [20-22]. The lower limit of the temperature range is due to the fact that the saline solution at 2m concentration would begin to freeze at about -7 degrees centigrade.

The raw data recorded by the strip chart recorder were in the form of photocell voltage traces. The procedure for normalizing and converting the photocell voltages so that the hemolysis kinetics were obtained will be discussed in chapter 7.

C. Control Experiments

The system was proven to be quite insensitive to uncertainities associated with the delivered mixture ratio and the light source intensity. However for purposes of reproducibility several control experiments were performed to assure consistant behavior of the system at different conditions.

The reference photocell voltage with no cells in the observation chamber was always set at 10 volts for each sodium chloride concentration level. This was accomplished through

adjusting the voltage supplied to the light source. This reference voltage value must be stable for the duration of each experimental run of about 10 minutes. However, since the reference voltage was not monitored during a 2 to 3 hour course of the entire experiment, the signal must remain stable for at least 3 hours. With the system warmed up, a drift of less than 2% was observed for a period of 4 hours. Considering the fact that the normalized voltages are very insensitive to the reference voltage, the electronics proved to be quite stable. The stability of the photocell signal checked at different temperatures revealed similar results.

The stability of the photocell voltage output was also checked for the observation chamber filled with cells at isotonic condition as well as 100% hemolysed suspensions. The photocell output remained constant to within 2% for periods of 10 minutes. At periods exceeding 20 minutes sedimentation causes the photocell output to drop slightly and for longer periods of time the sedimentation effect is reflected in an increase in the output voltage. Considering the 5 minute duration of each experimental run the photocell voltage was considered to be free of artifact, either due to cell sedimentation or changes in the photocell voltage.

The reproducibility of the delivery system was checked by

mixing the packed cells with isotonic saline. The delivered percent hematocrit at nominal operating condition was within .15% of the nominal value of 4%. This was verified at different temperatures and sodium chloride concentrations by virtue of the existence of a very reproducible zero time response corresponding to 0% hemolysis from run to run at the same conditions.

D. Possible Source of Error in Measured Hemolysis: Shear Effect as a Result of Rapid Mixing

As was discussed earlier the criteria for the injection flow rate were uniformity and reproducibility of the delivered mixture of packed cells and the test solution into the observation chamber. Since the packed cells are delivered through large tubings (6mm I.D.) at low flow rates (about 5 cm^3/sec) it is unlikely to shear the cells at all. However, the turbulent mixing of the packed cells and the test solution in the mixing unit will introduce some level of shear. To investigate the possible shearing effect on the reported results, the following control experiments were performed.

Following the standard procedure outlined in Chapter 5 a sample of 20% hematocrit blood was mixed with an identical solution (20% hematocrit blood) through the stop flow system. The

mixed solutions were collected and the procedure, using the same sample solutions, were repeated several times. The sample was then collected and checked for percent hemolysis, through spectrometric method and stop flow technique, with the result that no hemolysis had occurred as a result of mixing. It is important to realize that this does not mean that the mixing procedure does not introduce any shear effect.

The result of the above experiment merely suggests that an upper limit for the extent of the shear. That is we can only safely conclude that no hemolysis will result from mixing under isotonic condition. In fact the red cells may be sheared to an extent such that they become abnormally vunerable when exposed to hypertonic solutions. To investigate such a possibility the following experiment was carried out.

The desired ratios of blood and hypertonic solutions were mixed external to the stop flow in a beaker. The mixed solutions were then manually delivered directly into the observation chamber with a syringe and the system's response was recorded for several perturbation levels for several exposure times. These results along with results obtained for long exposure times using the spectrometric method (sample prepared as above) are tabulated in Table 6.1.

Table 6.1

Comparison of Percent Hemolysis For Externally Mixed and Manually Injected Red Blood Cells With the Ones Mixed and Delivered Through the Stop-Flow System

Molarity (m)	Exposure Time(sec) 30	40	60	90	150	300	n
2.0	0.0	0.0	.8+.8	2.5+1.6	6.3+1.4	10.2+1.5	4*
	0.0	.2+.3	.7+.7	2.3+1.3	5.5+1.6	9.5+1.6	12**
3.0	13.2+3.1	19.1+3.1	24.5+3.8	28.1+4.7	30.6+4.3	33.7+4.7	6*
	14.5+1.4	20.2+2.1	25.7+2.3	29.5+2.3	33.2+2.5	36.9+2.8	11**
4.0	67.3+9.7	75.6+9.6	80.4+8.2	82.3+7.9	83.5+7.2	86.5+6.7	5*
	71.5+8.8	79.4+8.1	85.1+6.6	88.2+5.0	90.1+3.7	91.4+2.8	12**

*:Manual injection

**:Stop flow

At a 2 molar perturbation level the conclusion is that no shear effect is present as the manually mixed results are statistically speaking identical with ones mixed through the stop flow device. For 3 and 4 molar perturbation levels the manually mixed results are slightly lower. The largest discrepancy, if there was one, appear in results for exposure times of 1 minute and longer. Since the analysis concerning kinetics only involved initial response, i.e. percent hemolysis for times less than one minute, the apparent discrepancy would not affect the analysis. Furthermore all the results reported in Table 6.1 are statistically equivalent for the given level of perturbation and exposure time. Finally the long exposure time results show a reasonable correlation with the stop flow system results (This will be discussed in Chapter VII). Therefore it is concluded that the shearing effect will only be appreciable and for that matter it is measurable only at long exposure times.

To further substanciate the above conclusion the kinetic measurements were performed at high injection pressures (high mechanical stress) for 3.0 and 4.0m NaCl concentrations at different temperatures. These results are presented in Tables 6.2-6.5. The results show significant increase in the amount of hemolysis at high injection pressures (compared to the nominal). Hemolysis at short exposure times (compared to the long exposure times) are shown to be less sensitive to the injection pressure.

TABLE 6.2

Percent Hemolysis as a Function of Injection Pressure (3m NaCl at 298K)

Exposure Time(sec)	Pressure(psi) 60 (n=5)	40 (n=5)	30 (n=5)	17(nominal) (n=15)
5	-	-	-	-
10	0.33+0.57	0.50+0.56	-	-
15	3.60+0.66	5.50+1.04	1.93+0.93	2.01+0.36
20	8.73+2.55	9.23+0.75	4.43+1.03	5.53+0.77
25	16.00+3.73	15.43+1.80	10.73+1.69	10.33+1.20
30	23.31+2.89	20.10+2.26	14.95+0.87	14.50+1.43
40	33.23+2.48	26.41+1.45	21.08+1.38	20.23+2.11
60	40.60+2.65	31.83+0.76	26.73+1.08	25.69+2.31
120	48.41+2.76	36.63+1.64	33.13+1.57	31.67+2.74
180	52.23+3.62	38.59+1.51	39.08+2.93	34.52+2.60
240	53.43+3.67	40.27+1.22	40.85+3.22	35.79+2.70
300	55.27+3.44	41.77+0.87	42.10+2.95	36.94+2.82

TABLE 6.3

Percent Hemolysis as a Function of Injection Pressure (3m NaCl at 268K)

Exposure Time(sec)	Pressure(psi) 40 (n=6)	30 (n=5)	20 (n=6)	15(nominal) (n=12)
5	-	-	-	-
10	-	-	-	-
15	0.88+1.14	1.40+1.25	-	-
20	2.55+1.63	3.77+0.68	0.13+0.23	-
25	4.75+2.09	6.33+1.19	1.17+1.20	0.88+0.43
30	8.35+2.01	9.67+1.14	3.87+3.47	4.54+1.35
40	18.12+2.46	13.90+0.98	7.07+5.20	8.06+1.86
60	33.65+3.17	22.20+3.08	12.83+6.79	12.83+3.76
120	59.63+7.05	47.20+5.00	32.23+5.78	31.72+4.52
180	71.10+5.91	65.07+5.88	47.67+3.75	46.52+3.26
240	76.85+4.59	68.90+4.42	55.57+3.56	53.46+3.85
300	80.25+3.35	71.43+3.11	61.20+4.81	58.66+4.96

TABLE 6.4

Percent Hemolysis as a Functionb of Injection Pressure (4.m NaCl at 298K)

Exposure Time(sec)	Pressure(psi) 60 (n=5)	40 (n=6)	30 (n=6)	18(nominal) (n=15)
5	6.83+1.65	3.30+2.86	1.10+0.57	1.52+0.38
10	30.27+3.43	20.83+6.83	10.48+1.91	9.28+2.24
20	76.20+2.55	71.02+9.12	55.93+2.37	50.54+8.09
30	87.32+3.06	84.50+1.80	79.11+1.97	71.48+8.84
40	91.00+1.10	87.87+1.80	86.43+2.00	79.36+8.07
60	93.30+0.58	90.53+2.34	90.80+2.19	85.14+6.64
120	95	93	93.05+1.39	89.38+4.11
180	95	93	93.85+1.55	90.56+3.43
240	95	--	94.00+1.43	91.07+3.10
300	95	--	94.15+1.29	91.45+2.78

TABLE 6.5

Percent Hemolysis as a Function of Injection Pressure (4.m NaCl at 283K)

Exposure Time(sec)	Pressure(psi) 30 (n=6)	20 (n=5)	17(nominal) (n=15)
5	1.58+0.55	1.17+1.20	0.61+0.70
10	8.58+1.78	6.23+2.45	6.11+1.70
20	32.52+5.14	26.73+6.86	24.77+2.53
30	65.65+5.69	48.67+9.11	49.60+4.53
40	84.12+2.94	70.02+5.24	71.34+2.76
60	94.30+0.70	78.62+10.10	88.70+1.98
120	97	95.32+1.59	95.93+0.79
180	—	96.12+1.39	96.41+0.86

Comparing the data in the last two columns of the Tables 6.2-6.5,as they are statistically equivalent, clearly shows that the injection pressure effect appears to be non-existant at low injection pressures. Therefore based on the results reported in this work, the mechanical stress due to the injection if present is only measurable at long exposure times.

CHAPTER VII

EXPERIMENTAL RESULTS

The experimental aspect of the present work is aimed at obtaining data which will be used to decouple the chemical and thermal effects which occur similtaneously during the freezing of living cells. It is intended to generate a complete data base in the form of rate information describing the kinetics of cell destruction for human red blood cells.

In this chapter the experimental results of damage histories for red cell populations subjected to chemical shock at different temperatures will be presented in the form of percent hemolysis as a function of exposure time. Specifically, the hemolysis kinetics of the human red blood cell population induced by sodium chloride solutions between 2m and 4m are presented for temperatures between -5 and 25 C. Furthermore the present results are compared with earlier works.

A.Hemolysis at Different Temperatures Due to Osmotic Perturbation:

The osmotic perturbation brought about by mixing the human red blood cells with hypertonic sodium chloride solution results in the shrinkage of the cells. If the concentration of the saline solution is high enough (>.8m) the cell will lyse and lose its hemoglobin content [32]. For a cell population this process is a time dependent (kinetic) process.

When a population of red blood cells is mixed through the stopflow system the hymolysis process is reflected in the increased intensity of light transmitted through the sample. The change in the transmitted light intensity is detecdted and recorded as a voltage output history of a photocell detection circuit. An increase in the photocell output is therefore directly related to the red blood cell hemolysis. It will be shown that at a given temperature, the higher the perturbation level the faster the photocell output will increase and consequently the faster the hemolysis kinetics. Figure(7.1) represents a typical photocell voltage output due to 2m and 3m isothermal hypertonic step changes of the extracellular solution at -5 C. Cells exposed to 2m concentration reach the minimum volume state in a finite time, represented by the initial drop in

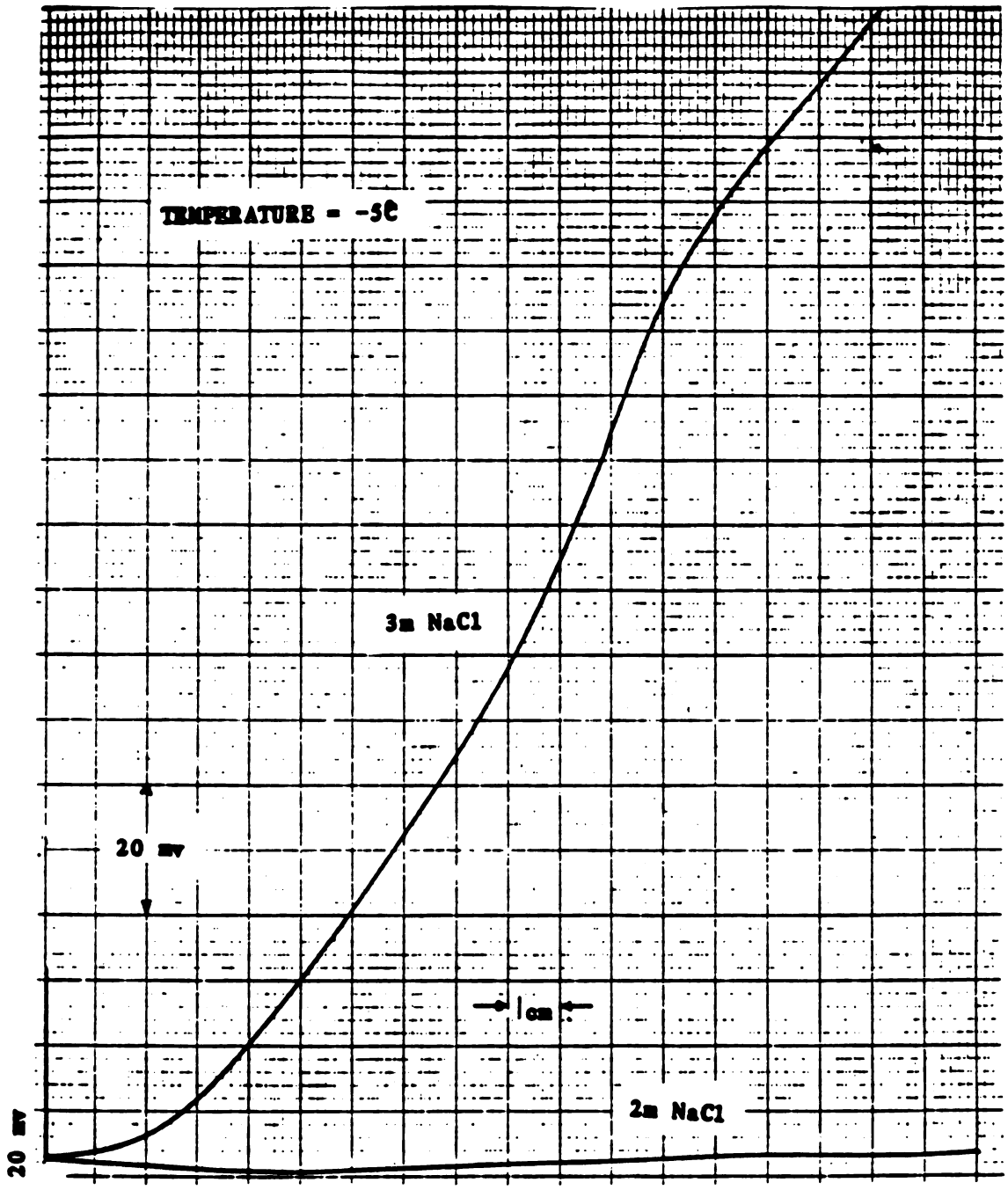

Figure 7.1: Typical Photocell Voltage Outputs Due to Isothermal Step Change of the Extracellular Concentration.

output voltage whereas at the 3m concentration level the cells reach minimum volume state instantaneously compared to the experimental time scale.

To translate the raw data in the form of photocell voltage as a function of exposure time into the desired hemolysis kinetics data the following procedure is employed. The photocell voltage at any instant of time is normalized with respect to the output voltage corresponding to the initial minimum volume, 0% hemolysis voltage level. The calibration curve (Figure 5.6) is then used to transform the normalized voltages to percent hemolysis. The hemolysis kinetic data are obtained for hypertonic sodium chloride concentrations of 2.5, 3.0, 3.5, and 4.0m at room temperature(25C), 10,5,0, and -5C. The result in the form of percent hemolysis as a function of exposure time for the above osmotic perturbation levels at different temperatures are presented graphically in Figures 7.2-7.6. As evident from these results the hemolysis kinetics at a given temperature are a function of the osmotic perturbation level as well as the exposure time. For example the results show that for an exposure time of 20 seconds at 25 C, while the 2m perturbation level produces no measurable hemolysis, about 50% of the cell population is hemolysed at the 4m level. Furthermore, the hemolysis kinetics are quite rapid at short times and as a larger portion of the population is hemolysed the rate of the hemolysis reaction process

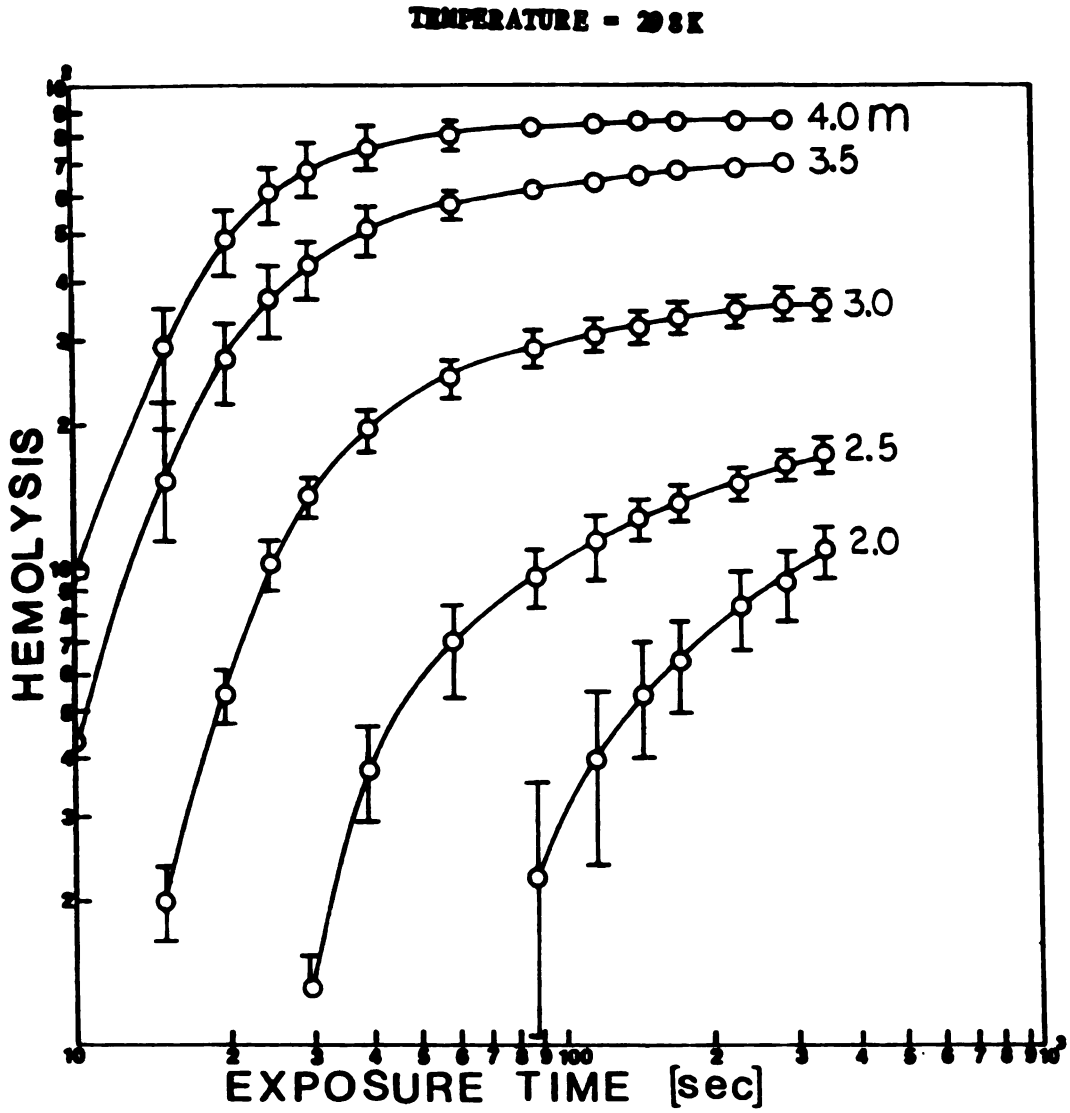

Figure 7.2: Percent Hemolysis as a Function of Exposure Time.

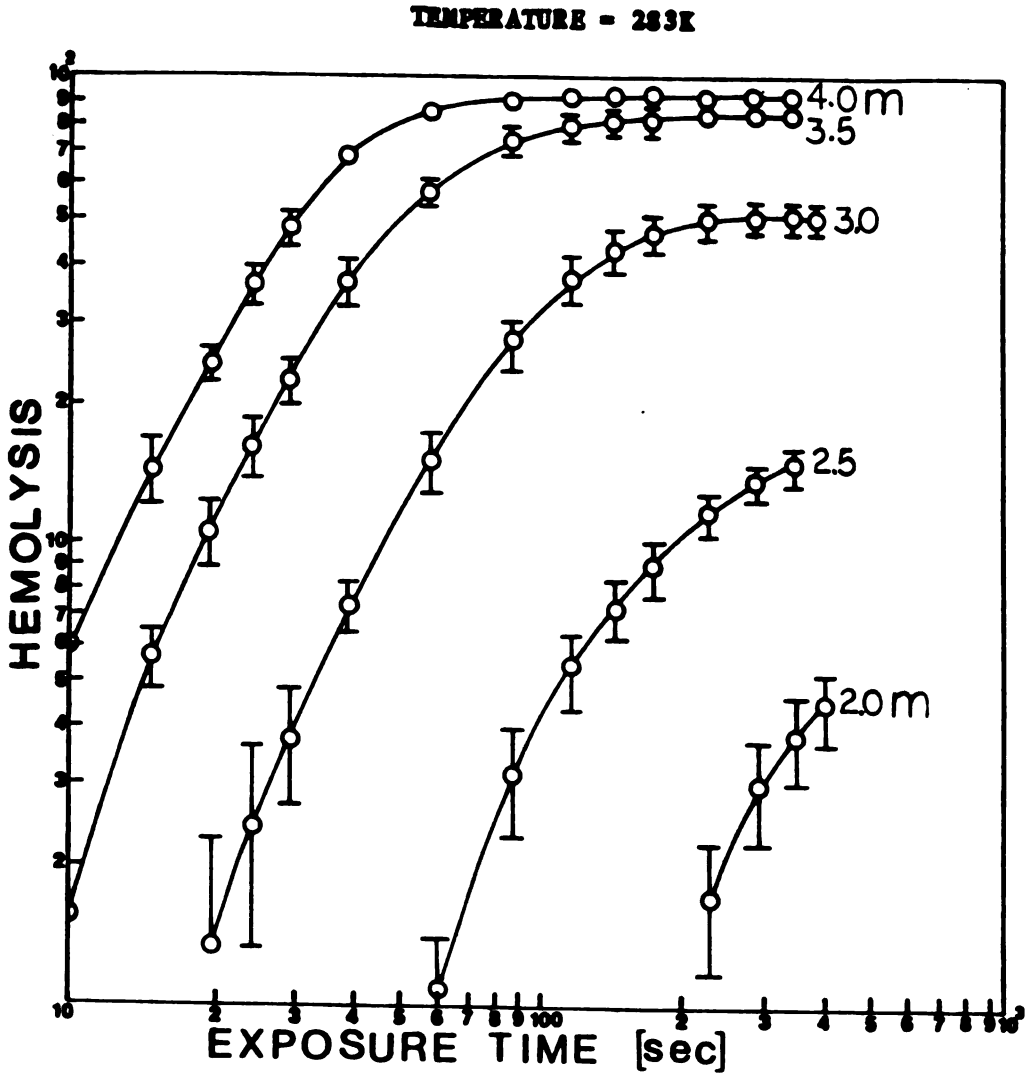

Figure 7.3: Percent Hemolysis as a Function of Exposure Time.

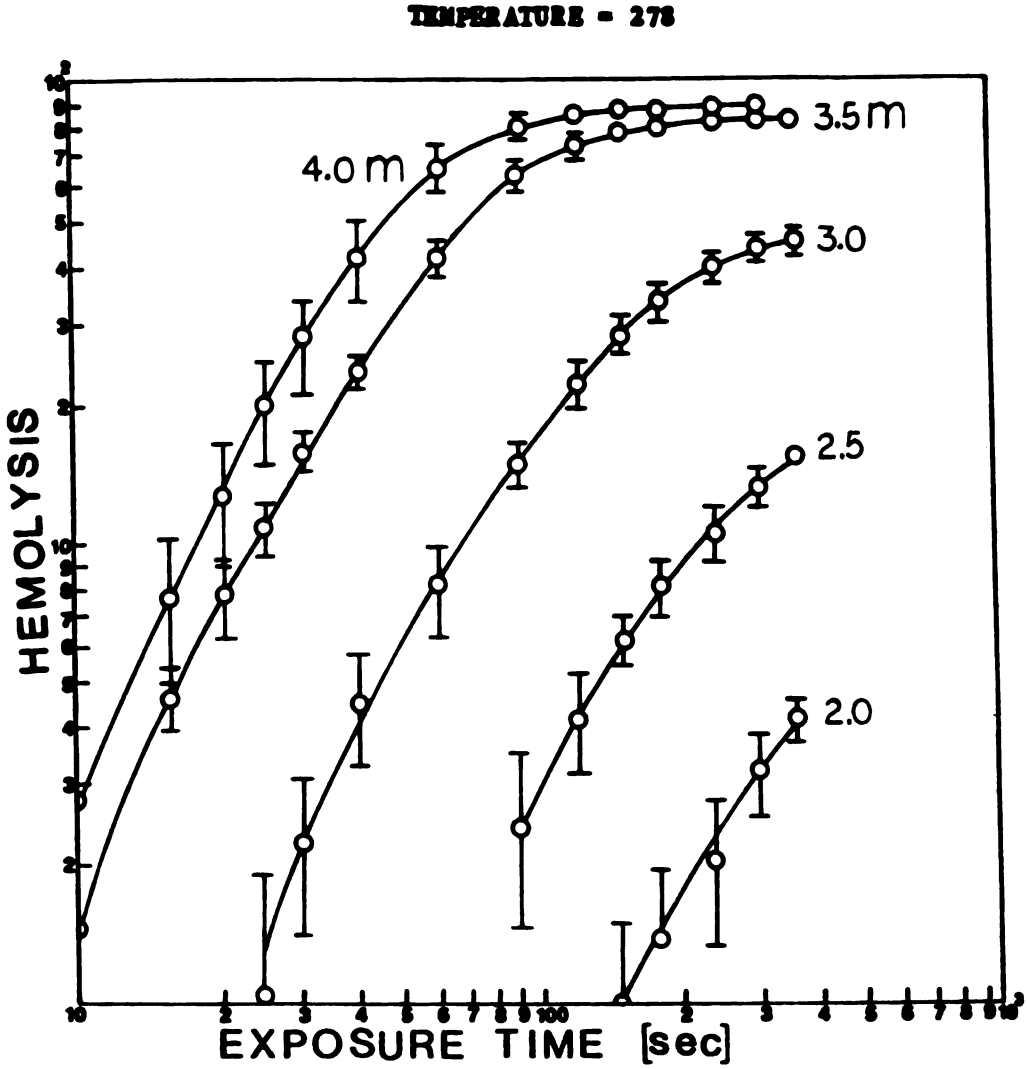

Figure 7.4: Percent Hemolysis as a Function of Exposure Time.

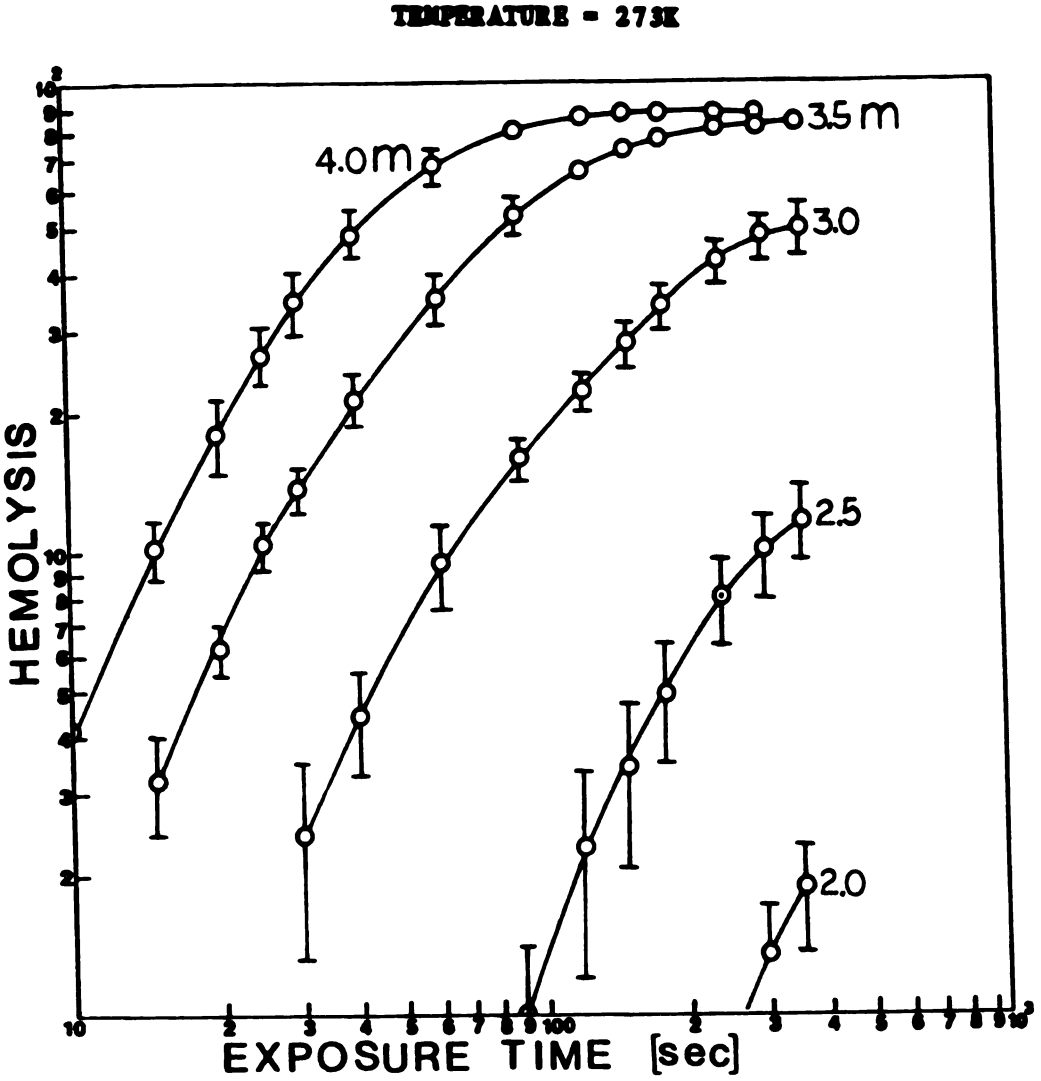

Figure 7.5: Percent Hemolysis as a Function of Exposure Time.

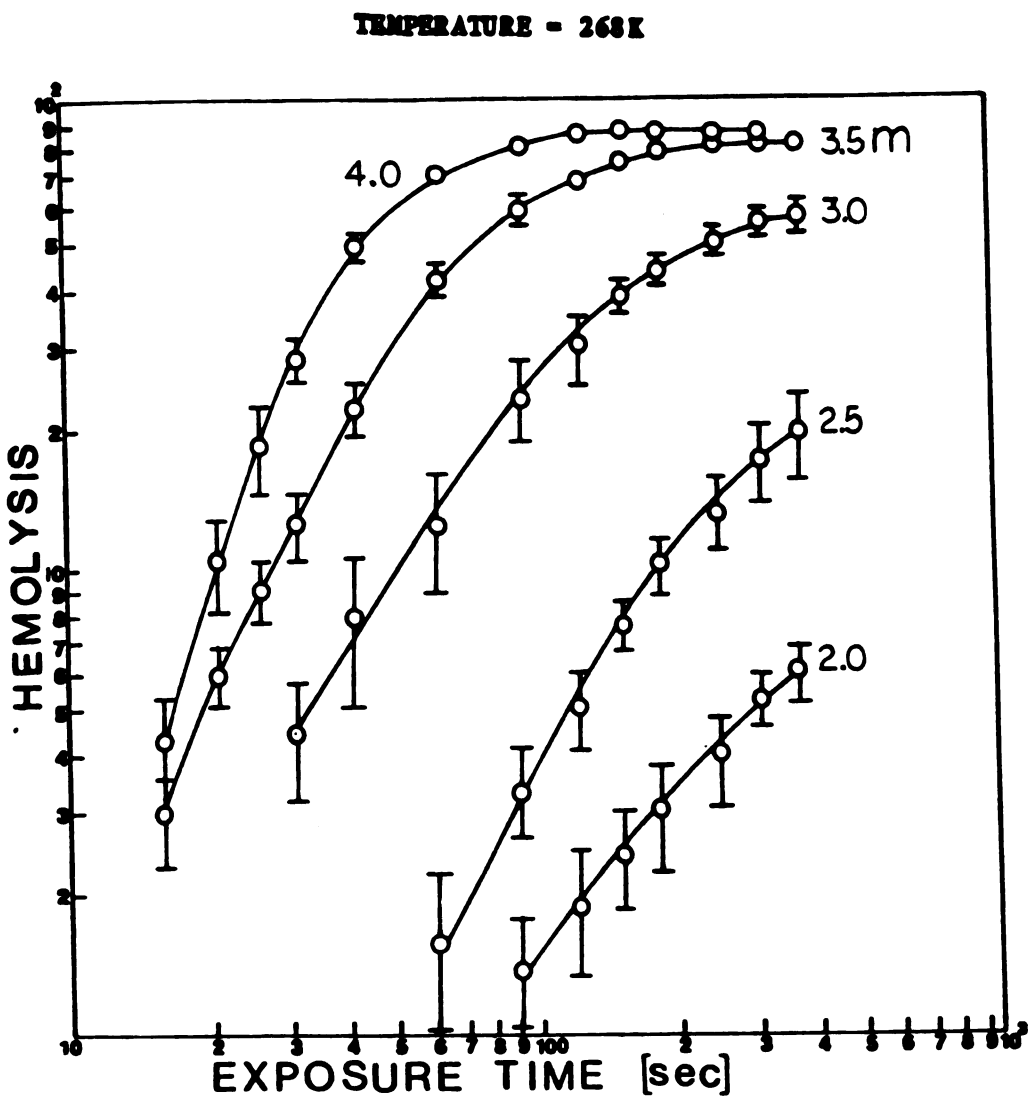

Figure 7.6: Percent Hemolysis as a Function of Exposure Time.

in the population shows a considerable decrease. This general pattern is observed for all the temperatures studied.

An important observation is that even though the level of hemolysis at a given temperature and time is higher for a higher saline concentration, nevertheless the rate of hemolysis reaction does not follow this trend. As a specific example, at relatively large times the reaction rate is quite slow for the 4m perturbation level, whereas the reaction rate at the 2m level is quite rapid. So far we have referred to hemolysis rate in the same manner as reaction rate is commonly addressed, this matter will be discussed in chapter 9. However, an attempt is made here to define the hemolysis rate for the present data. We define the rate of percent hemolysis RPH as

$$RPH = dH\%/dt \qquad [7.1]$$
$$= f(time)$$

As pointed out earlier it is evident from results presented in figures (7.2- 7.6) that RPH is a time dependent quantity. The time dependency is very pronounced for short times and for long times it approaches zero. In terms of the kinetics of the hemolysis reaction this implies that a kinetic analysis should emphasise short exposure time data as the long time data contains very little kinetic information since the system reaches

equilibrium. That is for a given NaCl concentration and isothermal temperature the damage process characteristically proceeds rapidly for early times and it is followed by a relatively abrupt transition to a considerably lower rate. This is especially pronounced at NaCl concentration greater than 2.5m. In this work the short time exposure data will be analysed in terms of reaction rate theory. At short times (less than 60 seconds) without loss of generality the ln(H%) is assumed to be a linear function of ln(time). Furthermore the linear dependency is only applied between two consecutive data points. Therefore for a given interval of time we have

$$\ln(H\%) = A\ln t + \ln B$$

$$H\% = Bt^{A} \qquad [7.2]$$

where t is time and A and B are constants. The values of A for different sodium chloride concentrations for various time intervals at given temperatures are tabulated in Table 7.1.

The calculated A values clearly demonstrate strong time and concentration as well as temperature dependency. Graphically speaking A represents the local slope of the hemolysis versus exposure time curve at an instant of time. For short exposure times the curvature of the curve is not pronounced and to a good approximation for small intervals it can be assumed to be linear

TABLE 7.1

"A" Values ($H_{\%} = Bt^{A}$) for Different Time Intervals

Time Interval (Sec.)	268K				273K				278K			
	4.0	3.5	3.0	2.5	4.0	3.5	3.0	2.5	4.0	3.5	3.0	2.5
10-15	4.857	4.536	---	---	2.249	2.932	---	---	2.494	2.814	---	---
15-20	3.130	2.398	---	---	1.986	2.273	---	---	1.830	1.898	---	---
20-25	2.579	1.901	---	---	1.789	2.375	---	---	2.033	1.505	---	---
25-30	2.418	1.803	8.999	---	1.524	1.539	6.377	---	1.799	2.110	4.261	---
30-40	1.966	2.033	1.995	---	1.575	1.575	2.095	---	1.472	1.394	2.463	---
40-50	0.897	1.591	1.152	1.529	0.823	1.257	1.915	---	1.111	1.417	1.468	---

Time Interval (Sec.)	283K				298K			
	4.0	3.5	3.0	2.5	4.0	3.5	3.0	2.5
10-15	2.150	3.193	---	---	2.894	---	---	---
15-20	1.830	2.187	---	---	1.813	2.094	3.518	---
20-25	1.824	1.907	2.656	---	1.027	1.345	2.800	8.091
25-30	1.518	1.887	2.399	---	0.644	0.864	1.860	4.372
30-40	1.260	1.699	2.246	---	0.364	0.573	1.158	2.964
40-50	0.537	1.111	1.843	---	0.173	0.326	0.589	1.524

(locally), again justifying the assumed functional form of H% given in Equation 7.2.

Based on the calculated A values the rate of percent hemolysis RPH is obtained for exposure times of 40 and 60 seconds. The RPH data are tabulated in Table 7.2 and are represented graphically in Figure 7.7. It should be noted that to obtain RPH values at a given time, concentration c, and temperature T, the following equation derived from Equation 7.1 is employed;

$$RPH(t,c,T) = H\%(t,c,T)*A(t,c,T)/t \qquad [7.3]$$

The results show that, except for the case of 2.5m concentration where RPH is decreased by decreasing temperature, decreasing temperature from ambient to 10C results in a sharp increase in the RPH. Decreasing temperature further does not seem to have a significant effect on RPH for the 4m concentration. An interesting point is that except for the cases of 4m and 2.5m concentrations the maximum RPH occurs at 10 C. That is increasing temperature beyond 10C in general seems to result in a decrease in RPH at the given times. The general pattern observed in Figure 7.7 can be deceiving as to arrive at rates at an instant of time the hemolysis kinetics are assumed to have the same characteristic times associated with them. This in fact is not the case, that is the characteristic time associated with hemolysis kinetics at a

TABLE 7.2

Rate of Percent Hemolysis at 40 and 60 Seconds

AT	-5°C		0°C		5°C		10°C		Rm Temp	
	40	60	40	60	40	60	40	60	40	60
4.0M	1.154	1.107	1.037	0.965	1.197	1.252	0.958	0.794	0.343	0.245
3.5M	0.912	1.159	0.682	0.763	0.858	1.016	1.045	1.093	0.247	0.325
3.0M	0.232	0.247	0.213	0.308	0.167	0.202	0.335	0.472	0.298	0.252
2.5M	0.040	---	---	---	---	---	---	---	0.145	0.179

TABLE 7.3

Initial Hemolysis Rate (%/sec.)

	-5°C	0°C	5°C	10°C	Rm Temp
4.0M	1.510	1.280	1.100	1.440	4.030
3.5M	0.650	0.670	0.950	1.030	1.770
3.0M	0.350	0.280	0.250	0.250	0.870
2.5M	0.031	0.046	0.060	0.080	0.180
	268	273	278	283	298

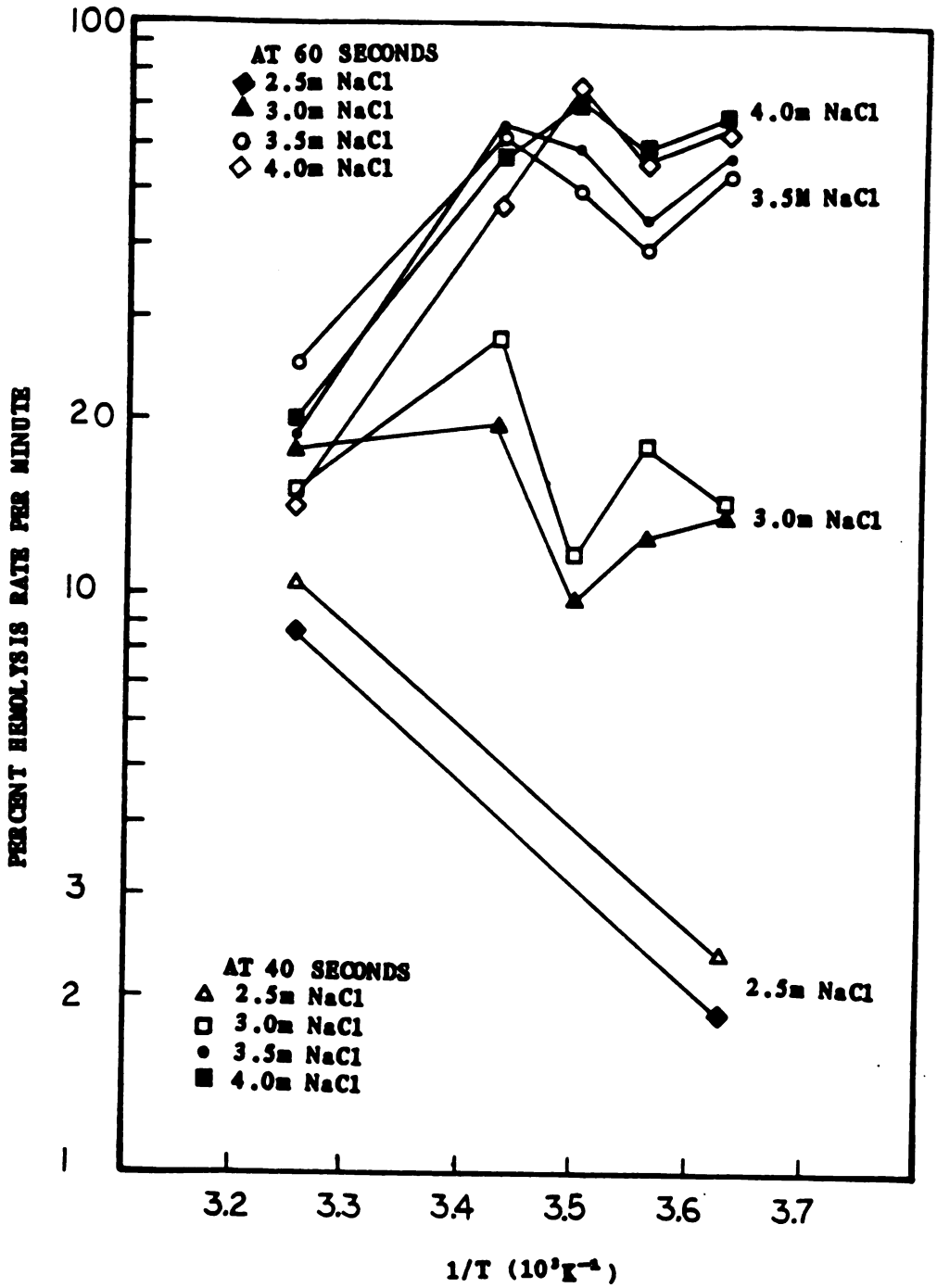

FIGURE 7.7: Initial Hemolysis Rate at 40 and 60 Seconds.

given condition is function of temperature. In other words the transition of the hemolysis process from rapid to slow is a function of temperature as well as NaCl concentration. For example, at 2.5m the hemolysis reaction is delayed by about one minute for cells at 0C compared to the room temperature response. Therefore the observed drop in RPH for -5C is largly due to the delayed response of the cells. To make this important point clear one can compare the hemolysis kinetics at a given sodium chloride concentration level as a function of temperature. For this the hemolysis responses of the cells at given concentrations are plotted for different temperatures in Figures 7.8-7.12.

The first and perhaps the most important observation is that the simple monotonically increasing hemolysis as a function of concentration trend observed for sodium chloride concentration does not hold true for the temperature. For instance for the case of 3m NaCl concentration, while the kinetic reaction is delayed for about 10-15 seconds at 5 ℃ compared to the other temperatures studied here, the final level of hemolysis is in fact higher for 5 ℃ as compared to 25 ℃. This implies that the instant of time at which significant hemolysis occurs is a function of temperature. In other words, the experimentally measured zero reaction time does not coincide with the zero mixing time. However the reaction rate at a given temperature might be rapid enough to overcome this shift or delay of measurable hemolysis as is the case for the

2.0m NaCl

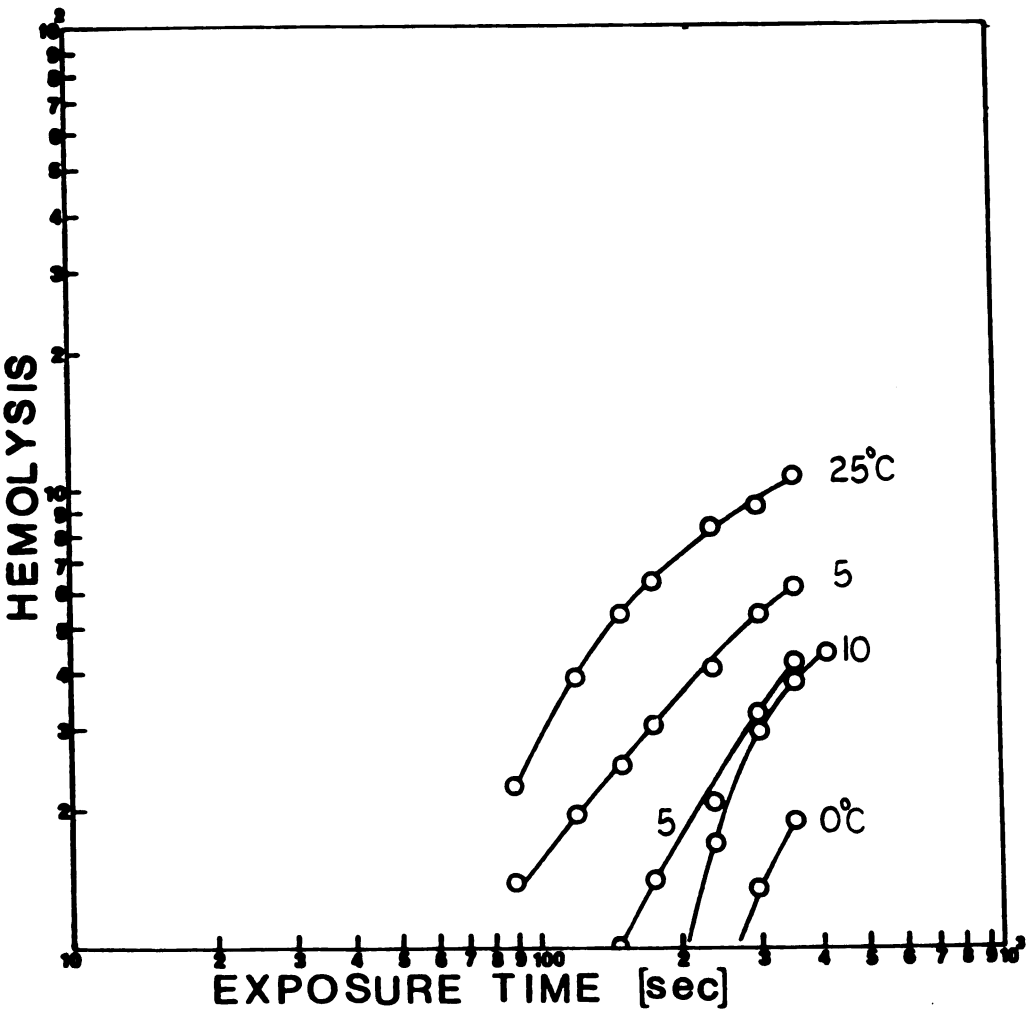

Figure 7.8: Percent Hemolysis as a Function of Exposure Time.

2.5M NaCl

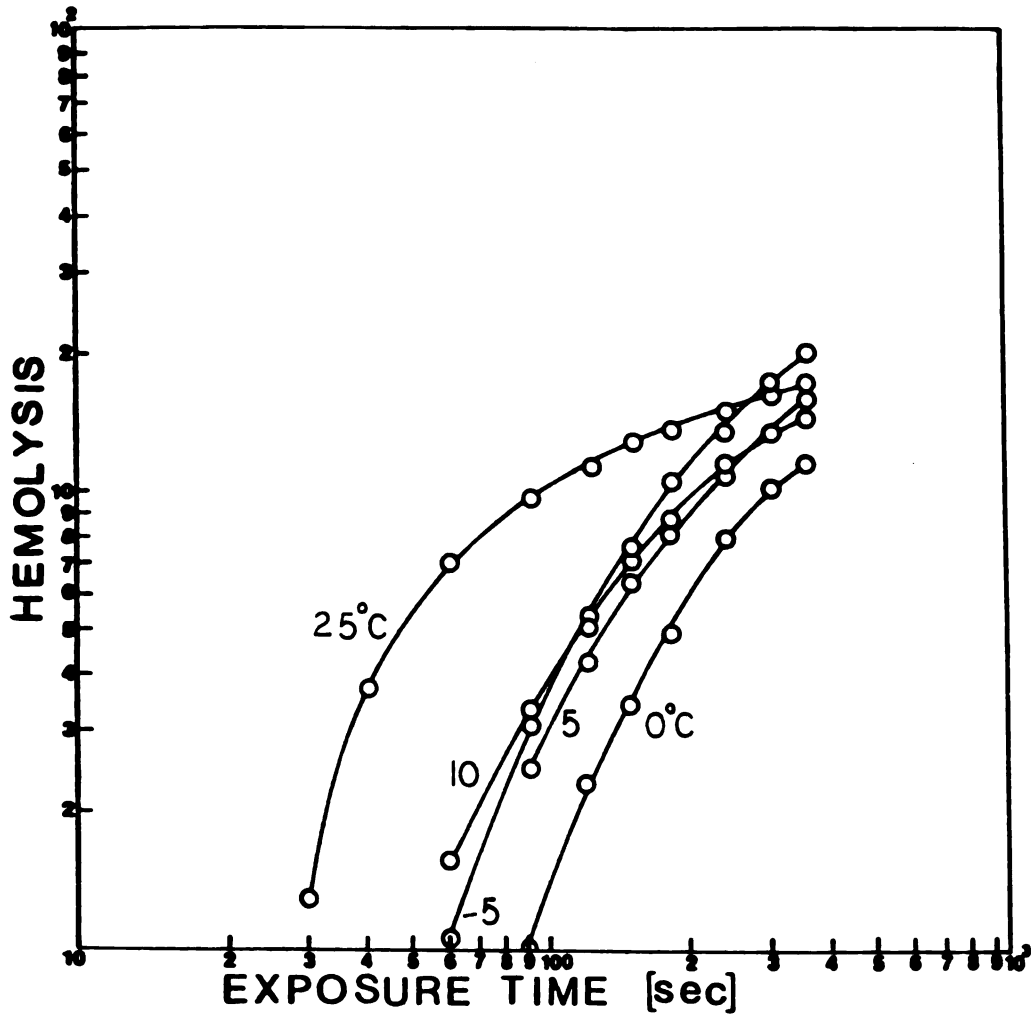

Figure 7.9 : Percent Hemolysis as a Function of Exposure Time.

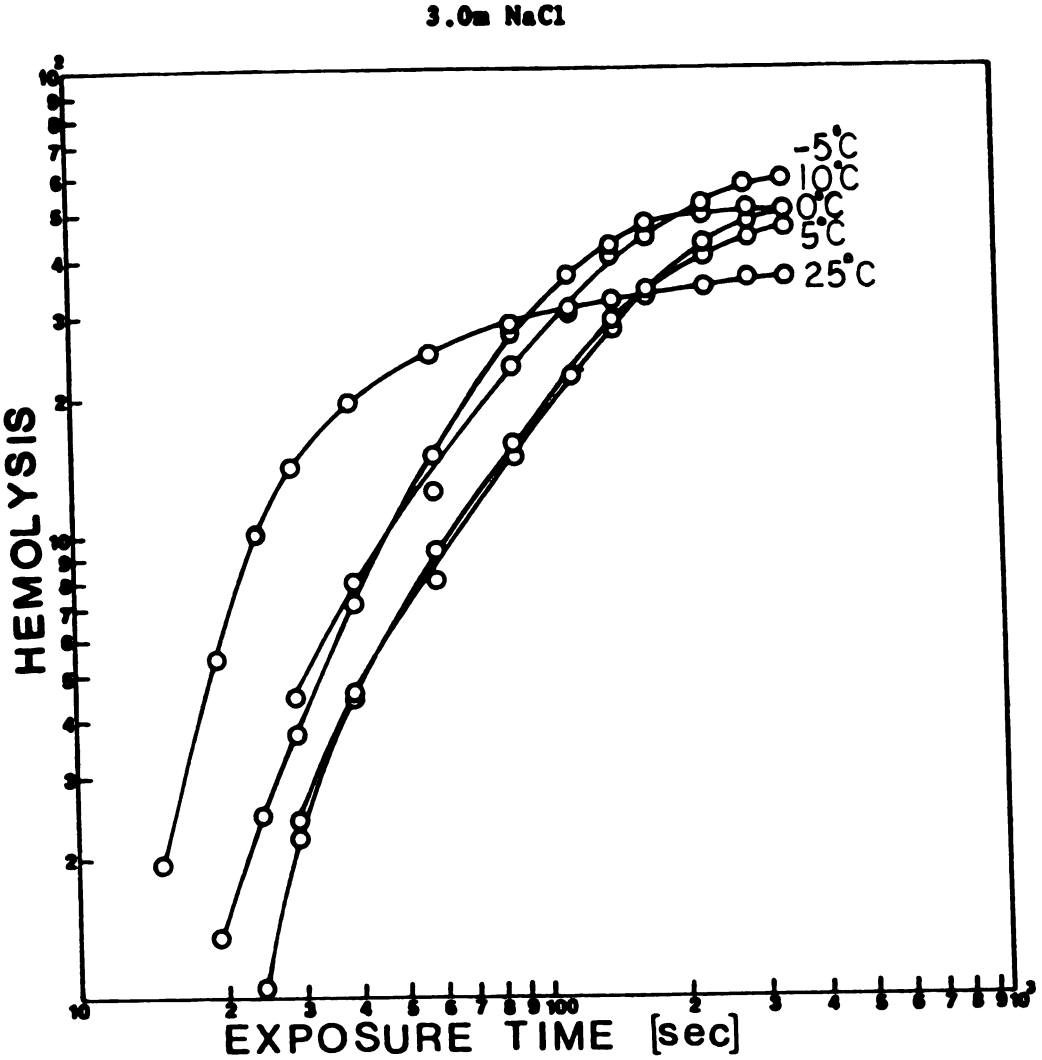

Figure 7.10: Percent Hemolysis as a Function of Exposure Time.

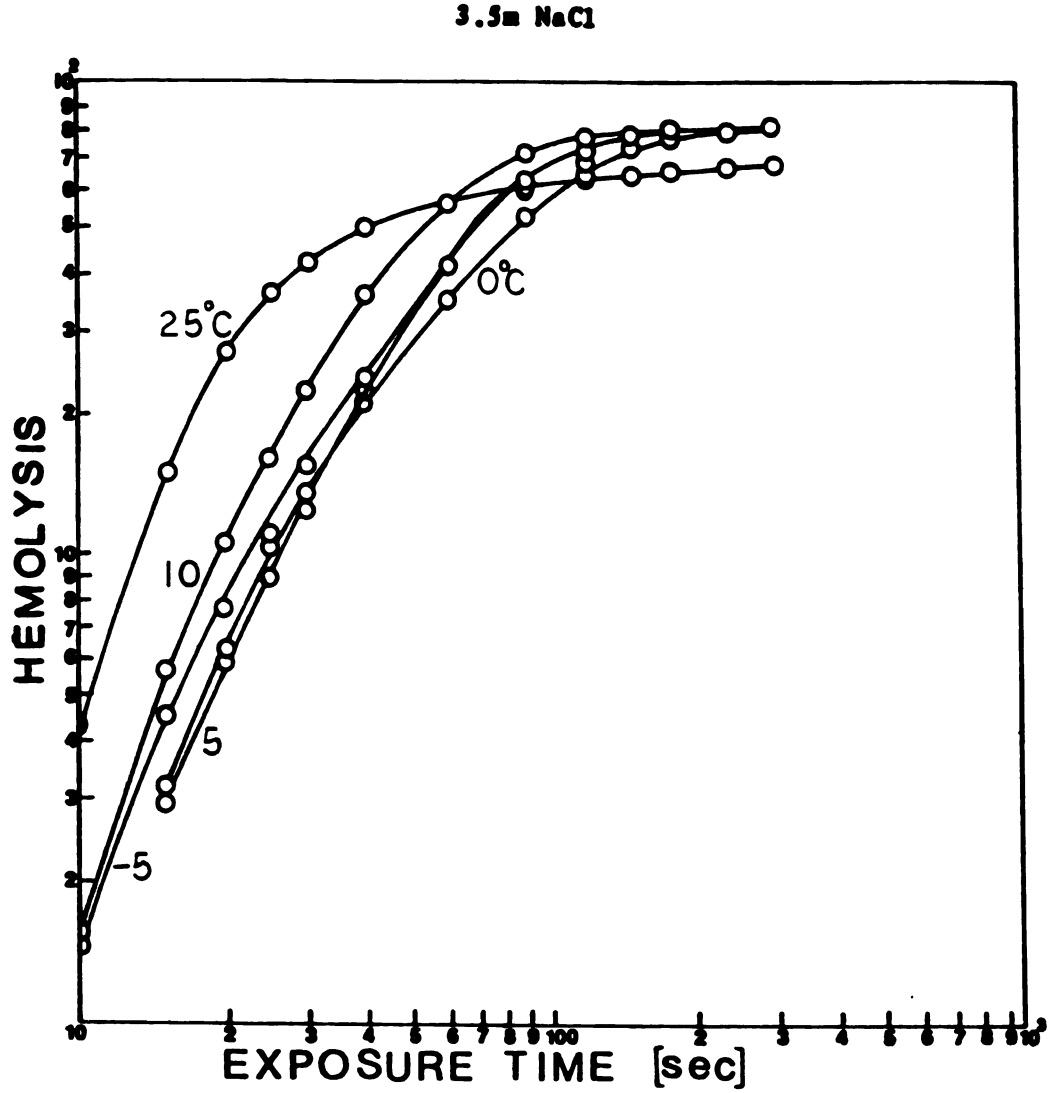

Figure 7.11: Percent Hemolysis as a Function of Exposure Time.

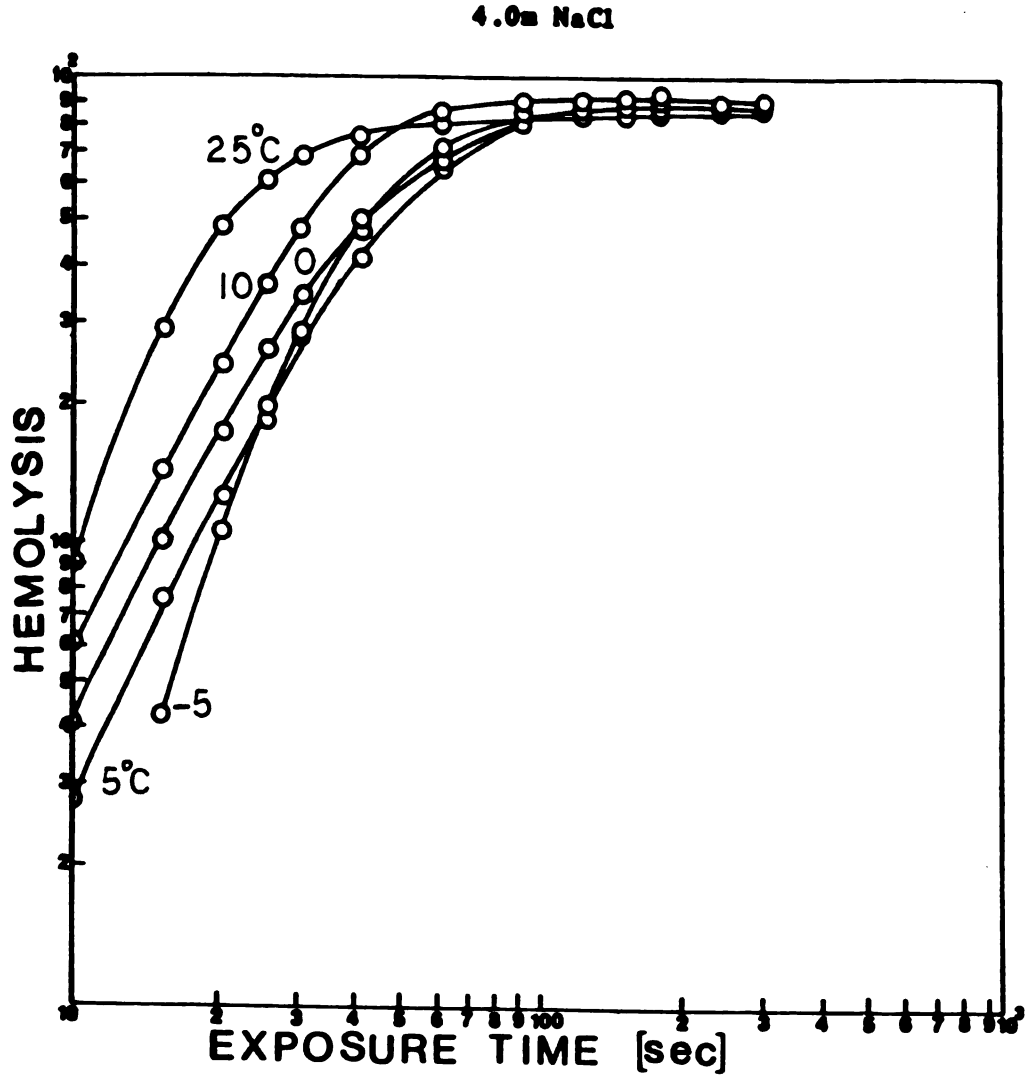

Figure 7.12: Percent Hemolysis as a Function of Exposure Time.

above example.

To overcome the difficulty due to the difference in characteristics of the kinetic response of the cell system at different temperatures, we will not fix the time at which the reaction rate is measured for all temperatures and concentration levels. Specifically, the time at which the reaction rate is measured at a given temperature will be determined independently for each case. To obtain this characteristic hemolysis reaction rate, hereafter referred to as the initial rate of percent hemolysis IRPH, the initial portion of each hemolysis curve is approximated as a straight line. Hence the slope of the early portion of the hemolysis history represents the initial rate of percent hemolysis for a given condition (temperature and concentration). In short the times at which IRPH is evaluated for each case depends on the concentration level and the absolute temperature of the experiment. The initial hemolysis rates for conditions considered here are tabulated in Table 7.3 and are represented graphically in Figure 7.13.

The initial hemolysis rate at temperatures 298K and 273K as a function of sodium chloride molarity are plotted in Figure 7.14. This figure clearly shows the effect of reduced temperature in substantially decreasing the initial hemolysis rate.

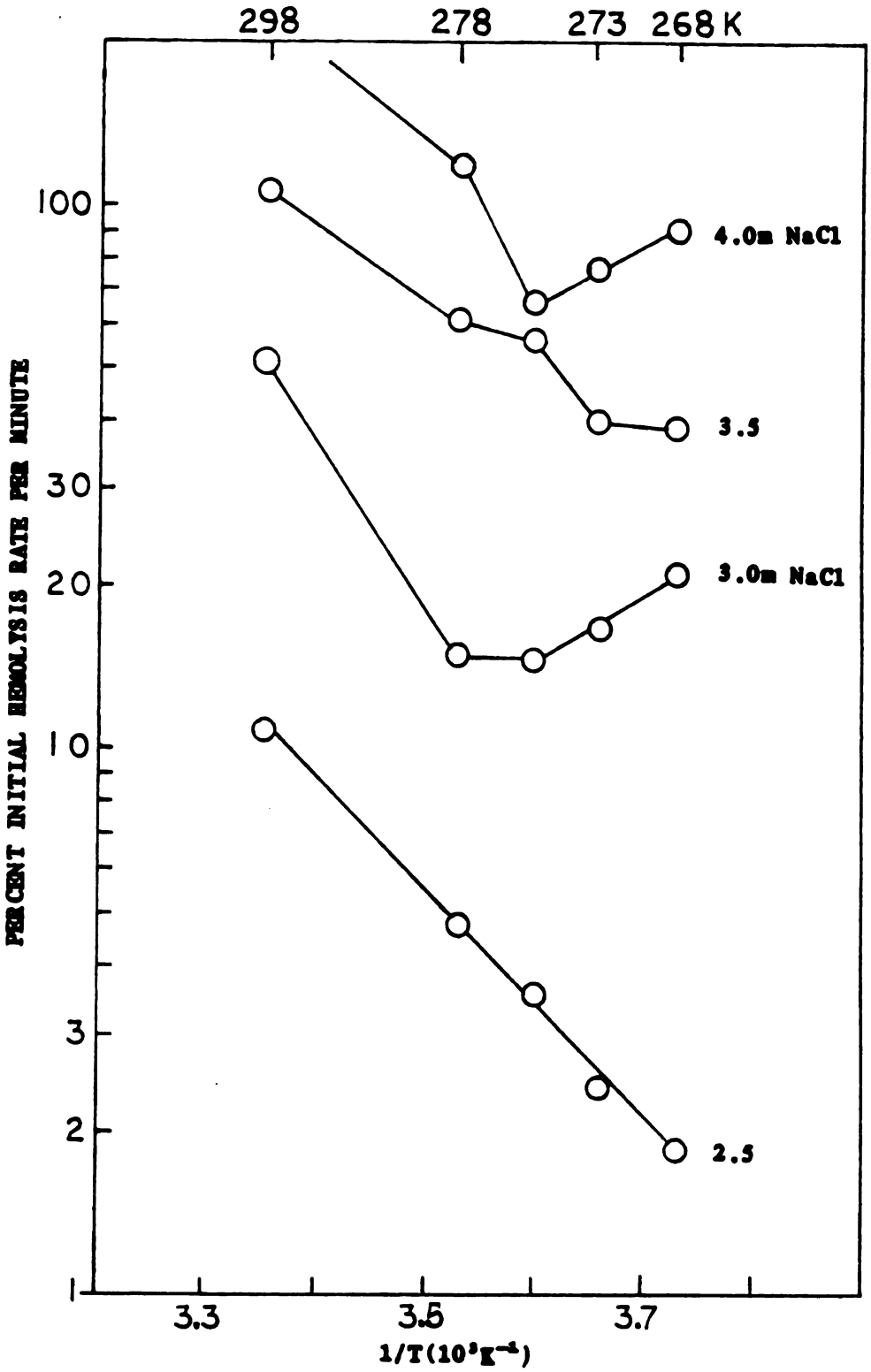

Figure 7.13: Initial Hemolysis Rate at Different NaCl Concentrations.

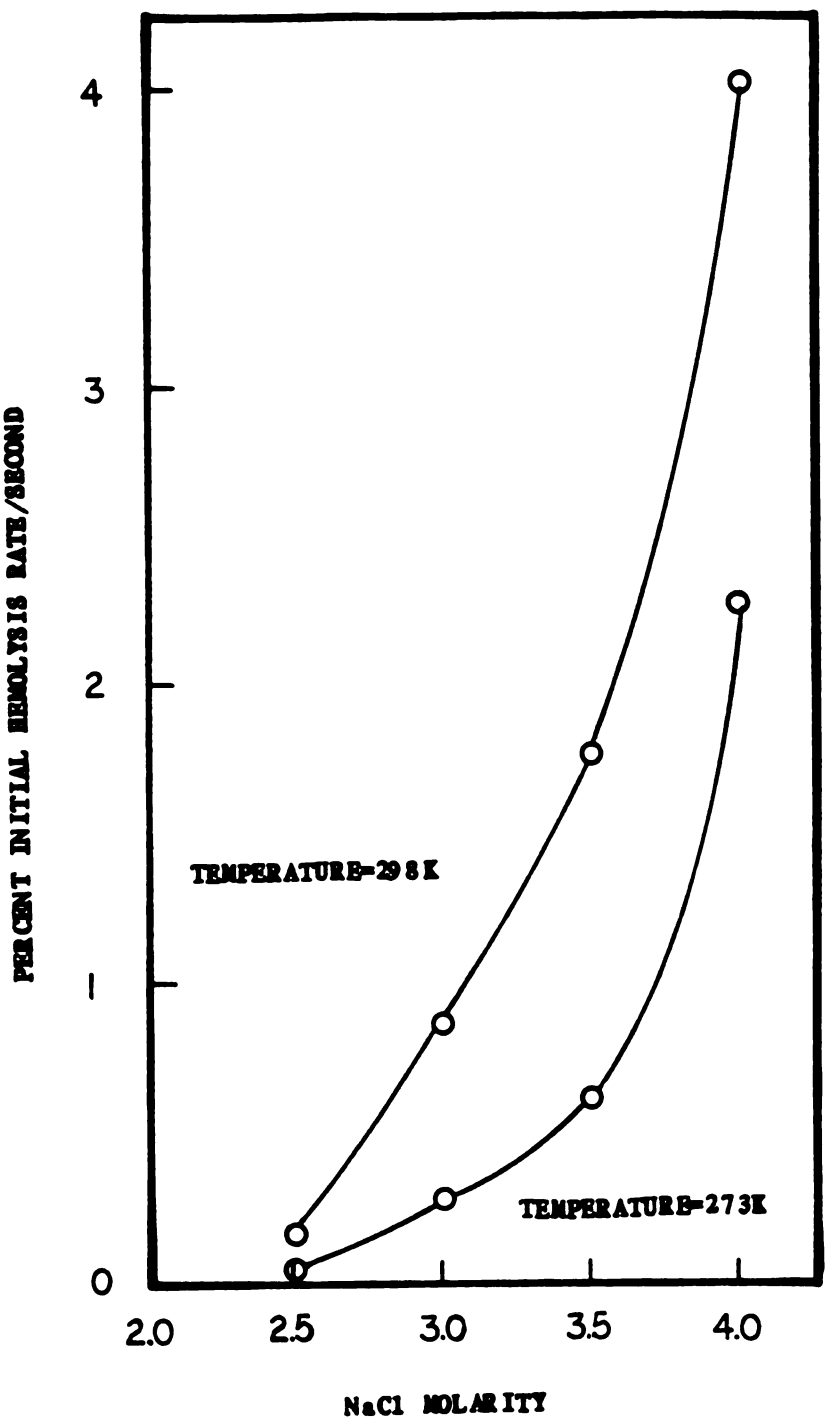

Figure 7.14: Percent Initial Hemolysis Rate Versus NaCl Molarity at 298K and 273K.

An important effect of temperature in delaying the hemolysis kinetics is revealed in Figure 7.15 where the hemolysis kinetics at room temperature for NaCl concentrations of 2.5m and 3.5m are compared with that of 2.5m and 4m at sub-ambient temperatures. It shows the striking effect, that for lowered temperature the extent of damage for short times is lower even for higher NaCl concentration level.

The percent hemolysis at molarities of 2.5 and 3 for exposure times of 1 and 3 minutes as a function of temperature are plotted in Figure 7.16. These results show that the dependence of the absolute amount of damage at 2.5m NaCl concentration as a function of temperature for 1 and 3 minute exposure times are quite similar. It also clearly shows a complicated temperature effect on hemolysis at a 3m concentration. For 1 minute exposure time the hemolysis level is decreased by decreasing temperature. However for the 3 minute exposure time decreasing the temperature either has no effect (at temperatures 0 and 5 $^{\circ}$C) or negative effect at temperatures (-5 and 10 $^{\circ}$C) on survival of the cells exposed to 3m NaCl.

<u>Temperature Effect:</u>

From the data presented in this chapter concerning the effect

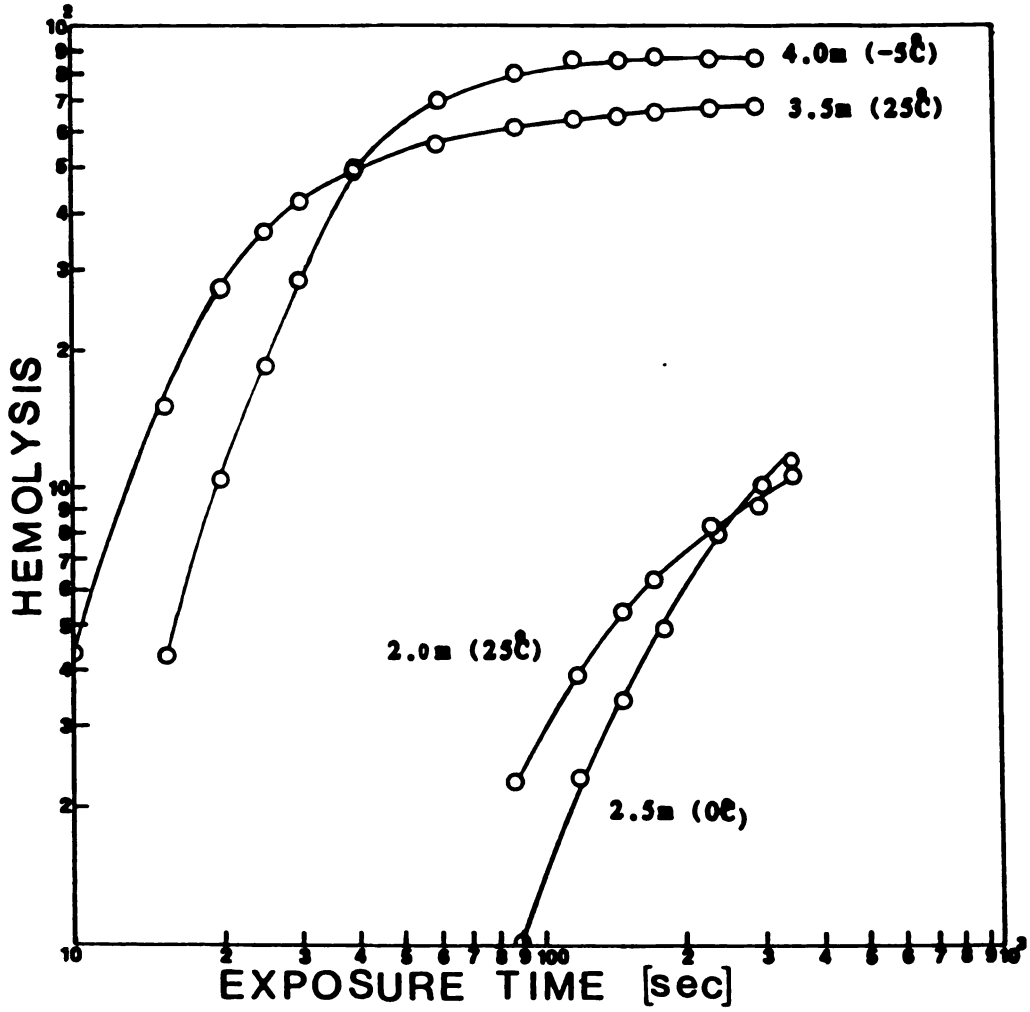

Figure 7.15: Comparison of Hemolysis Kinetics at Selected Temperatures and Concentrations of NaCl.

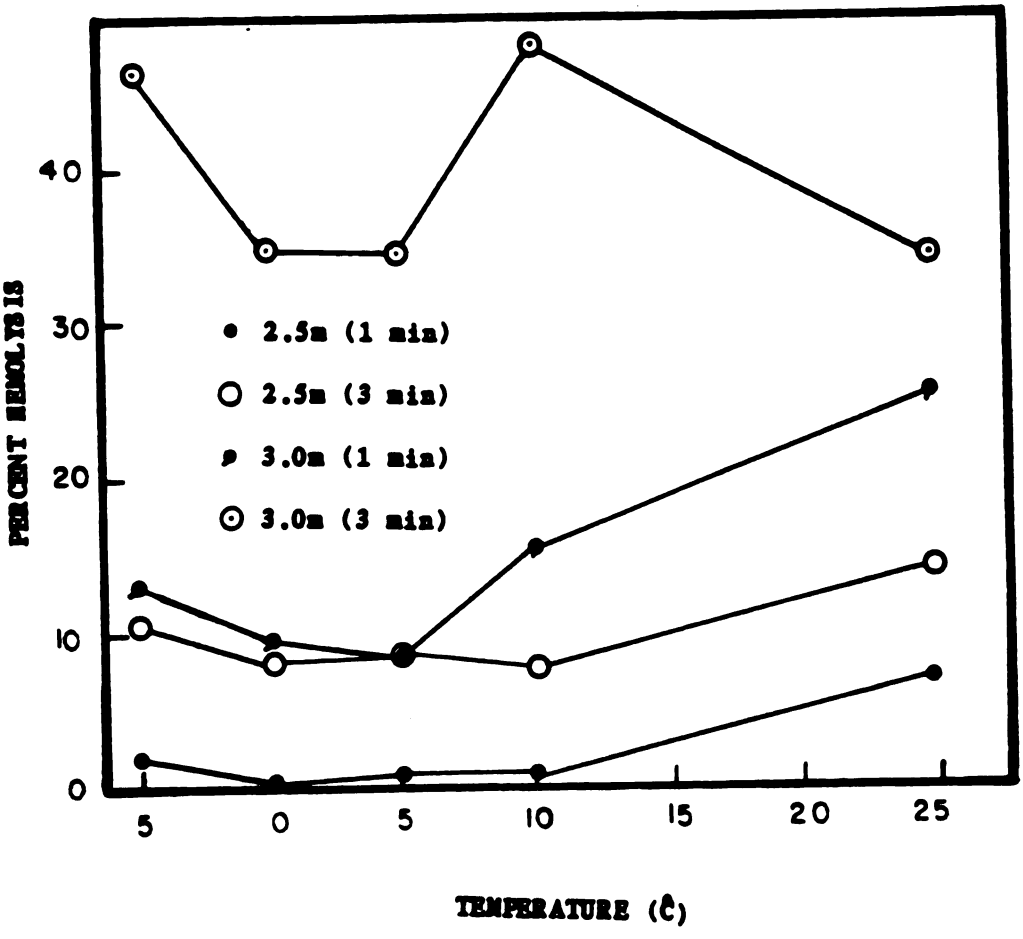

Figure 7.16: Percent Hemolysis for Exposure Times of 1 and 3 Minutes as a Function of Temperature.

of absolute temperature on the rate of the damage process, the following conclusions can be made:

1) The appearance (measurable occurance) of damage is delayed for sub-ambient temperatures at all concentrations. This effect is more pronounced at NaCl concentrations of 2 and 2.5m. The characteristic delay time associated with this effect is about 3.5 minutes for a 2m NaCl concentration and about 1 minute for the 2.5m case. It is on the order of seconds for higher concentrations.

2) At short times the destructive hemolysis reaction proceeds at faster rates at room temperature compared to lower temperatures. This behavior is more dramatic at the NaCl concentration of 2.5m where the initial hemolysis rate is .18 percent per second at room temperature compared to .031 percent per second at -5 C

3) For osmotic perturbations of 2m and 2.5m, the minimal amount of damage is induced when the experimental temperature is 0 C.

4) For osmotic perturbation levels greater than 2.5m the minimal total damage for the course of the experiments (about 6 minutes) occurs at the isothermal temperature of 25 C.

5) Characteristically the rate of the damage process is rapid at short times compared to that at long times for all temperatures and concentrations.

6) The transition of the rate of reaction from rapid to slow takes a fairly short time, particularly at NaCl concentrations greater than 2.5m, at room temperature compared to the responses at subambient temperatures. That is the transition and therefore curvatures at these instants are sharper at room temperature than at lower temperatures. The maximum level of damage is reached in 45 seconds for 4m concentration compared to 5 minutes required for 2m concentration.

7) At sub-ambient temperatures compared to room temperature the damage process proceeds at fairly higher rates for relatively long times. That is, the transition from initial rapid rates to final slow rates are smoother and delayed. This delay in the transition accounts for higher final damage levels at low temperatures for NaCl concentrations greater than 2.5m.

8) For 3.5m and 4m NaCl concentrations the damage kinetics and extent of damage for the experimental exposure times observed are insensitive to changes in sub-ambient temperatures.

9) For osmotic perturbation levels of 2 and 2.5m lowering the

absolute temperature results in reduction of the amount of damage for time period of up to 4 minutes. That is the red cells are able to sustain the osmotic stress for longer times at lower temperatures.

10) The largest effect of reduced temperature is observed when the isothermal temperature is dropped from 25 ℃ to 10 ℃. A further decrease of temperature has comparatively less significant effect on survival. For example, at 3 and 3.5m NaCl concentrations no appreciable difference in damage exists between data at 0 ℃ and 5 ℃.

B.Comparison of Present Experimental Results With Earlier Efforts

A major goal of the present work was to generate a reliable data base for hypertonic hemolysis kinetics at room temperature as well as sub-ambient temperatures. The incidence of reported hemolysis data in kinetic form for the red cell damage process as obtained by present research has been rare and for most cases unreliable. In this section we intend to justify the present effort both in light of its necessity and reliability. The specific earlier efforts we intend to compare our results to are due to McGrath and Jen [136,139].

McGrath has been a pioneer in the field of cryopreservation and the most complete study of the hypertonically induced hemolysis kinetics of human red blood cell populations to date is due to him. He used a stop flow system similar to the one developed for this work. Before attempting to compare the kinetic results we need to clarify an important point about the calibration protocol used to interpret the raw data in the form of the photocell voltages to the hemolysis form presented here.

The calibration protocols constitute the mechanism for transformation of the raw voltage histories into hemolysis kinetics and for this reason alone an erroroneus procedure at this stage makes any further analysis of the results meaningless. Due to disagreement between the calibration curve obtained in the present work and the ones used by McGrath and Jen, the first task is to justify the validity of the protocols reported here.

The comparison of the hematocrit calibration curve obtained for the present work with that reported by others is summarized in Figure 7.17 [136,137,139]. All the results follow the general trend as

$$V(\text{photocell voltage}) = a^{*}(\text{percent Hematocrit})^{b}$$

where a and b are constants. From Figure 7.17 it is clear that

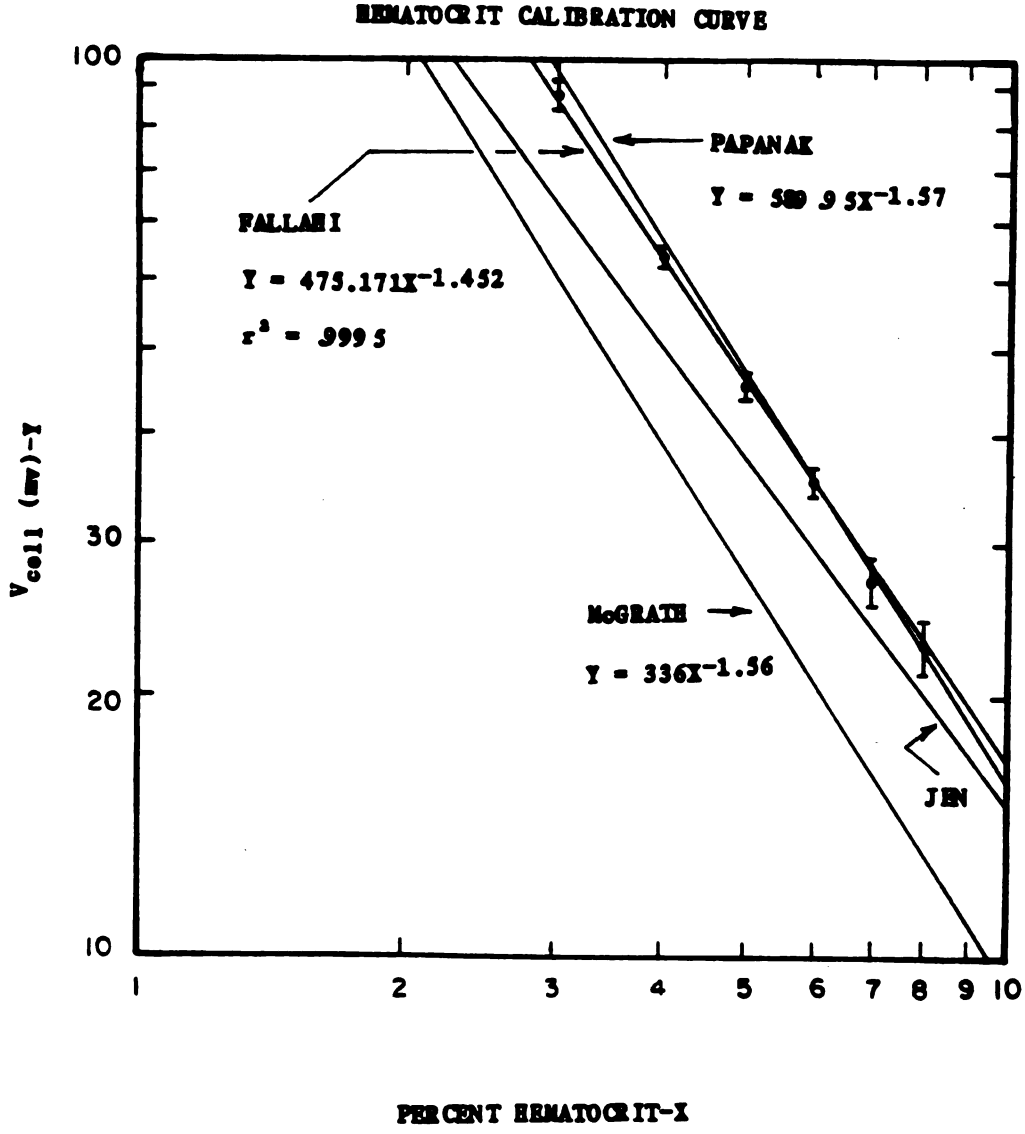

Figure 7.17: Normalized Photocell Voltage as a Function of Hematocrit.

the protocol due to Papanek is statistically equivalent to the result reported here while the other two protocols disagree.

The percent hemolysis calibration curves reported by earlier researchers are summarized along with the result obtained here in Figure 7.18. The author believes this calibration protocol, normalized photocell output as a function of percent hemolysis, should be independent of the experimental system variables such as light source and detection mechanism. The excellent agreement between the results of Papanak and the present results is therefore expected as the two results are statistically identical. However the results obtained by McGrath and Jen deviate sharply from the present results. It is very difficult to arrive at the source of these discrepancies. Nevertheless, it seems likely to be due to the size of the beam width with respect to the diameter of the observation chamber.

The results of percent hemolysis kinetics at room temperature obtained here are compared with that of other investigators in Figure 7.19. There appears to be considerable disagreement between the present results and results reported elsewhere. It is believed that the roots of the apparent discrepency lie in the calibration protocols. An important observation is that for the resulted reported by McGrath the initial hemolysis rates are independent of time. A is equal to 1 in Equation 7.2 for all

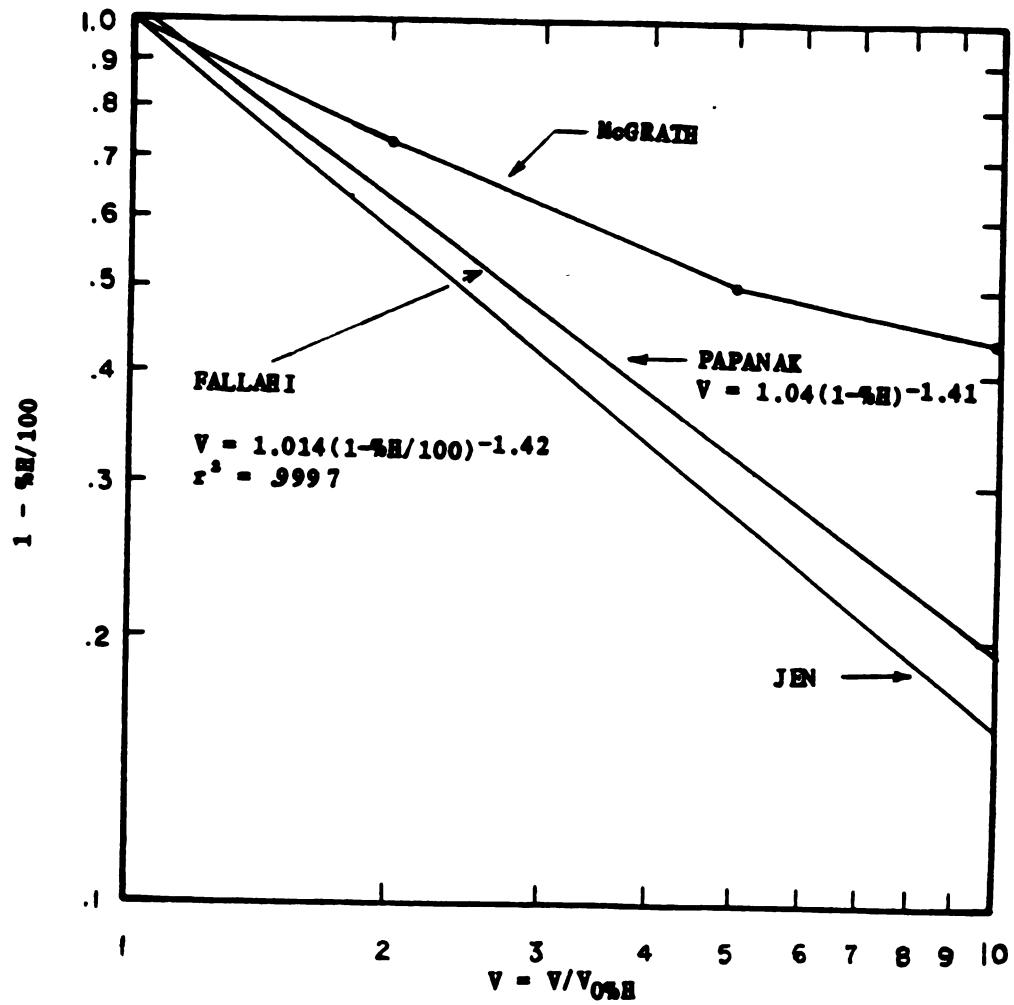

Figure 7.18: Comparison of Present Hemolysis Calibration Data with the Results Reported by Others.

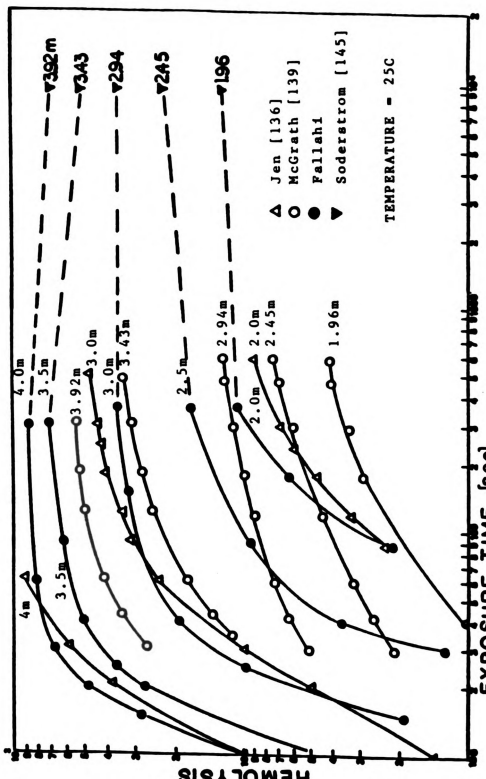

Figure 7.19: Comparison of Present Results with Results of Other Investigators.

concentrations. This is not believed to be the case as the present results show strong time, concentration and temperature dependency for initial hemolysis rates. Further the results obtained here compares far better with the long exposure time data of Soderstrom [145].

Lovelock using a different technique measured the red blood cell percent hemolysis for long exposure times (5 minutes) [8]. These results are significantly different from the results presented here. Lovelock to assess the damage ocurred (to the cells) during a hemolysis process, colorimetrically measured the quantity of hemoglobin released into the suspending solution (spectrometric technique). Here an attempt will be made to explain the author's viewpoint of Lovelock's data.

First of all it is not clear how the hemolysis at subzero temperatures were measured. For example; i)was the hemoglobin measurement carried out at room temperature or at the test temperature, ii) how was the time spent for colorimetery accounted for. Secondly,contrary to the present results, his results at a given NaCl concentration show very small (if any) temperature dependency . Furthermore there is a substantial discrepancy in his results which makes a direct comparison impossible. Finally a very disturbing observation is the trend of his hemolysis results for damage due to the dilution to isotonic condition (Table

2,[8]). According to Lovelock dilution from 1 M NaCl does not result in hemolysis of more than 3%. However dilution from 2.5 M NaCl results in two-fold greater damage than that at 2 M. Furthermore his results show no NaCl concentration dependence beyond 2.5 M. The major concern here is that if redilution to isotonic condition at 1 M NaCl is not damaging (insignificant), it does not seem realistic that it results in such a dramatic damage at 2.5 M. It is also difficult to accept that such a concentration dependence is for all practical purposes is the same for NaCl concentrations greater than 2.5M.

CHAPTER VIII

MECHANISM AND CAUSE OF CELL INJURY AS A RESULT OF EXTERNAL PERTURBATIONS

A. Cause and Mechanism of Injury

Biological systems are very sensitive to changes in environmental parameters such as temperature and electrolyte concentration. Such systems exposed to a freeze-thaw cycle are often severely damaged or killed. Substantial efforts in cryobiology have been centered on the problems of the causes and mechanisms of injury when biological sytems are exposed to low temperatures with special reference to freezing. The question of the cause of injury at slow cooling rates is generally believed to be the result of cell dehydration due to hypertonic exposure and/or freezing [22,24]. However, an understanding of the mechanism(s) of freezing injury is still lacking. This is mainly due to the microscopic and complex nature of the system with coupling which requires a knowledge of cellular behavior at the molecular level in response to environmental alterations. Several mechanisms for injury based on the macroscopic analysis of the

physico-chemical events associated with the freezing process have been hypothesised by different investigators [8,106,141]. Despite the diversity of the proposed mechanism they invariably agree on membrane damage to be the primary cause of injury.

1. Cause

The cause of injury when cells or tissue are cooled at supraoptimal rates has been determined convincingly and the damage is shown to be associated with the formation of intracellular ice during the cooling process [7,8,58]. It is known that both intracellular and extracellular ice formation results in damage [140]. It should be pointed out here that, while the lethality of the extracellular ice formation can be reduced or eliminated by the presence of protective agents, the intracellular ice formation is usually lethal [23]. However, the question of the cause(s) of injury when a cell is cooled (frozen) at suboptimal rates does not seem to have a unique answer. The general belief is that the cause(s) of slow freezing injury is a consequence of alterations in the intracellular as well as extracellular solutions. These so-called solution-effects are a result of extracellular ice formation. The solution effects include the solution concentration and excessive dehydration among others [8]. Hence, most if not all of the hypotheses put forth to explain the cause

of damage during freezing have been centered on the osmotic stress experienced by the cell due to depletion of water.

Lovelock (1953) suggested that the cause of damage to the human red blood cell at suboptimal cooling rates in the absence of protective agents is the increase in the concentration of the extracellular solutes during freezing [8]. He further proposed that the physio-chemical consequences of the concomittant increase in the intracellular electrolyte concentration is the major cause of damage. Miller and Mazur (1976) in agreement with Lovelock concluded that the cause of injury in a cell frozen at slow rates is due to the increase in the concentration of solutes of the suspending medium of the cell [21]. However, in contrast with Lovelock they emphasized the role of extracellular electrolytes as the cause of damage. Meryman (1968) proposed the idea of exceeding a maximum tolerable mechanical resistance to shrinkage as a result of increase in the concentration of the extracellular solutes [106]. According to Merymans' view, as water is frozen out of solution as a result of slow freezing the increase in the extracellular concentration leads to a reduction in the cell volume. This in turn brings about an increasing resistance to shrinkage due to the compression of the cell content. The damage to the cell membrane is then caused by the development of an osmotic pressure gradient across the cell membrane greater than that which can be compensated for by cell volume change. Since,

according to Meryman, the membrane damage results from osmotic stresses imposed on the cell membrane as a result of reduction in cell volume it is also called the "minimum cell volume" hypothesis.

Steponkus and Wiest (1978) on the other hand proposed that cells which osmotically shrink during freezing can tolerate only a certain increase in surface area during thawing [141]. Again the cause being due to an increase in the concentration of the extracellular solutes (hypertonic exposure).

Wolf and Steponkus showed that while the volume of isolated protoplasts negligibly changes due to tension in the plasma membrane (which approaches that tension necessary to lyse them), membrane area is considerably reduced [127]. They proposed that damage is due to exchange of material between the plasma membrane and a reservior of membrane material. That is loss of the membrane area during hypertonic exposure is the main factor responsible for cell lysis. According to this view, the cells that have shrunken (during freezing) will burst upon return to isotonic solution (thawing) due to the lack of sufficient membrane area for the cell to reach an osmotic equilibrium with the extracellular solution.

The forementioned hypotheses are in good agreement with the

fact that the primary cause of damage in slow freezing is either due to an increase in the concentration of non-permeant extracellular electrocytes (solution effects) or is a consequence of intolerable deformation of the cell membrane brought about as a result of area changes. That is injury could be directly linked with the lowered chemical potential of the solvent (water), due to the increased solute concentration, which is manifested as an osmotic stress. The osmotic shrinkage of the cell concurrent with one or more of the structural and functional alterations brought about as a result of lowering the temperature in general and ice formation in the extracellular region in particular is damaging. However, other complications induced by the presence of ice could result in stress (other than osmotic stress). Shear stress due to entrapment in the unfrozen channels between ice crystals is known to play important roles in determining the fate of a successful suboptimal freezing protocol [142].

2.Mechanism

The problem of understanding the mechanism of damage caused by exposure to low temperatures and hypertonic solutions as a result of slow freezing is yet to be completely understood. Concerning the general class of "solute effects" the general

belief in the field of cryobiology is that the freezing injury occurs at the membrane level. During the process of freezing and thawing the cell membrane goes through dramatic alterations regarding both its structure and function as a result of environmental changes. An important environmental alteration is associated with the removal of a major portion of the solvent water and the idea that freezing injury is primarily due to the dehydration enjoys a wide acceptance. This is a manifestation of the functional and structural importance of water in living systems. The removal of solvent water results in the lower chemical potential of water in the cell's residual suspending medium as a consequence of the increased solute concentration. The chemical potential of extracellular water could also be lowered by increasing the extracellular solute concentration. Lovelock reported that cell lysis as a result of freezing and thawing is duplicated by hypertonic exposure and dilution to isotonic condition in the absence of freezing [8]. This is the chief reason for equating the hypertonic exposure injury to the damge due to slow freezing in the field of cryobiology. However, one should always bear in mind that although it is known that in some cases (red cell for example) temperature drop alone is not damaging, it could cause detrimental damage once the membrane is altered as a result of hypertonic exposure. Leibo et al have observed that while cells subjected to hypertonic exposure generally shrink symmetrically (retaining their general geometry),

cells frozen slowly generally are distorted and contorted [143]. It is known that mechanical stress could lyse the cell [87]. This implies that the mere presence of the ice besides the osmotic pressure could be lethal as it could result in a severe distortion of the membrane.

Acel and Lorber (1924) were the first to propose that the red blood cell hemolysis as a result of hypertonic exposure is a consequence of the saline action on colloids forming part of the cell [144]. Soderstrom (1944) working on the same problem proposed a more clear picture in which he suggested the structural alteration of the membrane [145]. More precisely he proposed that the cell death is due to the fact that the membrane, as a result of hypertonic exposure, is structurally damaged in such a way that the hemoglobin content of the cell could flow out of the cell. He further suggested the idea of an actual dissolution of the protoplasmic framework of the cell caused by the action of concentrated salt solution. Lovelock (1953) proposed some form of injurious denaturation in the membrane caused by the action of concentrated electrolyte solution as an explanation for the cell injury [8]. He suggested that the red cell is hemolysed in the process of freezing and thawing as a result of the uptake of ordinarily nonpermeable ions such as sodium during the freezing. The resulting high intracellular sodium concentration leads to an intolerable level of swelling upon thawing. Based on his

experimental work, he further refined his hypothesis (1954 and 1955) and proposed the membrane dissolution theory [58,145]. It is suggested that hypertonic solution removes (by dissolving) membrane constituents resulting in the cell becoming increasingly permeable to solutes to such an extent that hemoglobin leaks from the cell [58,145]. Lovelock's idea that it is the intracellular electrolytes which play the important role has been contested by Mazur and co-workers [21,147] In contrast they emphasize the role of extracellular electrolytes and believe that the damage due to concentrating intracellular electrolytes during freezing is comparatively small.

Meryman (1968) in general agreement with Lovelock's hypotheses observed an increase in the intracellular sodium concentration as a result of hypertonic exposure of neutral salts as well as electrolytes [106]. He furthur reported that the sodium uptake is concurrent with the loss of intracellular potassium to the extracellular medium. From his work on the red blood cell Lovelock concluded that phospholipid is lost from the cell membrane to the environment and reported that the rate of loss increases abruptly at about 1400 mosm [145]. However, Meryman believes that the solute leak does not develop abruptly at any "minimum volume" or "critical osmolality" [106]. Meryman et al reported that the permeability of the red blood cell is altered due to excessive osmotic stress resulting in an inward leak of

solutes [110]. The inward leak of solute is lethal as upon return to isotonic suspension the cell will burst due to excessive swelling. The change in permeability characteristics of the cell and the release of membrane components, as referred to by Lovelock and Meryman, are interdependent. However, note that the changes in permeability characteristics of the cell membrane require minor actual structural alterations while much more severe structural changes of the membrane are required for the release of membrane constituents such as lipids and proteins [147]. That is the cell shrunken osmotically is more likely to be damaged during return to isotonic condition (thawing) than during hypertonic exposure (freezing).

Solvent water as was discussed earlier plays a fundamental role in regard to the non-covalent bonds between biomolecules. The ionic interactions are of utmost importance regarding the binding of the extrinsic proteins. It is also known that it is the water-membrane interactions which are primarily responsible for binding of drugs and hormones to the cell surface receptors [110]. In 1978 Volger et al working on isolated thylakoid membranes reported membrane protein release amounting up to 5% of the total membrane protein caused by increased salt concentration, even in the absence of freezing [36]. They suggested that the protein release in concentrated salt solution is caused by altered intramembrane ionic interaction. Volger et

al in agreement with Garber et al [110] concluded that the protein release and the change in membrane permeability is just a manifestation of the membrane damage and not the cause of it as was originally reported by Lovelock and others [58,106,144,145].

The hypotheses mentioned so far regarding the mechanism of damage to the cell membrane as a result of slow freezing are based on the fact that damage is due to increased solute concentration. In contrast to these views Mazur et al (1981) have reported their findings that show that slow freezing injury is far more dependent on the fraction of unfrozen water (solution) than it is on the solute concentration [142]. More precisely they conclude that the survival of a slowly frozen red blood cell is much more sensitive to the amount of water in the remaining unfrozen solution that it is on the amount of the salt (Nacl) in the solution. This supports the idea that the mere presence of extracellular ice could be lethal [143], and is a manifestation of the importance of the state of water associated with membrane constituent molecules. It is known that a certain amount of structurally important water called "bound water" does not have the osmotic properties of the bulk water [142]. The bound water is unfreezable and is an absolute requirement for the integrity of the membrane system. It is believed that the removal of water associated with the membrane protein for example due to freezing leads to denaturation of the protein [149,150].

From the foregoing arguments it is clear that no matter what the mechanism of the injury (in slow freezing) it is the result of dehydration which results in removal of membrane material. It is the osmotic water loss and the subsequent reduction in cell volume which triggers the string of events leading to damage. The mechanism through which the cell volume reduction could result in cell lysis is not clear. At this point we would like to examine the mechanism by which membrane material is lost as a result of events associated with slow freezing in light of morphological changes accompanying such events. The normal shape of red blood cell is a bioconcave discoid and it is known that perturbations in the suspending medium of the cell such as chemical agents could easily result in numerous morphological transformations [82]. Cell death as a result of environmental perturbations is always preceeded by some form of shape changes [86]. Different types and levels of perturbations result in a range of shape changes such as echinocytosis, myelin figures, envagination and endocytotic vesiculation [86,153-156]. An important parameter which influences the cell shape is the tonicity of the cell suspending medium. The shape changes as a result of exposure to typical lysins which eventually leads to lysis are described in detail by Ponder [86]. As a result of hypertonic exposure the membrane becomes creanated and while the effective area of the membrane remains constant the cell volume is decreased. As a result of membrane creanation the cell could develop into cup-shaped

stromatocytes or echinocytes. In the absence of the loss of membrane surface area by the breaking-off of such structures the process for most cases appears to be reversible [45,46]. It is known that the temperature controls all processes associated with living systems, specifically sub-zero temperatures play an important role in such processes. Williams proposed that osmotic stress due to freezing for example not only results in reduction of the cell volume but also cell surface area [157]. According to Williams the membrane material is lost during the shrinking process (hypertonic exposure) and the cell is lysed when it is returned to the isotonic condition. The cell bursts due to insufficient membrane material available to provide the required area for osmotic equilibrium. This is in line with Steponkus's maximum tolerable area increment hypothesis for spinach protoplast lysis which has also been observed to be the damaging mechanism for the red blood cell [106,130,158].

Araki (1979) reported that the red cell membrane treated with hypertonic saline at sub-zero temperatures results in the release of microvesicles [45]. He found that the vesicles contain a larger amount of lipid and less protein compared to the native red blood cell membrane. From his experimental results he concluded that the low temperatures induce lipid and protein segregation in the membrane. In 1982 Araki et al further reported segregation between different classes of lipids as well [46]. They also

showed that the membrane-constituent segregation is a temperature dependent process.

The hypotheses discussed here all point to the fact that the membrane constituent molecules are lost due to excessive osmotic stress. In the next section the membrane dissolution theory will be discussed further.

B. Theoretical Argument in Support of a Loss of Membrane Material (Dissolution Theory)

The extracellular perturbations such as low temperature and/or hypertonic exposure produce a complex set of events which could lead to a cellular damage. The dominant factor in determining the fate of the cellular system is clearly the osmotic stress. The mechanism of cellular injury as was discussed in the previous section is not clearly understood. However it is now clear that the primary site of damage is the cell membrane and the major consequence of the freezing and hypertonic exposure is an irreversible preferential aggegation or dissolution of macromolecules comprising the cell membrane. In this section attention will be centered on the mechanism of the loss of membrane material and a theoretical argument in support of this

notion will be presented. Specifically a model will be presented and the loss of membrane material will be considered as a consequence of cell volume reduction. Before we can attend to the difficult question of an equation of state for the membrane system, we need to clarify the important parameters of interest in such a considertion, namely the surface tension and surface pressure.

1. SURFACE TENSION-SURFACE PRESSURE

The following discussion is developed in light of the fact that surface tension is equal to negative surface pressure [87]. That is, membrane surface pressure and tension are used interchangably throughout this work. The membrane tension is a direct consequence of a hydrostatic pressure gradient across the cell membrane [87]. When a cell is in osmotic equilibrium with the environment there exists a small pressure gradient across its membrane, hence the cell membrane in the natural (force free) state is under negligible, if any, tension [87]. Cells under osmotic stress have well recognizable geometrical configurations, a reflection of membrane tension. In the tension free state the effective surface area per molecule $\bar{A}_o$ is such that the free energy per molecule, G, is minimized. According to Tanford for a

spherical vesicle the surface tension is zero in the absence of a hydrostatic pressure gradient across the membrane

$$2\gamma = (\partial G/\partial A)_{n,v,T}$$
$$= 0 \qquad [8.1]$$

where 2γ is the membrane tension, n is the number of molecules within the membrane, T is temperature, and v is the membrane volume [73].

For some cases it is known that cell shrinkage results in the reduction of the cell surface area as well as its volume [108,141]. There is also evidence that volume reduction due to osmotic stress is accompanied by a surface pressure build up in the membrane [159]. That is the driving force for expulsion of membrane-residing molecules and therefore membrane injury is the existence of an intra-membrane pressure. Positive pressure exists during osmotic shrinkage and the surface pressure is negative (tension) during osmotic swelling.

According to the analytical argument outlined in chapter 3 based on a lipid vesicle model system, reduction in the area of the cell membrane is only possible through two modes. If the vesicle is to respond to environmental perturbation through the first mode, where the number of molecules comprising the membrane

is conserved (closed system), the magnitude of the free energy per molecule will increase. This then results in changing the area per molecule away from the force free state value. The increased interfacial pressure could result in buckling and failure of the membrane and subsequently lysing. The membrane system could also respond through the second mode, where the number of molecules in the membrane is not conserved (open system). In this case an interfacial pressure will develop due to close packing of molecules as before. This, as pressure is related to the number density [87], implies that the mechanism by which the interfacial pressure is relaxed is through the loss of membrane-residing molecules.

Langmuir has shown that a reduction in surface area of lipid monolayers results in the development of tangential pressure within the interface [160]. Once the potential energy stored as a surface pressure exceeds the hydrophobic forces responsible for the planar assembly of molecules within the interface the molecules are forced out of the lipid interface [161]. The loss of individual molecules from the cell membrane such that for example lipid molecules leaving the membrane and becoming dissolved in the environment is not likely to be the case. This is due to extremely low solubility of the membrane components in water (lipid: water ratio of 10^{-4} which is a reflection of high energy expenditure for the process [73,172]. That is if a

molecule is forced out of the membrane system, there is a favorable energy path for reincorporation.

An alternative mechanism is that the molecules leave the membrane as clusters. That is, once forced out they will assemble into stable configurations such as micells or microvesicles. This implies that once the components are lost it is highly unlikely that they could be reincorporated back into the membrane. This is found to be the case in several instances. For example for red cells treated with hypertonic salt at low temperatures [40,41,42]. However, the observations such as membrane creanation and rod formation in living cells and liposomes suggest that the molecules could leave the membrane plane and still remain physically attached to it for some time before it is pinched off [43,44]. Therefore a more realistic approach is to assume that the membrane system is capable of exchanging material with a reservior. Although the specific mechanism involved is not clearly understood the reservior approach has gained a wide support.

According to Wolfe the equilibrium tension in a membrane capable of exchanging material with a reservior is given as

$$2\gamma = 2\Delta G/\bar{A} \qquad [8.2]$$

where ΔG is the free energy difference per molecule between the

reservior and the membrane at the force free state (tension ~ 0) and $\bar{A}$ is the effective area per molecule in the membrane [162].

The existence of a membrane material reservior explains several observed behaviors associated with biomembranes and liposomes. When the membrane is subject to tension as is the case for swelling in the hypotonic condition, according to Equation 8.2 the internal free energy of the system increases. Therefore this creates a favorable energy condition for incorporation of reservior material into the membrane. This process will result in relaxation of membrane tension to the equilibrium level. On the other hand if the membrane is stressed such that molecules are forced to pack closer (cell shrinkage and negative membrane tension) the internal free energy of the system is again increased. The energy is minimized by forcing molecules into the reservior.

So far we have talked about "a" reservior, however the reservior referred to in this work could consist of several components or smaller reserviors distributed all over the membrane.

2. Thermodynamic Development of Equation of State of Bilayer Membrane-Supporting the Loss of Membrane Material

The theory developed here is aimed at arriving at an equation describing the size (volume) of a model membrane system (liposome) as a function of the extraliposomal solute concentration. The liposome is chosen as our model system which is a three component system comprised of lipid, sucrose or Nacl, and water. Before proceeding with the thermodynamic argument, let us outline the basic assumptions:

1) Interfacial region is assumed to be impermeable to solute (semipermeable membrane).
2) The osmotic response of the liposome is assumed to be a reversible process.
3) Constant temperature process.
4) No chemical reaction is involved.
5) Non-Planar geometry.

The vesicle at equilibrium is under mechanical constraint manifested in the spherical geometry ofsuch a system which results in a surface tension T. The mechanical constraint is arrived at through the following force balance argument.

The forces acting on the surface could be classified into normal and tangential forces. At equilibrium any change in tangential force TdA is balanced by subsequent change in the

normal force (P'-P")dv, where P' and p" are internal and external pressures respectively.

Hence

$$(P'-P")dV = TdA \qquad [8.3]$$

Equation 8.1 for spherical geometry gives

$$(P'-P")=2T/r \qquad [8.4]$$

where r is the radius of the curvature. The above mechanical constraint and the physico-chemical constraint make up our equilibrium conditions. Due to low solubility of lipid in water ($1:10^4$) the system consists of two compartments divided by a semipermeable membrane. Therefore the system could be illustrated as in Figure 8.1. For the membrane, permeable to water but impermeable to solute, the physico-chemical equilibrium condition is when the chemical potential (partial molal Gibbs free energy) of permeant molecule in this case water inside and outside the membrane are equal;

$$\mu_w^i = \mu_w^o$$

The existance of a semipermeable membrane results in an osmotic pressure. Thus the equilibrium condition could be written as

$$\mu_w^i(T,P+\pi,n) = \mu_w^o(T,P,n)$$

where π is the osmotic pressure.

At this point let us relate the osmotic pressure to the solvent content of each component. The chemical potential in general is written as

$$\mu_i(T,P,n) = \mu_i^o(T,P) + RT\ln a_i + Z_i f\xi$$

where a_i is the activity of the ith specie, and $Z_i f\xi$ is identically zero for nonelectrolytes. Expanding the μ_i^o about P_o using Taylor series expansion we have

$$\mu_m^o(T,P) = \mu_i^o(T,P) + (P-P_o)(\partial\mu_i/\partial P)_{T,P_o} + \text{Higher order terms}$$

For the system under consideration here the standard pressure P_o is generally taken to be the atmospheric pressure and it is deleted from the equation. As a result it is understood that the pressure is the excess pressure. The above expression for the chemical potential for a component with negligible compressibility is written as

$$\mu_i^o(T,P) = \mu_i^*(T) + \bar{V}_i P$$

where

$$\bar{V}_i = (\partial \mu_i / \partial P)_T$$

= Partial molar volume

Now for the osmotic equilibrium;

$$\mu_w^i(T) + \bar{V}_w(P+\pi) + RT\ln a_w^i = \mu_w^o + \bar{V}_w P + RT\ln a_w^o$$

or

$$\bar{V}_w \pi = RT\ln(a_w^o / a_w^i)$$

The water activity can be expressed as

$$a_w = \gamma_w X_w$$

where γ_w is the activity coefficient, and X_w is the mole fraction of water.

For an ideal solution, γ_w is equal to 1 and this condition is approached for a dilute solution. As the vesicles are formed in a very low solute concentration to a good approximation $a_w^i = 1$, therefore

$$\pi = RT/\bar{V}_w \ln(a_w^o)$$

$$= RT/\bar{V}_w \ln(X_w^o / \bar{V}_w)$$

$$= RT/\bar{V}_w \ln[n_w^o / (n_w^o + n_s^o)]$$

$$= -RT^{o}\ln(1+n_s^o/n_w^o)/\bar{V}_w$$

with the dilute assumption,

$$n_s^o << n_w^o \quad \text{and} \quad n_s^o/n_w^o << 1$$

expanding the logarithm we have

$$\pi = RT(n_s^o/n_w^o)/\bar{V}_w$$

where n_w is the number of moles of water and n_s is the number of moles of solute.

Rewritting the physico-chemical equilibrium condition as

$$\mu_w^o(T)+\bar{V}_w P^o+RT\ln a_w^o = \mu_w^o(T)+\bar{V}_w P^i+RT\ln a_w^i$$

we have

$$RT\ln a_w^o = RT\ln a_w^i + \bar{V}_w(P^i - P^o)$$

Now, as $n_s << n_w$, $n_s/n_w << 1$ the above equation could be written as

$$RT(n_s^o/n_w^o) = RT(n_s^i/n_w^i) - \bar{V}_w(P^i - P^o) \quad [8.4]$$

Substitutiong for the left hand side of Equation 8.4 from Equation 8.3 we have

$$\pi = RT(n_s^i/n_w^i)/\bar{V}_w - (P^i - P^e) \qquad [8.5]$$

Again as the system is assumed to be dilute;

$$V_{cell} = V = \bar{V}_w n_w^i + \bar{V}_s n_w^s$$
$$\simeq \bar{V}_w n_w^i \qquad ; \quad n_w^i >> n_w^s$$

Therefore Equation 8.5 becomes

$$\pi = RTn_s^i/V - (P^i - P^e) \qquad [8.6]$$

Substituting for $P^i - P^e$ from the mechanical constraint, Equation 8.1., we have

$$\pi = (RT/V)n_s^i - (2\bar{T}/r) \qquad [8.7]$$

The surface pressure for a bilayer system is given by [87]

$$T = \gamma(T) - ncT/(A - n\bar{A}_e) \qquad [8.8]$$

Where A is the total area of the bilayer, $\bar{A}_e$ is the excluded area

per molecule, c is a constant equal to 4k where k is Boltzman's constant, n is the number of molecules in the bilayer, and γ is the interfacial free energy density. In the snatural (force free) state T is equal to zero and we have [87]

$$\gamma = cT/(\bar{A}_o - \bar{A}_o)$$
$$= 70 \text{ dyn/cm}$$

where

$$\bar{A}_o = 68\text{Å}^2$$

If the initial vesicle volume is denoted by V_o, then

$$\pi_{initial} = RTn_s^i/V_o \qquad [8.9]$$

Now with Equations 8.8 and 8.9, Equation 8.7 becomes

$$\pi = (V_o/V)\pi_o + 2ncT/r(A - n\bar{A}_o) - 2\gamma/r$$

where for spherical geometry

$$\pi = (V_o/V)\pi_o + 2ncT/(3V-rA_o) - 2\gamma/r \qquad [8.10]$$

The excluded area per molecule $\bar{A}_o$ from monolayer studies is approximated by a value of 38 Å^2. Therefore as $\bar{A}_o$ is taken to be equal to 68 Å^2 we have

$$A_e = \varepsilon A_o \quad \text{and} \quad \varepsilon = 38/68$$

Equation 8.10 after some algebraic manipulation becomes

$$\pi V = \pi_o V_o + K/[1-\varepsilon(r_o/r)^3] - 2\gamma(V/r) \quad [8.11]$$

where

$$K = 2/3nRT.$$

The behavior of the second term on the right hand side of Equation 8.11 is very interesting. The denominator becomes zero at $r=(.56^{**}.5)r_o$ which implies the vesicle could not be shrunken beyond this size. Equation 8.11 predicts the volume response of the liposomes very well for sucrose concentration of .1M. Compared to the experimental values of D. Callow [95] Equation 8.11 gives

Actual Sucrose Conc.	Calculated Sucrose Conc.*
.1	.0996
.1	.1031
.1	.102

* The sucrose concentration is calculated based on the measured volume of the vesicle through Equation 8.11.

The minimum cell criteria arrived at in Equation 8.12 in order not to conflict with the observed behavior of such systems must mean that the closed system assumption is not valid. That is to say the system shrinks beyond r_e by losing the membrane constituents.

CHAPTER IX

THERMODYNAMIC AND KINETIC TERATMENT OF HEMOLYSIS

A. Introduction:

The fate of living systems is governed by harmonious chemical and physical processes which occur continuously in such systems. The stability of a biological system is likely to be increasingly jeopardised as these reactions are altered and the system is removed further from what might be considered a normal or physiological equilibrium state. These reactions and processes involve the transfer and transformation of both energy and matter. Thermodynamic study and analysis of such systems is of immense practical value as it is on the basis of thermodynamics that one can study the energy changes.

In most biological systems, at physiological temperatures and pressures some biological reactions proceed at very slow rates conferring stability on living systems. When such a system is removed too far from its physiological equilibrium state, some reactions which are normally exceedingly slow take place with

extreme rapidity with often deadly results. The result of perturbing the system away from its equilibrium state to various extents can be useful in establishing quantitative measures of the amount of damage expected for a given mode and magnitude of perturbation. This could also result in a suggested mechanism by which the damage process occurs.

One example of this stability problem arises when cryopreservation of a biomaterial is attempted. For freezing damage, the perturbations considered in this study are the increasingly concentrated solutes in solution and the reduction in absolute temperature.

Thermodynamics offers a self-contained logical structure based on a set of far-reaching phenomenological laws. Thermodynamics is one of the few disciplines of physical sciences which is largly independent of any assumptions or hypothesis regarding the nature of the fundamental particles (molecular and atomic theory of matter) and it considers only observable, macroscopic changes. Based on the detailed elaboration of thermodynamic laws, predictions may be made concerning the effect of operationally definable quantities, such as pressure, temperature and composition, for very complicated chemical and physical situations. For instance, thermodynamic laws enable one to relate the events associated with a chemical reaction, to the

observed behaviour of energy. The real strength of a thermodynamics study lies in the fact that the physical and chemical phenomena are described in terms of easily controlled variables such as pressure, volume, temperature and composition. Since it does not depend on "mechanism" per se , and on events at the sub-macroscopic level, such as are used in theories of molecular structure and kinetics, it can not contribute directly to such molecular theories. However, thermodynamics complements and offers a good check on such theories. This is accomplished by means of interpreting the thermodynamically attained parameters or constants at a molecular level or comparing such values with the ones calculated from molecular theory.

As was pointed out in an earlier chapter, in this study we were concerned with the osmotic shock aspect of "solution effect" freezing injury. That is, the data presented quantify the damage histories to be expected when human erythrocytes are subject to step changes in osmotic concentration (from an isotonic to a hypertonic condition) at various isothermal set points. It is well known in cryobiology that frozen-thawed cell recovery can be very sensitive to the rates of freezing and thawing [20-23]. It is therefore important to study the damage process on a rate basis in order to correlate the extent of damage with the time of exposure to any temperature or concentreation.

B.Hemolysis-Reaction

The red blood cell (RBC) exposed to a hypertonic concentration of sodium chloride (Nacl) is hemolysed as a consequence of Nacl interacting with the cell. In light of chemically reacting systems (mixtures), this reaction could be modeled as

$$RBC + NaCl \rightarrow RBC^{*} + NaCl$$

where RBC^{*} represents a partially hemolysed RBC population.

An important point to note is that in the analysis of the hemolysis kinetics presented here only the initial portion of the RBC response will be considered.

In such a system, the degree and rate of hemolysis depends on the tonicity (level of salt concentration) as well as the RBC concentration and temperature [163]. The cell concentration dependence is only significant at concentrations an order of magnitude larger than the concentrations considered in this work [163].

Concerning classical chemically reacting systems, there are

generally two main reasons for studying the rates of reactions. The first is the prediction of the dependency of the rate of the reacting mixture on a number of controllable factors such as pressure and temperature. This is of major practical importance as it would enable us to arrive at an optimum rate for which the reacting mixture will move to its equilibrium state. For instance, from an industrial point of view it is desirable for the reactions to proceed very rapidly in order to save time and produce more (save money).

From the cryopreservation point of view it is of utmost importance to acquire a detailed knowledge of the temperature dependency of the reacting mixtures namely sodium chloride and red blood cell. This knowledge could help reduce the uncertainty involved in the design of a working freezing protocol by gaining valuable insight with regard to freezing and thawing rates. The reactions to proceed very rapidly in order to save time and produce more (save money).

The mechanism is the final goal of the more chemically oriented study. Over looking such elementary and intermediate reactions does not effect the generality of our analysis.

The rationale for this is that for a series of consecutive reactions the overall rate is determined by the rate of passage of

activated complexes (molecules with enough energy to take part in reaction) over the highest energy barrier. From the stand-point of the theory of absolute reaction rates, it is sufficient, provided that equilibrium is established between the various intermediate states, to consider only the equilibrium between the initial state and the rate-determining activated state. Therefore all intermediate states can be neglected [164].

C.Rate Law and Rate Constant

In chemical kinetics the rate of reaction R at constant temperature, based on the historic mass action rate law form, is conventionally presented as a function of the composition of the system in the general form of

$$\begin{aligned} R &= f(\text{Reactants and products}) \\ &= -d[A]/dt \\ &= f([A],[B],[C],\ldots) \end{aligned} \qquad [9.1]$$

Where A,B, and C, etc. are reactants and products. The above expression which gives the rate of reaction R as a function of concentrations, is customarily referred to as the "rate law" for the reaction under consideration.

The complete mathematical characteristics and functional form of the rate law are often very complicated. However, one can considerably reduce the complexity of the rate law by proper choice of experimental conditions. Therefore, the rate law almost always reduces to the form

$$R = K(T)[A]^x[B]^y[C]^z \qquad [9.2]$$

Where K is some coefficient independent of concentrations, but usually dependent on the temperature; it is called the rate coefficient or the rate constant.

The statement of the rate law, given the composition and temperature of the reacting mixture and the experimental value of the rate constant K, permits the prediction of the rate. It also gives the order of the reaction where, the order of a reacton is the sum of powers to which the concentrations of the components are raised in the rate law.

The rate law for the system of (RBC + salt) takes the form

$$R = -d[RBC]/dt$$
$$= K(T)[RBC]^x[Na^+]^y[Cl^-]^z \qquad [9.3]$$

All the kinetic data are generated at nominal RBC concentration

level of 4% (Hematocrit) for different sodium chloride concentrations ranging from 1M to 4M. That is, reagents $[Na^+]$ and $[Cl^-]$ are in great excess throughout the course of each experiment so that their concentrations remain virtually constant. Therefore, the rate law could now be written as

$$R = K_p(T, [Na^+], [Cl^-])[RBC]^x \qquad [9.4]$$

where K_p is a psuedo-reaction rate constant.

$$K_p = K(T)[Na^+]^y[Cl^-]^z.$$

Once the reaction rate for the suggested rate law is evaluated, the next task would be that of determining how such rates vary with temperature and with the degree of tonicity of the suspending media of the red blood cells.

The kinetic data is in the form of a hemolysis time history, therefore to relate the rate as defined in Equation 9.3 to percent hemolysis we can write

$$\%\text{Hemolysis} = \%H$$
$$= 100\%([RBC]_o - [RBC]_t)/[RBC]_o \qquad [9.5]$$

where $[RBC]_o$ and $[RBC]_t$ refer to the initial and instantaneous

intact RBC concentrations. Thus

$$d[\%H]/dt = 100\%R/[RBC]_o \qquad [9.6]$$

solving Equation 9.6 for R we have

$$R = [RBC]_o/100\% \cdot d[\%H]/dt$$

Now Equation 9.4 could be written as

$$R = K'_p(T, [Na^+], [Cl^-], [RBC]_o)[RBC]_t^x \qquad [9.7]$$

where

$$K'_p = K_p(T, [Na^+], [Cl^-])[RBC]_o/100\%$$
$$= K(T)[Na^+]^y[Cl^-]^z[RBC]_o/100\%$$

but from Equation 9.5 we have

$$[RBC]_t = [RBC]_o - [\%H][RBC]_o/100\%$$

Therefore Equation 9.7 becomes

$$R = K'_p([RBC]_o - [\%H][RBC]_o/100\%)^x$$
$$= K'_p[RBC]_o^x(1 - [\%H]/100\%)^x \qquad [9.8]$$

Substituting for R from Equation 9.8 in Equation 9.6 we have

$$d[\%H]/dt = 100\%K'_p[RBC]_o^{x-1}(1 - [\%H]/100\%)^x \qquad [9.9]$$

In the above equation, K'_p and $[RBC]_o$ are constants for a given experimental run because T, $[Na^+]$, $[Cl^-]$, and $[RBC]_o$ remain unchanged for a given experimental run, so Equation 9.9 could now be written as

$$d[\%H]/dt = K_p^*(1 - [\%H]/100\%)^x \qquad [9.10]$$

where

$$K_p^* = 100\%K'_p[RBC]_o^{x-1}$$
$$= K_p[RBC]_o^x$$

To integrate Equation 9.10, write:

$$d[\%H] = -d(1 - [\%H]/100\%)100\%$$
$$= -dA(100\%)$$

where A is the percent red blood cell survival.

Then Equation 9.10 becomes

$$-dA/dt = K_p^*A^x/100$$

or

$$A^{-x}dA = -K_p^*dt/100 \qquad [9.12]$$

Next, the 1st and 2nd order hemolysis reaction rate laws will be discussed and the results of each rate law model will be presented later. The rationale for not considering the zeroth order reaction rate law lies in the fact that the kinetics of the hemolysis process shows a strong concentration and temperature dependence.

1. First Order Reaction Rate Law

If x=1 in the differential rate law (Equation 9.12); i.e. the forward reaction rate depends only on the concentration of some reactant A. The rate law is then

$$A^{-1}dA = -K_p^* dt/100$$

This integrates to give

$$A = A_0 e^{-\alpha} \qquad [9.13]$$

where

$$\alpha = K_p^* t/100$$

and

$$A_0 = A(t=0)$$
$$= 1$$

This well known rate law is obeyed in radioactive decay of an unstable nucleus and bacterial growth processes. Now, if our system is to obey the 1st order rate law, a plot of ln[A] vs time should give a straight line with slope equal to $-K_p^*/100$. The initial hemolysis data is fitted into the above relationship and the rate constant K_p^* for given temperature and solute concentration are tabulated in Table 9.1. The results show a good fit for this rate law with correlations at different conditions ranging from .9756 to .9991. The rate constant for a given solute concentration as a function of inverse temperature is plotted in the Appendix. This kind of plot could be used to infer the mechanism of the hemolysis process.

2. Second Order Reaction Rate Law

The rate law Equation 9.12 for x=2 results in

$$A^{-2}dA = -K_p^*dt/100$$

which is the second order rate law. This integrates to give

$$A^{-1} = K_p^*t/100 + A_o^{-1} \qquad [9.14]$$

Where A_o is the constant of integration and is evaluated by

TABLE 9 .1

Reaction Rate Constant and Activation Energies For 1st and 2nd Order Reaction Rate Laws

		1st Order Rate Law			2nd Order Rate Law		
C(m)	T(K)	K_p^*	$\Delta G^{\#}$ (Kcal/mole)	r^2	K_p^* (sec^{-1})	$\Delta G^{\#}$	r^2
	298	0.190	18.43	.9830	0.190	18.43	.9962
	283	0.064	18.08	.9922	0.061	18.11	.9994
2.5	278	0.061	17.78	.9967	0.065	17.74	.9964
	273	0.048	17.58	.9916	0.051	17.55	.9967
	268	0.060	17.13	.9916	0.060	17.13	.9908
	298	0.840	17.54	.9935	0.962	17.47	.9855
	283	0.453	16.98	.9897	0.543	16.88	.9805
3.0	278	0.234	17.04	.9973	0.259	16.98	.9953
	273	0.261	16.66	.9991	0.290	16.60	.9987
	268	0.380	16.14	.9954	0.472	16.03	.9933
	298	2.396	16.92	.9775	3.651	16.68	.9943
	283	1.840	16.19	.9932	0.921	16.58	.9807
3.5	278	0.881	16.30	.9860	1.019	16.22	.9760
	273	1.086	15.89	.9975	1.523	15.70	.9643
	268	1.268	15.50	.9945	0.638	15.87	.9938
	298	4.90	16.50	.9810	11.26	16.01	.9838
	283	3.80	15.78	.9820	2.87	15.94	.9623
4.0	278	2.23	15.79	.9756	1.80	15.91	.9623
	273	2.41	15.45	.9940	2.57	15.42	.9896
	268	2.65	15.11	.9865	2.43	15.16	.9630

requiring that at t=0, $A=A_o$. Equation 9.14 is the integrated rate law for a second-order reaction. The initial hemolysis data is fitted into the above form and the rate constant K_p^* for given temperature and solute concentration are tabulated in Table 9.1. The results show good fit with correlations ranging from .9301 to .9994. Comparing the results for first and second order rate laws indicates that the derived rate constants are not too much different to substantially effect the free energy of activation. Therefore it is impossible to choose one rate law over the other on this basis. However, the fact that the 2.5m results are very close for both rate laws can be interpreted to indicate that the reaction process (the damage mechanism) is somewhat different than those at higher solute concentration levels.

3. Mechanism

Mechanism in chemistry is defined as, the detailed way through which the reactants are converted into products. The kinetic study from a chemistry point of view is not complete unless the study reveals the mechanism of the chemical reaction. Information about the mechanism is gained from a detailed knowledge about the rate of reaction under various temperature, pressure, and composition conditions. This is why the kinetic study in general is very complicated and often controversial. The

rate at which equilibrium is attained and the position of equilibrium play important roles in the study of reactions. Changes of activation parameters, free energy $\Delta G^{\neq}$, entropy $\Delta S^{\neq}$, and enthalpy $\Delta H^{\neq}$ can be obtained from the equilibrium reaction rate constant. The equilibrium state is generally independent of the mechanism, whereas the rate at which the reaction proceeds to the equilibrium state depends on the mechanism.

D. Thermodynamics of Reaction Rates

1. The Temperature Dependence of the Rate of Reaction: The Arrhenius Equation

The Arrhenius rate law marks the origin of modern kinetic theory. With very few exceptions the rate of reaction decreases exponentially with a decrease in temperature. Arrhenius [166] to account for the temperature dependency of the inversion rate of sucrose, put forth the idea that the variation of the specific rate or rate constant K of the reaction with respect to temperature is expressed as;

$$K = Z\, e^{-E_a/RT} \qquad [9.15]$$

where Z is the "frequency factor" or pre-exponential factor and E_a is the "energy of activation" or more correctly the "experimental activation energy" of the reaction. It is apparent from Equation 9.1 that by determining the value of K at several temperatures, the plot of logK vs 1/T will yield the activation energy from the slope of the curve and the frequencey factor from the intercept with the lnK axis.

The activation energy, E_a, of the reaction (chemical or physical) represents the energy that the molecule must posses if it is to take part in the reaction (activated state). The determination of the activation energy is an important objective of any kinetic investigation. The frequency factor (sometimes called the "collision number" or "collision frequency") Z, for a reaction which is the consequence of the collision of two molecules may be regarded as the number of collisions per second. Where $\exp(-E_a/RT)$, is a measure either of the probability of the occurrence of the activated state or a measure of the fraction of the total number of molecules which have proper level of activation energy to take part in the reaction (fraction with energies greater that E_a). The frequency factor is usually found to depend on temperature, however, unless the temperature range is very large, the temperature effect is almost always negligible[164].

Chemical reactions depend very strongly on temperature and most are found to follow the Arrhenius rate law. Provided that the temperature range is not large, certain physical processes also follow the Arrhenius rate law. The Arrhenius rate law Equation 9.1 is justified on a theoretical basis from either collision theory or the theory of absolute reaction rates. Even though the former approach is intuitively more appealing the latter is more elegant. Nevertheless neither theory is able to predict the activation energy except for very simple cases.

2. Free Energy and Entropy of Activation

The equilibrium constant $K^{\neq}$ for a reacting system(chemical or physical) is given by

$$K^{\neq} = C_1 / C_2$$
$$= N_1 / N_2$$

where

C_1 = Concentration in activated state

C_2 = Concentration in initial state

N_1 = No. of molecules in activated state

N_2 = No. of molecules in initial state

The assumption that the activated complex is in thermodynamic equilibrium with the reactants involved in the reaction allows one to arrive at thermodynamic parameters of the reaction by an equilibrium thermodynamic analysis. Therefore, the equilibrium constant $K^{\neq}$ may be expressed in terms of the standard free energy of the process or sometimes called Gibbs function of activation or simply "free energy of activation", $\Delta G^{\neq}$, by means of the familiar thermodynamic equation (definition)

$$-\Delta G^{\neq} = RT\ln K^{\neq} \qquad [9.16]$$

The specific reaction rate or more generally the rate constant K can be shown to have the form

$$K = kTK^{\neq}/h \qquad [9.17]$$

where k is Boltzmann's constant and h is Plank's constant and it is assumed that the rate constant is expressed in terms of concentrations of the reactants and products[167]. Equation 9.17 is the Eyring equation for the rate constant of a reaction. Introducing $K^{\neq}$ from Equation 9.16, it follows that

$$K = (kT/h)e^{\Delta G^{\neq}/RT} \qquad [9.18]$$

Since a Gibbs function is related to the entropy and enthalpy by

$$G = H - TS$$

this for constant temperature process leads to the introduction of the entropy of activation, $\Delta S^{\neq}$, and the enthalpy of activation $\Delta H^{\neq}$;

$$\Delta G^{\neq} = \Delta H^{\neq} - T\Delta S^{\neq} \qquad [9.18']$$

Introduction of this expression into Equation 9.4 leads to

$$K = (kT/h)e^{-\Delta H^{\neq}/RT}e^{\Delta S^{\neq}/R} \qquad [9.19]$$

where $\Delta H^{\neq}$ and $\Delta S^{\neq}$ are generally referred to as the "heat of activation" and "entropy of activation" respectively. Equation 9.19 resembles the Arrhenius equation (Equation 9.15) except that $\Delta H^{\neq}$ appears instead of E_a and according to this equation the frequency factor is

$$Z = (kT/h)e^{\Delta S^{\neq}/R} \qquad [9.20]$$

From Equation 9.20 it is apparent that a negative entropy of activation results in a low frequency factor while a positive entropy of activation results in a high frequency factor.

At this point it is essential to discuss the respective interdependency of $\Delta G^{\neq}$, $\Delta H^{\neq}$, and $\Delta S^{\neq}$ and their consequent effect on the rate of a reaction. Comparing Equations 9.17 and 9.18 it is clear that it is the free energy of activations $\Delta G^{\neq}$ which is the determinant of the rate of the reaction. This is especially important for reactions in liquids where large values of $\Delta H^{\neq}$ are compensated by high values of $T\Delta S^{\neq}$, whereas in many gas reactions, since the entropy of reaction does not vary greatly, the $\Delta H^{\neq}$ may appear to play an important and deterministic role [167]. In general, any factor decreasing the free energy of activation $\Delta G^{\neq}$ will result in increasing the rate. This fact is explored to advantage where certain substances, called catalysts, are employed to increase the rate of the reaction by lowering the free energy of activation.

3. Experimental Activation Energy

An experimental activation energy can always be attained even when the rate coefficient does not follow the Arrhenius rate law form given by Equation 9.15 through the defining statement [166];

$$E_a = RT^2(\partial \ln K/\partial T)_v \qquad [9.21]$$

It is desirable to incorporate the experimental activation energy, E_a, into Equation 9.19 in place of $\Delta H^{\neq}$ as E_a can be found from the reaction rate constant, K, through Equation 9.21. Equation 9.17 may be written as

$$\ln K = \ln k/h + \ln T + \ln K^{\neq} \qquad [9.22]$$

Where upon differentiation with respect to temperature we have

$$\partial \ln K/\partial T = 1/T + \partial \ln K^{\neq}/\partial T \qquad [9.23]$$

but from Equation 9.21

$$\partial \ln K/\partial T = E_a/RT^2 \qquad [9.24]$$

also from Equation 9.16 we have

$$\partial \ln K^{\neq}/\partial T = \Delta G^{\neq}/RT^2 - (1/RT)\partial \Delta G^{\neq}/\partial T$$
$$= \Delta H^{\neq}/RT^2 - \Delta S^{\neq}/RT - (1/R)\partial \Delta G^{\neq}/\partial T \qquad [9.25]$$

but since

$$-\Delta S^{\neq} = \partial \Delta G^{\neq}/\partial T$$

Equation 9.25 becomes

$$\partial \ln K^{\neq}/\partial T = \Delta H^{\neq}/RT^2 \qquad [9.26]$$

Therefore with Equations 9.24 and 9.26, Equation 9.22 becomes

$$E_a/RT^2 = 1/T + \Delta H^{\neq}/RT^2 \qquad [9.27]$$

solving for E_a gives

$$E_a = RT + \Delta H^{\neq} \qquad [9.28]$$

Now introducing the $\Delta H^{\neq}$ as given by Equation 9.28 into Equation 9.19 results

$$K = (kT/h)e^1 e^{\Delta S^{\neq}/R} e^{-E_a/RT} \qquad [9.29]$$

The data fitting procedure is discussed in detail, in the Appendix. The in Figures 7.2-7.6 were fitted to produce the reaction rate constants tabulated in Table 1 and Table 2 in the Appendix. These reaction rate constants are then used in Equations 9.16 and 9.26 to yield $\Delta G^{\neq}$ and $\Delta H^{\neq}$ respectively. The thermodynamic parameters $\Delta G^{\neq}$, $\Delta H^{\neq}$, and $\Delta S^{\neq}$ along with the reaction rate constant K_p are presented in Tables 9.1 and 9.2.

From Table 9.2 it is evident that $\Delta G^{\neq}$ decreases with respect to decreasing temperature and increasing osmotic concentration. All $\Delta S^{\neq}$ values except one (believed to be due to an artifact) are negative. The $\Delta H^{\neq}$ values range from positive to negative but in most cases are positive. Furthermore the rate constant K_p increases with increasing osmotic concentration.

TABLE 9 .2

Activation Parameters For 1st and 2nd Order Rate Laws

		1st Order Rate Law			2nd Order Rate Law		
C(m)	T(K)	$\Delta G^{\neq}$ (Kcal/mole)	$\Delta S^{\neq}$	$\Delta H^{\neq}$ (Kcal/mole)	$\Delta G^{\neq}$	$\Delta S^{\neq}$ (cal/mole C)	$\Delta H^{\neq}$
	298	18.43	-23.33	10.78	18.43	-21.33	12.07
	283	18.08	-36.67	7.70	18.11	-48.67	4.34
2.5	278	17.70	-50.00	3.88	17.74	-56.00	2.17
	273	17.58	-65.00	-1.65	17.55	-61.00	.90
	268	17.13	-90.00	-6.99	17.13	-84.00	-5.38
	298	17.54	-37.33	6.41	17.47	-39.33	5.75
	283	16.98	-12.62	13.40	16.88	-9.67	14.14
3.0	278	17.04	-32.00	8.14	16.98	-28.00	9.20
	273	16.66	-90.00	-7.91	16.60	-95.00	-9.34
	268	16.14	-104.00	-11.73	16.03	-114.00	-14.52
	298	16.92	-48.67	2.42	18.68	-6.67	14.69
	283	16.19	-13.33	2.42	16.58	-39.34	5.45
3.5	278	16.30	-30.00	7.96	18.22	-88.00	-8.24
	273	15.89	-80.00	-5.95	15.70	-35.00	6.15
	268	15.56	-78.00	-5.40	15.87	34.00	24.98
	298	16.50	-48.00	2.20	16.01	-4.67	14.62
	283	15.78	-23.00	9.27	15.94	-5.33	14.43
4.0	278	15.79	-33.00	6.62	15.91	-52.00	1.45
	273	15.45	-68.00	-3.11	15.42	-75.00	-5.06
	268	15.11	-68.00	-3.11	15.16	-52.0	1.22

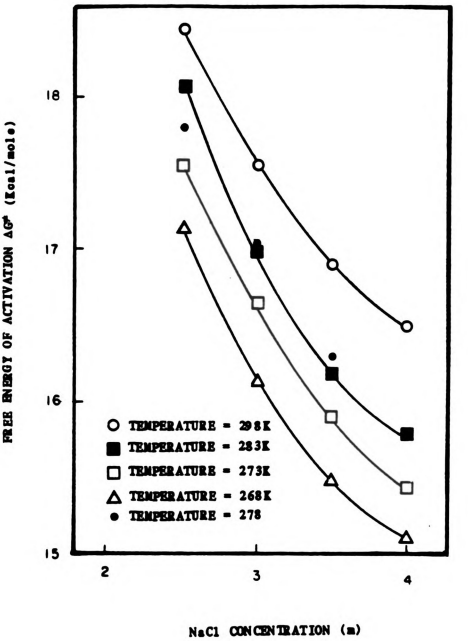

Figure 9.1: The Relationship Between Free Energy of Activation and NaCl Concentration for 1st order Reaction Model.

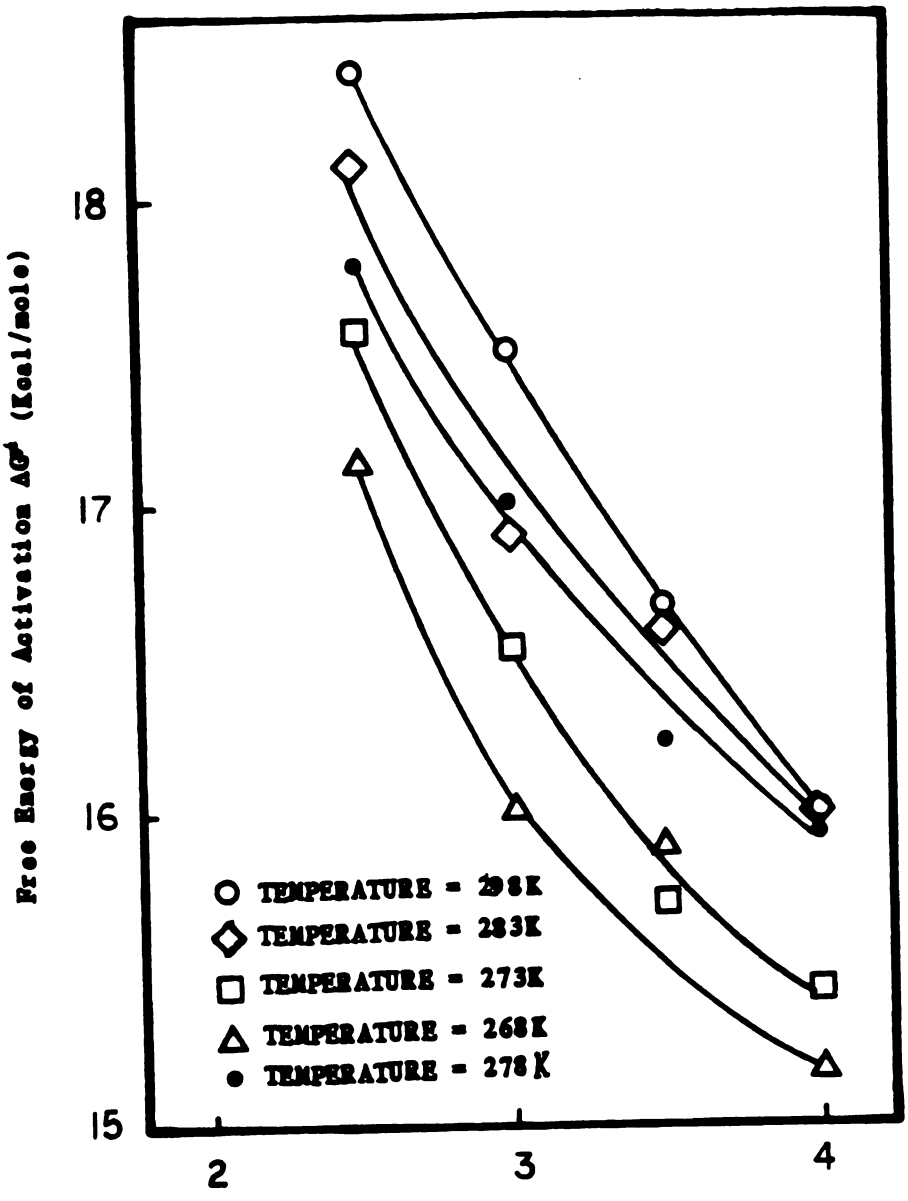

Figure 9.2: The relationship Between Free Energy of Activation and NaCl Concentration for 2nd order Reaction Model.

The free energy of activation $\Delta G^{\ddagger}$ for the hypertonic hemolysis process has been plotted in Figures 9.1 and 9.2 as a function of extracellular sodium chloride concentration for different temperatures for 1st and 2nd order rate laws respectively. The data show slight deviation from a linear relationship. Since the reaction rate will increase exponentially as the free energy of activation decreases (see Equation 9.18), the negative slopes of these curves indicate that an increasingly hypertonic NaCl solution will greatly enhance the initial rate of the destructive reaction process. The room temperature data is somewhat less effected by NaCl concentration as indicated by smaller slope. The lowest $\Delta G^{\ddagger}$ values are recorded for the lowest temperature studied, 268K, at a given concentration of sodium chloride.

The reaction constant for the hemolysis process, k , has been plotted in Figures 9.3 and 9.4 as a function of extracellular NaCl concentration for different temperatures for 1st and 2nd order absolute rate laws respectively. The data show that the reaction constant K_p increases with increasing concentration for all temperatures. The largest rate of increase is observed for temperatures 298 and 283K. The concentration dependency of the reaction constant is similar for temperatures below 278K. Lowering the set point temperature generally results in lowered reaction rate constant. That is the initial rate of the

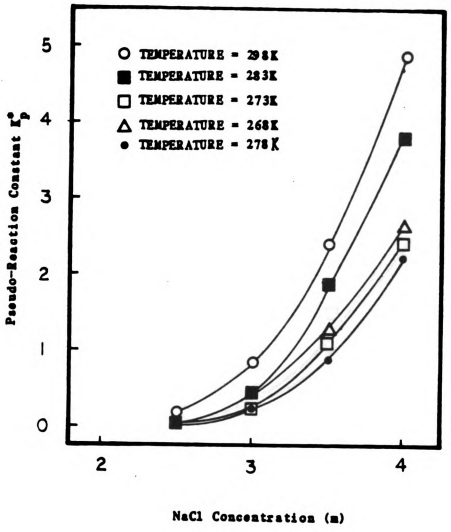

Figure 9.3: The NaCl Concentration Dependence of Pseudo-Reaction constant K_p^* for 1st order Reaction Model.

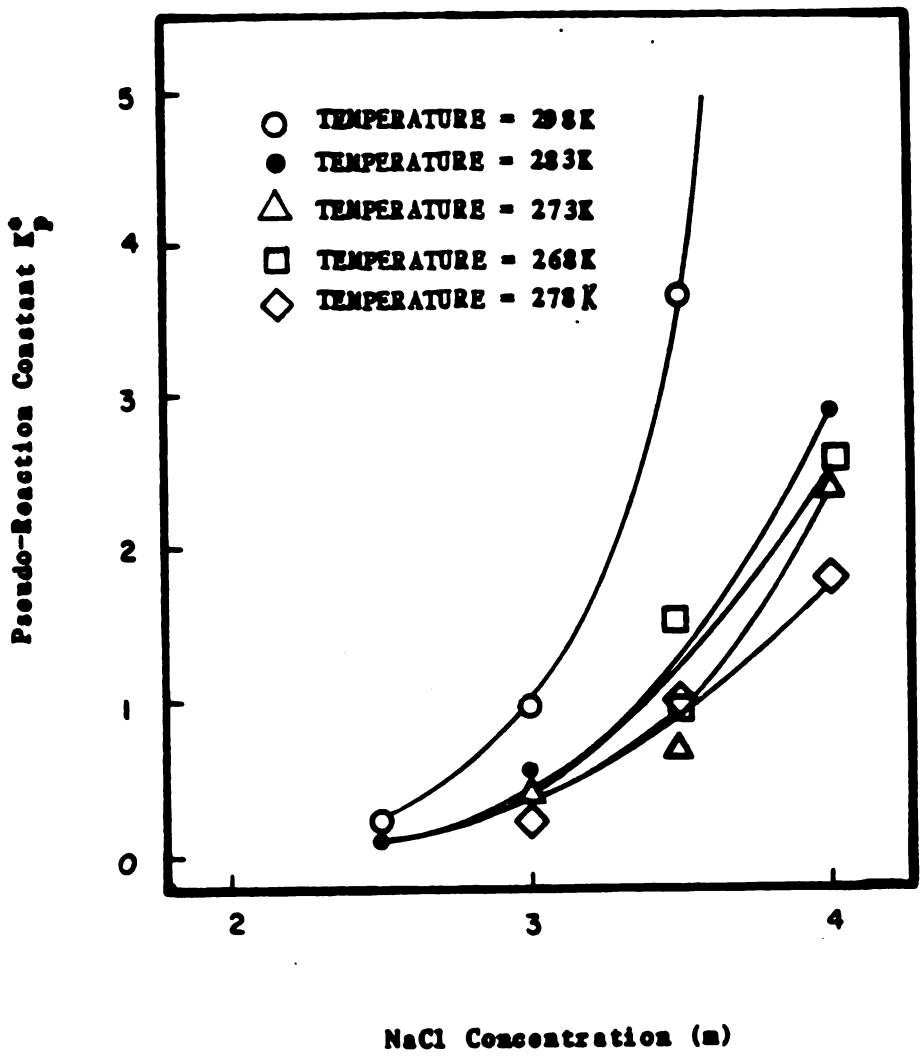

Figure 9.4: The NaCl Concentration Dependence of Pseudo-Reaction Constant K_p^* for 2nd order Reaction Model.

destruction process is reduced by reducing temperature. The lowest K_p values for 2.5m NaCl occurs at 273K where for higher NaCl concentrations it occurs at 278K.

At this point it is interesting to compare the K_p and $\Delta G^{\neq}$ behaviors based on the above observations. The temperature at which K_p is minimal (278K) does not coincide with the temperature corresponding to maximal $\Delta G^{\neq}$ values (298K). Furthermore, the temperature at which $\Delta G^{\neq}$ is minimal (268K) does not correspond to maximal K_p values (298K). This indicates a very complicated and strong temperature dependency of the hemolysis process.

The entropy of activation $\Delta S^{\neq}$ has been plotted as a function of the enthalpy of activation $\Delta H^{\neq}$ for the 1st and 2nd order rate laws in Figures 9.5 and 9.6 respectively. The 1st order and 2nd order activation parameters show quite similar span and behavior. It is also evident that graphs of $\Delta S^{\neq}$ vs $\Delta H^{\neq}$ show parallel relationship with osmotic concentration, i.e., the $\Delta S^{\neq}$ and $\Delta H^{\neq}$ values at a given NaCl concentration are related by the simple linear equation

$$\Delta S^{\neq} = a\Delta H^{\neq} + b \qquad [9.30]$$

This is referred to as a thermodynamic compensation law [170],

since as is apparent from Equation 9.19, variation of one parameter for example $\Delta S^{\neq}$ in the positive direction is compensated for by variation of $\Delta H^{\neq}$ in the negative direction. In other words whatever the contribution of any process or mechanism to $\Delta S^{\neq}$, exactly the same contribution is contained in $\Delta H^{\neq}$. This in fact is the chief reason for the observed small variation in $\Delta G^{\neq}$ for different temperatures and concentrations. The temperature $T_c=1/a$ is called the compensation temperature [170].

From the least square fit of the data presented in Figures 9.5 and 9.6, the following results are obtained;

1st order rate law:

$$\Delta S^{\neq} = 3.635 \cdot 10^{-3} \Delta H^{\neq} - 60.064$$

$$T_c = 275.06 \text{ K}$$

2nd order rate law:

$$\Delta S^{\neq} = 3.644 \Delta H^{\neq} - 60.440$$

$$T_c = 274.43 \text{ K}$$

Such a linear relationship between $\Delta H^{\neq}$ and $\Delta S^{\neq}$ has been observed for several physical and chemical processes [168-170].

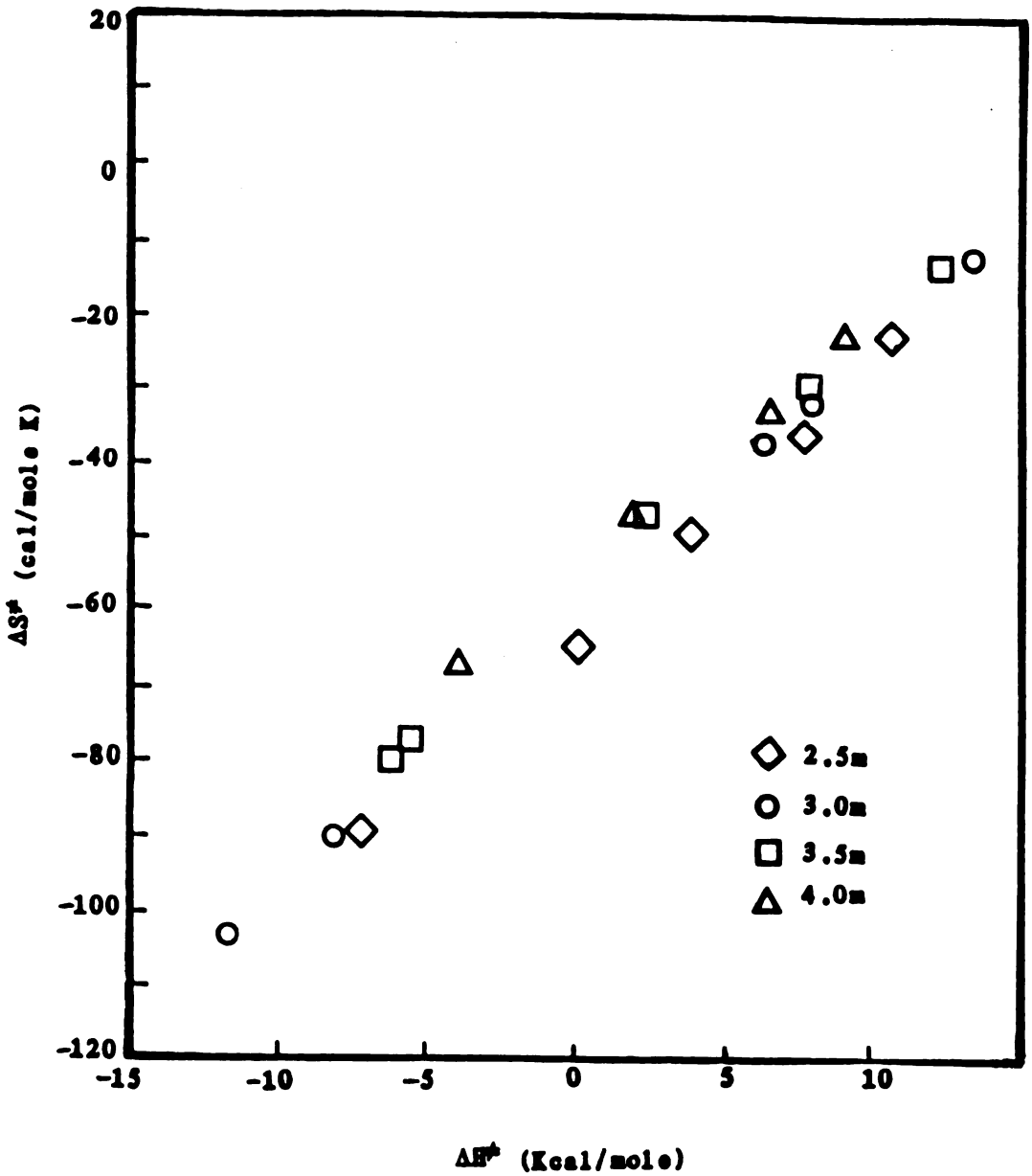

Figure 9.5: The Relationship Between the 1st Order Eyring Activation Parameters $\Delta S^{\ddagger}$ and $\Delta H^{\ddagger}$ for Hypertonic NaCl-induced Hemolysis for 1st Order Reaction Model.

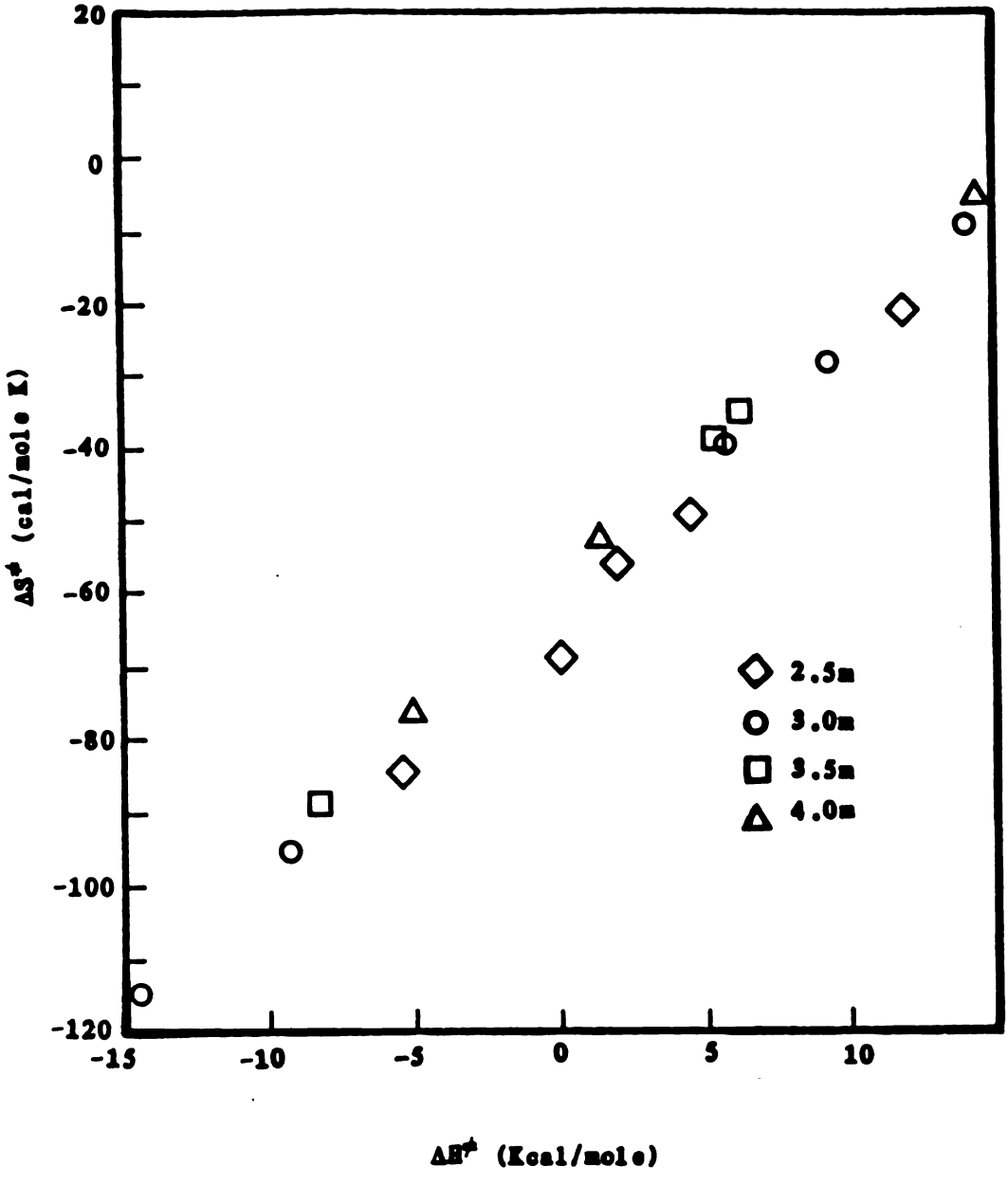

Figure 9.6: The Relationship Between the 2nd Order Eyring Activation Parameters $\Delta S^{\ddagger}$ and $\Delta H^{\ddagger}$ for Hypertonic NaCl-induced Hemolysis for 2nd Order Reaction Model.

It has been argued that this apparent linear behavior is wholly artifactual [171]. That is the linear relationship between $\Delta S^{\neq}$ and $\Delta H^{\neq}$ of a reaction is of no significance. However, the respective intercepts in Figures 9.5 and 9.6 are significant.

The $\Delta S^{\neq}$ intercepts are -60.064cal/K and -60.440cal/K for 1st and 2nd order rate laws respectively. This intercept (i.e. b in Equation 9.30) is called the intrinsic entropy of activation $\Delta S^{\neq}_{o}$. Substituting for $\Delta S^{\neq}$ in Equation 9.18' from Equation 9.30 we have;

$$\Delta G^{\neq} = \Delta H^{\neq}(1 - T/T_c) - T\Delta S^{\neq}_{o} \qquad [9.31]$$

For $\Delta H^{\neq} = 0$;

$$\Delta G^{\neq} = -T\Delta S^{\neq}_{o} \qquad [9.32]$$

From the above equation then, $\Delta G_{o}^{\neq}$ the intrinsic activation energy is temperature dependent and varies from 16.10 to 17.90Kcal/mole and 16.20 to 18.01Kcal/mole for 1st and 2nd order rate laws respectively. On the other hand from Equation 9.30 we have;

$$\Delta H^{\neq} = \Delta H^{\neq}_{o} + T_c\Delta S^{\neq} \qquad [9.33]$$

where

$$\Delta H^{\neq}_{e} = -b/a$$

$$= 16.5213 \text{ Kcal} \qquad \text{(1st order rate law)}$$

$$= 16.5867 \text{ Kcal} \qquad \text{(2nd order rate law)}$$

Substituting for $\Delta H^{\neq}$ from Equation 9.33 in Equation 9.18' we have;

$$\Delta G^{\neq} = \Delta H^{\neq}_{e} + (T_c - T)\Delta S^{\neq} \qquad [9.34]$$

For $\Delta S^{\neq} = 0$,

$$\Delta G^{\neq} = \Delta H^{\neq}_{e}$$

That is when the entropy of activation is equal to zero the free energy of activation is equal to the intrinsic enthalpy of activation.

If we consider the $T_c\Delta S^{\neq}$ in Equation 9.33 to represent the structural contribution to the enthalpy of activation, it is evident from Equation 9.34 that the structural contribution to the free energy is $(T_c - T)\Delta S^{\neq}$. Since $(T_c - T)$ ranges from about +8 to -24K, the structural contribution to $\Delta G^{\neq}$ is much smaller than that of $\Delta H^{\neq}$. In fact this is the major if not the only reason for the observed compensation law and therefore comparatively small variation of $\Delta G^{\neq}$ values (tabulated in Table 9.2). This means $\Delta G^{\neq}$

is mostly made up of the intrinsic enthalpy $\Delta H^{\ddagger}_{e}$ as $(T_c - T)\Delta S^{\ddagger}$ ranges from -1.41 to 1.91Kcal/mole and -1.43 to 1.94Kcal/mole for 1st and 2nd order rate laws respectively.

The structural contribution, $(T - T_c)\Delta S^{\ddagger}$, to $\Delta G^{\ddagger}$ deserves an interpretation. This term in Equation 9.34 as discussed above will change sign as temperature is decreased below T_c. That is for temperatures less than T_c the structural contribution is negative (as $\Delta S^{\ddagger}<0$) and for temperatures greater than T_c the structural contribution is positive. This in terms of $\Delta G^{\ddagger}$ means that it is less for temperatures below T_c compared to those at temperatures higher than T_c, i.e., the energy barrier height is decreased for temperatures below T_c. However, the above argument does not necessarily mean that the reaction will proceed faster at lower temperatures. To clear this very important point the following argument is presented.

The behavior of the cell and therefore its fate depends primarily on the amount of water remaining in the cell. In other words, the rate of reaction depends on the water conductivity of the cell membrane. The cell membrane permeability K_w is temperature dependant and according to Jacobs is given by the following general form [171];

$$K_w = K_g \exp[b(T-T_g)] \qquad [9.35]$$

where

$$T_g = 293K \quad , \quad b = .0325K^{-1}$$

and K_g is the red blood cell membrane permeability at temperature T_g, and b is called the permeability temperature coefficient [172]. Therefore we have;

$$K_w(T=298)/K_w(T=268) = 2.65$$

That is the resistance of the cell membrane to transport of water across it is increased by a factor of 2.65 for temperature 268K compared to 298K. Since the damage is a function of water remaining in the cell, the hinderance of water transport is directly responsible for the observed comparatively slower kinetics at sub-ambient temperatures. It is to say that the loss of cell water and therefore damage is postponed at low temperatures.

The $(T - T_0)\Delta S^{\neq}$ values for different reaction conditions are tabulated in Table 9.3 for 1st order rate law.

TABLE 9.3

$(T - T_c)\Delta\bar{S}^{ex}$(cal/mole °C)

Concentration	Temperature(K)				
(m)	268	273	278	283	298
2.5	-.630	-.130	.150	.293	.303
3.0	-.728	-.180	-.096	.101	.485
3.5	-.546	-.160	.090	.107	.633
4.0	-.476	-.136	-.099	.184	.624

It is clear from these data that the $(T-T_c)\Delta S^{\neq}$ decreases for a given concentration level by decreasing the temperature of the reacting mixture. The fact that the numerical value of T_c is close to the freezing point of water is significant, emphasizing the important role played by water in the reaction process.

Another important observation is the abrupt increase in the structural contribution to the free energy of activation at 298K compared to the value at 283K for concentrations greater than 2.5m. The positive values of $(T - T_c)\Delta S^{\neq}$ for temperatures greater than T_c is an indication of the extent of the disorder in the activation state. The author believes it is at this disordered stage where membrane molecules are desorbed into water.

The thermodynamic properties for desorption of long chain hydrocarbon molecules shows that the free energy of desorption is a positive quantity and increases with chain length [172]. Furthermore, where smaller molecules gain entropy upon desorption into water the entropy of desorption becomes negative for larger molecules. This is believed to be due to the orientation and partial immobilization of the water molecules around the hydrocarbon chains [173].

The data represented in Figures 9.5 and 9.6 are qualitatively in agreement with the trends of the thermodynamic properties of

the long chain hydrocarbon desorption process. The negative values of $(T - T_c)\Delta S^{\neq}$ in Table 9.3 for temperatures below T_c represents the fact that: even though the activation process results in a more ordered state, the structural contribution to the free energy of activation is negative.

Since the rate of the reaction is controlled by $\Delta G^{\neq}$, this means that at temperatures below T_c the reaction velocity is higher. The author believes this is an indication of a brittle state where the interactions between membrane molecules are weakened and subsequently the membrane is susceptible to damage. However, as mentioned earlier, the water conductivity of the cell membrane is drastically lowered at these temperatures. Therefore the likelihood of the membrane structure collapsing due to the substantial loss of water in a short time is considerably reduced.

The forgoing argument implies a partial desorption of hydrocarbons or proteins from the membrane into the aqueous medium. According to Davis and Rideal, a molar $=CH_2$ group requires a ΔG of +810 calories to pass into the aqueous solution from the oil-water interface [172]. If the intrinsic free energy of activation $\Delta G^{\neq}_0$ (for $T=T_c$ or $\Delta S^{\neq}=0$) for the NaCl induced hemolysis is compared to this figure of 810 calories/mole, the approximate number of $=CH_2$ groups participating in the activation process is found to be 20. Considering the average number of $=CH_2$

groups per hydrocarbon molecule of 28-48 [173], it is clear that the derived number of 20 $=CH_2$ groups indicates that the activated complex or the transition state consists of a half-desorbed hydrocarbon molecule.

The entropy lost by the aqueous media per $=CH_2$ group immersion is about 5 cal/mole K [173]. If the intrinsic entropy of activation $\Delta S^{\neq}_0$ is divided by the value 5 cal/mole K, then the approximate number of $=CH_2$ groups involved in the activated complex is found to be 12. Both estimated number of $=CH_2$ groups involved in the transition state indicate that at this state the molecules are still partially attached to the membrane. Finally, the present data are in agreement with the hyphothesis that the activation mechanism for cell membrane damage due to hypertonic NaCl solution is a partial desorption of the membrane components.

CHAPTER X

CONCLUSION AND SUGGESTIONS FOR FURTHER WORK

A. Conclusion

The physiochemical alteration of cells as a result of freezing during a cryopreservation protocol at sub-optimal cooling rates is known to be due to the coupled effects of lowered temperature and the increased solute concentration. The living cell in the absence of protective agents is usually injured as a result of exposure to these thermal and chemical perturbations which occur simultaneously during freezing. An understanding of the effect of these two major factors is essential for the design of an optional freeze-thaw protocol. The major goals of this work were :

1) To develop an experimental system and technique for a decoupled measurement of the amount of damage incurred due to a desired thermal and chemical alteration of the cells,
2) To generate a complete data base in the form of hemolysis kinetics for the human red blood cell,
3) To analyse the cell responses to imposed perturbation in

terms of thermodynamic and kinetic principles.

The outcome of a freeze-thaw protocol greatly depends on the dynamic events produced by the removal of the system from its physiological equilibrium state, as the cell recovery is intimately dependent on the cooling and warming rates. Unfortunately information on cell hemolysis has either been of a static type or of a questionable nature. However, it has been clearly shown that in order to quantify the freezing injury due to the simultaneous variations of the temperature and concentration, decoupled studies of these coupled factors resulting in information in the form of hemolysis kinetics are essential.

To decouple the chemical and thermal effects an improved stop flow system equipped with temperature control with the potential for measurement of the red cell destruction dynamics has been designed and developed. The stop flow technique provides very rapid mixing and therefore the damage dynamics for short times (order of seconds) are obtained. This technique represents a definite advantage over the standard technique for hemolysis measurement of the blood sample (on the order of several minutes). Even though the experimental principles of the stop flow technique were already known, because of the biological nature of the problem, several vital modifications were necessary in order to obtain reliable results. The hemolysis rate data for the human

red blood cell population induced by several hypertonic sodium chloride concentrations have been obtained. With the aid of the thermal control capabilities of the system the temperature dependence of the chemical perturbation has also been studied for several isothermal sub-ambient temperature conditions. The stop flow system proved to be capable of generating the hemolysis data in the desired rate format. However, it was found that extreme care in terms of a complete understanding of the operating characteristics of the system is required. The results obtained here indicate that the chemical perturbations (increased salt concentration) at a given isothermal condition were similar at all temperatures. However, the thermal perturbations at a given sodium chloride concentration level proved to indicate a temperature dependent process. For kinetic analysis the hemolysis process is treated as a chemcial reaction of the blood cell sample and sodium chloride. The temperature and the sodium chloride concentration dependence of the hemolysis kinetics is studied in terms of the 1st and 2nd order rate law for short exposure times. The rational for this is that the forward reaction rate of the destructive hemolysis process is characteristically very rapid at short times compared to that at relatively long times for all temperatures and concentrations. The thermodynamic activation parameters, free energy of activation, activation enthalpy, and activation entropy associated with these kinetics have been analysed.

Biological systems are very sensitive to changes in environmental parameters such as temperature (resulting in so called thermal shock) and electrolyte concentration (resulting in so called osmotic shock). Several mechanisms for injury based on the macroscopic analysis of the physio-chemical events associated with the thermal and osmotic shock have been hypothesized by a number of investigators. Despite the diversity of the proposed mechanisms they invariably agree that the hemolysis produced by either perturbation modes to cause damage primarily at the membrane site. Specifically evidence with respect to the loss of membrane components induced by such environmental alterations is mounting. Therefore, in the present work, the thermodynamic activation parameters associated with the hemolysis kinetic process have been analyzed. It is shown that the trends of the thermodynamic properties are in agreement with that of a desorbtion process involving long chain hydrocarbons.

The conclusions concerning the temperature effect on the hemolysis kinetics data obtained here, are presented in chapter VII. Furthermore a complete analysis and conclusions regarding the derived thermodynamic activation parameters are presented in chapter IX. In addition, a complete discussion of the hypothesized mechanism for cellular injury along with a theoretical argument in support of dissolution theory is presented in chapter VIII. Therefore in this section we would like to

consider a proposed mechanism for the cell freezing injury in light of the present results and analysis.

Cells exposed to hypertonic solutions go through shape changes. The membrane becomes distorted and the effective area of the membrane decreases while the volume remains constant. The fact that red cells under stress become spherical during osmotic shrinkage implies that the intracellular membrane pressure should increase [108,126,127,173-175]. As pressure is related to the number density of molecules at the membrane , the increased membrane pressure results in membrane constituents becoming closely packed [87]. The van der Waals forces between the hydrocarbon tails favor close packing. On the other hand, the mutual interactions of the ionic or Zwitter-ionic polar head groups do not favor such close packing. Now according to Equation 2.1, the concentration of free ions at the membrane surface should decrease i.e., softening of the ice like structure of the hydration shell. This means that the mutual interactions between ions in the hydration shell (bound water) becomes weaker as a result. That is the shrinkage of the cell membrane produces a tendency for the bilayer constituents to leave the plane of membrane. Since the lipid bilayer surface in an aqueous solution is nonhomogeneous, the tendency of the membrane surface to expand will only be confined to certain local "weak" parts of the membrane. Therefore as a result of increased pressure in the

membrane, the membrane components are forced out of the plane of the membrane. This could result in evagination and microvesicle formation which break off from the membrane. This hypothesized behavior has been observed in monolayers (see Ref. [175] for review). Such vesicle release from the cell membrane, either into the intracellular or extracellular compartments has been observed for erythrocytes and plant protoplasts [45,46,130,174]. If such release of membrane effective area exceeds the critical limit, the cell upon thawing, can not return to its isotonic volume and therefore it may be lysed. Furthermore, if the osmotic stress is severe enough the loss of membrane area could lead to a formation of holes in the membrane through which hemoglobin could be lost so that the cell becomes hemolysed.

Evidence concerning the alteration in the cytoskeleton network in red cell in response to hypertonic exposure has been presented [45]. The membrane interaction with the spectrin-actin cytoskeleton network has been suggested to be responsible for the red cell (membrane) shapes and therefore lysis of the cell [52-57]. This idea is definitely in line with the above argument. Once the cell is shrunken to a critical configuration the cytoskeleton interaction with membrane molecules will be greatly enhanced. The cytoskeleton network is made up of much larger molecules (proteins) compared to lipid molecules at the membrane. Therefore, several lipid molecules could associate with one

protein molecule thereby, creating a local macroscopic alteration in the membrane. This again could result in evagination and microvesicle formation. Boroske et al. studied the effect of osmotic shrinkage on egg-lecithin liposomes. They found that during osmotic shrinkage the vesicle remained or became spherical and their radii decreased linearly with time. They reported formation of finger-like perturbances and daugther vesicles under osmotic shrinkage and concluded that a loss of active wall area takes place during the process. Since the liposomes lack any type of supporting skeletal network, one can not assume that the cytoskeletal network in for example blood cell membrane plays the dominant role in hemolysis. The author believes that the cytoskeleton plays an important role once the membrane is shrunken close to the critical limit and the cell volume has been considerably reduced.

In an effort to offer some insight regarding the likely mechanism and process of re-structuring of the membrane system as a result of extracellular perturbations leading to damage, a hypothetical model will be given here. According to this model the membrane system under osmotic stress is forced to go through a loss of membrane constituents to the extra- and/or intracellular environment. The loss of molecules from the membrane is thought to start at a structurally weak loci. Molecules are released in the form of micelles and/or microvesicles. Here we will consider

the case of hypertonic exposure. The author believes the release of membrane components, according to our model, takes place in the following manner;

1) Exposure to hypertonic solution results in increase in the molecular number density, a direct consequence of intracellular pressure. This is envisioned as the membrane proceeding from state A to state B in Figure 10.1. Consequently the ice-like structure of the hydration shell is softened. In other words, the concentration of free ions at the membrane surface decreases.

2) In state B as the molecules begin to pack closer, the van der Waals interactions between the hydrocarbon tails and ionic interactions between the head groups are altered. Due to the nature of these interactions the hydrocarbon tails favor close packing, whereas the head groups do not favor close packing. Therefore, the close packing of molecules in the plane of the membrane creates an imbalance. This is conceptually reflected in state C as kink formations on the membrane surface.

3) These structures are finally forced completely out of the cell membrane. The re-structured molecules may stay attached to the mother cell or be released in the form of micelles or microvesicles.

The forementioned process will alter the membrane permeability to solutes. It will eventually result in formation of holes in the membrane large enough for the encapsulated molecules to leave the cell and cause lysis. Concerning the low temperature preservation, the author believes the molecular re-arrangment due to the external perturbations will be drastically altered (unfavorable) during cooling process of a freez-thaw cycle.

B. SUGGESTIONS FOR FURTHER WORK

The improved experimental apparatus, namely the stop-flow system, equipped with temperature control has been developed and shown to be an excellent tool to measure the destruction dynamics of the red blood cells over a wide range of temperatures. In the course of producing the thermal shock data the temperature of the blood sample is dropped below the room temperature value in two to four seconds. It needs to be determined whether or not the initial temperature drop predisposes the cells to thermal stress severe enough to effect the kinetics at long exposure times. To accomplish this, the author suggests; 1) subject the cells to several cycles of temperature drops (at cooling rates experienced by the cells during a typicla experiment) before the final run, 2) initially cool the blood cells to the same temperature as the test solution. Comparing the data presented in this work with those

obtained in 1 and 2 above should shed light on the question of the effect of initial temperature drop on the hemolysis kinetics.

It has been attempted in this work to show that the shear stress incurred during mixing does not effect the kinetics of damage process. An effort should be made to measure and classify the stress levels imposed on the red blood cells going through the mixing chamber. It is needed to exaggerate such a mechanical stress in order to determine how this could effect the hemolysis kinetics at sub-optimal cooling rates. Another approach would be to use less turbulent mixing scheme where the mechanical stress would be non-existant or minimal, and compare the results with the data reported in this work.

The long exposure time hemolysis data obtained here and elsewhere show that a few percent of the cell population sustain severe hypertonic conditions for long periods of time. This implies the possibility that in any given population of the red blood cells there may exist a small population of "super" cells which are remarkably different from the "normal" cells. A study of population-characteristic variance need to be undertaken to determine whether such super cells exist. For example, it is feasible to separate these cells (if they exist) from others by hemolysing say 90% of the cells and through a proper technique removing the perturbing element (thermal and/or chemical).

A major contribution would require an effort concerning the detailed molecular as well as atomic interactions and magnitude of forces involved in the membrane system. Such studies should bring about elegant statistical mechanics studies of the membrane sytem both at experimental and theoretical levels.

An important contribution would be to study the hemolysis kinetic process employing completely different experimental approach. One such approach would be through a photometric study utilizing a diffusion chamber developed in this laboratory. For this the major task is to arrive at a calibration technique. This could be accomplished through an image analysis technique. For example, the diffusion chamber could be used in conjunction with a light microscope. The microscope image can then be digitized. Once a reliable correlation between the light intensity passing through the cell (damaged or healthy) is established, the hemolysis kinetic data could be inferred at any extracellular concentration at any desired temperature.

Finally, in order to fully understand the role of membrane constituents (lipids and proteins) in an aqueous environment in relation to stability of the membrane system, a theoretical kinetic model of the activation process initiated here should be used as a starting point. Such study should consider both thermal and chemical perturbation modes (the essential parameters involved

in cryopreservation process). The forementioned approach is perhaps most significant in a sound scientific approach to understand and design an optimal protocol for cryopreservation of blood.

REFERENCES

REFERENCES

1. Huggins, C. E., "Frozen Blood", Annals of Surgery, 643-649, (1964).

2. Saldier, R. M. F. S., "Preservation of Mammalian Spermatoza by Freezing", Laboratory Practice, Vol. 15, 413-417, (1966).

3. Mueller, F. O., Casey, T. A., and Trevor-Roper, P. D., "Use of Deep-Freez Human Cornea in Full Thickness Grafts", British Medicine Journal, Vol. ii, 473-475, (1964).

4. Lehr, H. B., Berggren, R. B., Lotke, P. A., and Coriell, 1.1, "Permanent Survival of Preserved Skin Antografts", Surgery (St. Louis), Vol.56, 742-746, (1964).

5. Leibo, S. P., Mazur, P. and Jackowiski, S. C., "Factors Affecting Survival of Mouse Embryos During Freezing and Thawing", Exp. Cell Res., Vol.89, 79-88 (1974).

6. Mazur, P., and Ribo, S. P., Farant, J. and Chu, E. H. T., "A Two Factor Hypothesis of Freezing Injury", Exp. Cell Res. 711: 345-355, (1972).

7. Leibo, S. P., Farrant, J., Mazur, P., Hanna, M. G., Smith, L. H., "Effects of Freezing on Marrow Stem Cell Suspensions: Interactions of Cooling and Warming Rates in the presence of PVP, Sucrose or Glycerol", Cryobiology, Vol. 6, No. 315-332, (1970).

8. Lovelock, J. E., "The Hemolysis of Human Red Blood Cells By Freezing and Thawing. Biochemica et Biophysica Acta, Vol. 10, 414-426, (1953).

9. Meryman, H. T., "Freezing Injury and its Prevention in Living Cells", Annu. Rev. Biophys. 3, 341-363, (1974).

10. Mitchell, C. D., and Hanahan, D. J., "Solubilization of Certain Proteins from the Human Erythrocyte Stroma", Biochemistry 5, 51-57, (1966).

11. Sonzu, H., Nei, T., and Sato, T., "Hemolysis and Release of Phospholipids of Human erythrocytes caused by Freeze-Thawing or Exposure to Hypertonic Salt Solution", Low Temp. Sci., Vol. B29, 75-82, (1971).

15. Polge, C., Smith, A. V., and Parkes, A., "Revival of Spermatozoa after Vitrification and Dehydration at Low Temperatures", Nature, Vol. 164, 166, (1949).

16. Meryman, H. T., and Kafig, E., "Rapid Freezing and Thawing of Whole Blood", Proc. Soc. Exp. Bio. Med. 90, 587-589, (1955).

17. Rowe, A. W., "Preservation of Blood at the New York Blood Center by slow-Glycerol, Rapid-Freeze Technique", In: Int. Working Conference Freeze-Preservation of Blood, 44-50. U.S. Office of Naval Research Report DR-143, (1967).

18. Huggins, C. E., "Practical Preservation of Blood by Freezing", In: Red Cell Freezing- A Technical Workshop. Presented by Committee on Workshops of the American Association of Blood Banks, 31-53, (1973).

19. Leibo, S. P., and Mazur, P., "Freezing of Bacteriophage T4:Temperature and Rate Effects as a Function of Salt Concentration", Virology, Vol. 38, 558-566, (1969).

20. Leibo, S. P., and Mazur, P., "The Role of Cooling Rates in Low-Temperature Preservation", Cryobiology, Vol. 8, 447-452, (1971).

21. Miller, R. H. and Mazur, P., "Survival of Frozen-Thawed Human Red Cells as a Function of Cooling and Warming Velocities", Cryobiology, Vol. 13, 404-414, (1976).

22. Mazur, P. and Schmidt, J., "Interactions of Cooling Velocity, Temperature, and Warming Velocity on the Survival of Frozen and Thawed Yeast", Cryobiology, Vol. 5, 1-17, (1968).

23. Mazur, P., Leibo, S. P., Farrant, J., Chu, EH. Y., Hanna, M. G., Smith, L. H., "Interactions of Cooling Rate, Warming Rate and Protective Additive on the Survival of Frozen Mammalian Cells", The Frozen Cell, J. and A. Churchill, London 69-88, (1970).

24. McGrath, J. J., Cravalho, E. G., and Huggins, C. E., " Hela cell Freezing Injury: Intracellular Ice Formation and Survival as a Function of Cooling Velocity", Cryobiology, Vol. 11, 549, (1974).

25. Lovelock, J. E., "The Mechanism of Protective Action of Glycerol against Haemolysis by Freezing and Thawing", Biochemica et Biophysica Acta, Vol. 11, 28-3d6 (1953).

26. Mazur, P., "Causes of Injury in Frozen and Thawed Cells", Fed. Proc. Amer. Soc. Exp. Biol., Vol. 24, 175-182 (1965).

27. Levin, R. H., Cravalho, E. G., and Huggins, C. E., "Effect of Hydration on the Water Content of Human Erythrocytes", Biophysical J., Vol. 16, 1411- 1425 (1976).

28. Mazur, P., "Kinetics of Water Loss from Cells at Subzero Temperatures and the likelihood of Intracellular Freezing", J. Gen. Physiol., Vol. 47, 347-365, (1963).

29. Uehiyama, M., Cravalho, E. G., Diller, K. R., and Huggins, C. E., "Intracellular Water Content of Saccharomyces Cerevisiae During Freezing at Constant Cooling Rates", Cryobiology, Vol. 10, 517-518, (1973).

30. Silvares, C., "A Thermodynamic Model of Water and Ion Transport Across Cell Membrane During Freezing and Thawing: The Human Erythrocytes", Ph.D. Thesis. Massachusetts Institute of Technology, Cambridge, Mass., (1974).

31. Ferguson, J. R., "The Thermodynamics of the Freezing and Thawing of Biological Cells", M. S. Thesis, Cornell University, (1980).

32. Farrant, J., "General Observations on cell Preservation", In: Low Temperature Preservation in Medicine and Biology, ed. by M. J. Ashwood- Smith and J.

33. Cravalaho, E. G., Hugins, C. E., Diller, K. R., Watson, W. W., "Blood Freezing to -272.29 C (-458.12 F)", Presented at the 9 th Annual Meeting, Society of Cryobiology, July 30-August 3, 1972, Washington, D. C.

34. Meryman, H. T., "Review of Biological Freezing", In: Cryobiology, ed. by H. T. Meryman, Academic Press, London, 1-114, (1966).

35. Jensen, M., and Oettmeier, W., "Effects of Fre Temperature Preservation in Medicine and Biology", ed. by M. J. Ashwood-Smith and J.

33. Cravalaho, E. G., Hugins, C. E., Diller, K. R., Watson, W. W., "Blood Freezing to -272.29 C (-458.12 F)", Presented at the 9 th Annual Meeting, Society of Cryobiology, July 30-August 3, 1972, Washington, D. C.

34. Meryman, H. T., "Review of Biological Freezing", In: Cryobiology, ed. by H. T. Meryman, Academic Press, London, 1-114, (1966).

35. Jensen, M., and Oettmeier, W., "Effects of Frecoupling of Phosphorylation from Electron Transport in Chloroplasts", Plant Physiol, Vol. 42, 1343-1350, (1967).

39. Herber, U., Volger, H., Overbeck, V., and Santarius, K. A., "Membrane Damage and Protection During Freezing", In: Advances in chemistry (O. Fennema, Ed.), Series 180, 159-189, Amer. Chem.

Association in Human Erythrocytes", J.Cell Biochem., Vol. 18, 49-65, (1982).

53. Branton, D., Cohen., C. M., Tyler, J., "Interactions of Cytoskeletal Proteins On the Human Erythrocyte Membrane", Cell, Vol. 24, 24-32, (1981).

54. Johnson, R. M., Taylor, G., Meyer, D. B., "Shape and Volume Changes in Erythrocyte Ghosts and Spectrin-Actin Networks", J. Cell Biol., Vol. 86, 371-376, (1980).

55. Mohandas, N. Shohet, S. B., "Control of Red Cell Deformability and Shape", Curr. Top. Hematol, Vol. 1, 71-125, (1978).

56. Sheet Z, M. P., Wang W. P., and Kreutzer, D. C., "Polyphosphoinositides as Regulaters of Membrane Skeletal Stability", White Cell Mechanics, 87-94, (1984).

57. Kirkpatrik, F. H., "Spectrin: Current understanding of its Physical, Biochemical, and Functional Properties", Life Sciences, Vol. 19, 1-18, (1982).

58. Lovelock, J. E., "Physical Instability and Thermal Shock in Red Cells", Nature(London), Vol. 173, 659-661, (1954).

59. Wool, I. G., "Structure and Function of Eukaryotic Ribosomes", Ann. Rev. Biochem., 48:719-754 (1979). sk. 60. Bretscher, M. S., "Membrane Structure: Some General Principles"' Science 181:622-629 (1973).

61. Unwin, P. N. T., and Henderson, R., "Molecular Structure Determination by Electron Microscopy of Unstained Crystalline Specimens", J. Mol. Biol. 94: 425-4401 (1975).

62. Quinn, P. J., "Molecular Biology of Cell Membrane", Mcmillan London, (1976).

63. Stein, W. D., The movement of Molecules Across Cell Membranes, Academic, New York, 1967.

64. Finean, J. B., "Biophysical Contribution to Membrane Structure", Quart. Rev. Biophysics, 2:1 (1969).

65. Ladbrooke, B. D., Chapman, D., "Thermal Analysis of Lipids, Proteins and Biological Membranes", Chem. Phys. Lipids, 3:304.(1969).

66. Schneider, M. J. J. and Schneider, A. S., "Water in Biological Membranes: Adsorption Isotherms and Circular Dichroism as a Function of Hydration", J. Membrane Biol., 9, 127-140

(1972).

67. Clifford, J. Properties of Water in Capillaries and thin films. In: Water, A Comprehensive Treatise, Vol. 5. Franks, Ed. Plenum. London, 75-132 (1975).

68. Finch, E. D., and Schneider, A. S., "Mobility of Water Bound to Biological Membranes Aproton NMR Relaxation Study", Biochemica et Biophysica Acta, 406, 146-154 (1975).

69. Schneider, A. S., Middaugh, C. R., and oldewurtel M. D., "Role of Bound Water in Biological Membrane Structure: Fluorescence and Infraved Studies", J. Supramolecular Structure, Vol. 10, 265-275 (1975).

70. Tait, M. J. and Franks, F., "Water in Biological Systems", Nature, Vol. 230, 91-94 (1971).

71. Kauzman, W., In a Symposium on the Mechanism of Enzyme Acr Bound to Biological Membranes Aproton NMR Relaxation Study", Biochemica et Biophysica Acta, 406, 146-154 (1975).

69. Schneider, A. S., Middaugh, C. R., and oldewurtel M. D., "Role of Bound Water in Biological Membrane Structure: Fluorescenc John Wiley (1980).

74. Wintrobe, D. A., Morowitz, H. J., and Prestegrand, J. H. Biophysical J., Vol. 20, 169-179, (1977).

75. Rothman, J. E., and Lenard. J., "Membrane Asymmetry", Science, 195: 743-753 (1977).

76. Bretscher, M. S., "Membrane Structure: Some General Principles", Science, Vol. 8, 622-629, (1973).

77. Singer, S. J., "The Proteins of Membranes", J. Colloid and Interface Sci., Vol. 58, 452-458, (1977).

78. Singer, S. J. and Nicolson, G. L., "The Fluid Mosaic Model of the Structure of Cell Membranes", Science, NY. 175, 720-731.

79. Steck. T. L., "The Organization of Proteins in the Human Red Blood Cell Membrane", J. Cell Biol., Vol. 62, 1 (1974).

80. Jan, L. Y. and Revel, J. P., "Ultrastructural Localization of Rhodopsin in the Vertebrate Retina", J. Cell Biol. Vol. 62, 257-273, (1974).

81. Henderson, R. and Unwin, P. N. T., "Three-dimensional Model of Purple Membrane Obtained by Electron Microscopy", Nature, Vol. 257, 28-32, (1975).

82. Bessis, M. Living Blood Cells and their ultrastructure. Berlin-Heidelberg- New York, Springer-Verlag, (1973).

83. Beck, J. S., "Echinocyte Formation: Atest case for Mechanisms of Cell Shape Changes", J. Theor. Biol., Vol. 71, 515-524, (1978).

84. Grunze, M., Haest, C. W. M., and Deuticke, B., "Lateral Segregation of Membrane Lipids and Formation of Stable Rod-Shaped Membrane Projections in Erythrocytes Treated with Long-Chain Alcohols", Biochimica et Biophysica Acta, Vol. 693, 237-245, (1982).

85. Canham, P. B., Parkinson, D. R., "The Area and Volume of Single Human Erythrocytes During Gradual Osmotic Swelling of Hemolysis", can. J. Physiol. Pharmacol., Vol. 48, 369-376, (1970).

86. Ponder, E. Hemolysis and Related Phenomena, Grune and stratton, N.Y., (1948).

87. Evans, E. A., Skalak, R., Mechanics and Thermodynamics of Biomembranes. CRC press, (1980).

88. Fung, Y. C., "Theoretical Consideration of Elasticity of Red Cells and Small Blood Vesseles", Fed. Proc. Fed. Am. Soc. Exp. Biol., Vol. 25, 1761-1769, (1966).

89. Jacobs. R. E., Hudson, B., and Anderson, H.C., "A Theory of Chain Melting Phase Transition of Aqueous Phospholipid Dispersions", Proc. natr. Acad. Sci. U. S. A., Vol. 72, 3993-3997, (1975).

90. Eisenberg, M., Gresalfi, T., Riccio, T., and McLanghlin, S., "Adsorption of Monovalent Cations to Bilayer Membranes Containing Negative Phospholipids" ,Biochem., N. Y., Vol. 18, 5213-5223, (1979).

91. Lee, A. G., "Lipid Phase Transition and Phase Diagrams", Biochim. Biophys. Acta, Vol. 472, 237-281, (1977).

92. Glasstone, S., Physical Chemistry, Van Nostrand, N. Y., (1946).

93. London, F., Phys. Chem., Vol. B11, 22, (1930).

94. Morris, G. J., and McGrath, J. J., "The Response of Multilamellar Liposomes to Freezing and Thawing", Cryobiology, Vol. 18, 390-398, (1981).

95. Callow, R., "Thermodynamic Modelling and Cryomicroscopy of

Large Unilamellar Liposomes", M. S. Thesis, Dept. Mech. Eng. MSU, (1983).

96. Singer, S. J., and Nicolson, G., L., "The Fluid Mosaic Model of the Structure of the Cell Membranes", Science, Vol. 175, 720-731, (1972).

97. Gorter, E., and Grendel, F., "On Bimolecular Layers of Lipids on the Chromocytes of the Blood", J. exp. Med., Vol. 41, 439-443, (1925).

98. Danielli, J. F., and Davson, H. A., "A Contribution to the Theory of Permeability of Thin Films", J. Cell Comp. Physiol, Vol. 5, 495-508, (1935).

99. Davson, H., and Danielli, J. F., "The Permeability of Natural Membranes", 2nd ed. London Cambridge Unive. Press, (1952).

100. Robertson, J. D.,In: Cellular Membrane in Development (ed. M.Locke), New York: Academic Press, 1-81, (1964).

101. Mueller, P., Rudin, D. O., Tien, H. T., and Wescott, W. S., "Reconstitution of Cell Membrane Structure in vitro and its Transformation into an Excitable System", Nature, Vol. 194, 979-980, (1962).

102. Tien, H. T., Bilayer Lipid Membranes (BLM), Theory and Practice, Dekker, New York, (1973).

103. Curatolo, W., Sakura, J. D., Small, D. M., and Shipley, G. G., "Protein- Lipid Interactions: Recombinants of the Proteolipid Apoprotein of Myelin with Dimyristoyllecithin", Biochemistry, N. Y., Vol. 16, 2313-2319, (1977).

104. Curatolo, W. Verma, S. P., Sakura, J. D., Small, D. M., Shipley, G. G., and Wallach, D. F. H., "Structural Effects of Myelin Proteolipid Apoprotein on Phospholipids: a Raman Spectroscopic Study", Biochemistry, N. Y., Vol. 17, 1802-1807, (1978).

105. Segrest, J. P. and Kohn L. D., "Protein-Lipid Interactions of the Membrane Penetrating MN-glycoprotein from the Human Erythrocyte", in protides of the Biological Fluids-21st Colloquium (H. Peeters, ed.). Pergamon Press, N. Y. 183-190, (1973).

106. Meryman, H. T., "Modified Model for the Mechanism of Freezing Injury in Erythrocytes", Nature (London), 218 No. 5139, 333-336, (1968).

107. Rall, W. F., Mazure, P., and Sonzu, H., "Correlation Between the Survival of Slowly Frozen Human Red Cells and of the Unfrozen Portion of the Extracellular Medium at Various Subzero Temperatures. II. Survival Versus Composition of the Extracellular Medium", Cryobiology, Vol. 13, 650, (1976).

108. William, R. J., and Hope, H. J., "The Relationship Between Cell Injury and Osmotic Volume Reduction. III Freezing Injury and Frost Resistance in Winter Wheat", Cryobiology, Vol. 18, 133-145, (1981).

109. Meryman, H. T., "The ExceCorrelation Between the Survival of Slowly Frozen Human Red Cells and of the Unfrozen Portion of the Extracellular Medium at Various Subzero Temperatures. II. Survival Versus Composition of the Extracellular Medium", Cryobiology, Vol. 13, 650, (1976).

108. William, R. J., and Hope, H. J., "The Relationship Between Cell Injury and Osmotic Volume Reduction. III Freezing Injury and Frost Resistance in Winter Wheat", Cryobiology, Vol. 18, 133-145, (1981).

109. Meryman, H. T., "The Exce CRC Press, Boca Raton, Florida, (1983).

112. Frank, H. S., and Evans, M. W., "Free Volume and Entropy in Condensed Systems. III. Entropy in Binary Liquid Mixtures; Partial Molal Entropy in Dilute Solutions; Structure and Thermodynamics in Aqueous Electrolytes", J. Chem. Phys., Vol. 13, 507, (1945).

113. LeNeveu, D. M., Rand, R. P., Parsegian V. A., "Measurement of Forces Between Lecithin Bilayers", Nature, Vol. 259, 601-603, (1976).

114. Farrant, J. and Woolgar, A. E., "Human Red Cells Under Hypertonic Conditions; a Model System for Investigating Freezing Damage. I. Sodium Chloride", Cryobiology, Vol. 9, 9-15, (1972).

115. Solomon, A. K., "Properties of water in red cell and synthetic membrane", Biomembrane, Vol. 3, 299-330, (1972).

116. Horowitz, S. B. and I. R. Fenichel, "Solute diffusional Specificity in hydrogen-bonding systems", J. Phys. Chem., Vol. 68, 3378, (1964).

117. Pimentel, G. C. and A. L. McClellan, "The Hydrogen Bond. W. H. Freeman and Company", San Fransisco, Section 2,4.7 52, (1960).

118. Fung, Y. C. B., Tong, P., "Theory of the Splering of Red

Blood Cells", Biophysical J., Vol. 8, 175-198, (1968).

120. Jenkins, J. T., "Static Equilibrium Configurations of a Model Red Blood Cell", J. Math Biology, Vol. 4, 149-169, (1977).

119. Deuling, H. J., Helfrich, W., "Red Blood Cell Shapes as Explained on the Basis of Curvature Elasticity", Biophysical J., Vol. 16, 861-868, (1976).

121. Chien, S., Luse, S. A., Bryant, C. A., "Hemolysis During Filtration through Micropores: Scanning Electron Microscopic and Hemorheologic Correlation", Microvasc. Res., Vol. 3, 183, (1971).

122. Evans, E. A., Waugh, R., Melnik, L., "Elastic area Compressibility Modulus of Red Cell Membrane", Biophys. J., Vol. 16, 585, (1976).

123. Reeves, J. P., and Dowben, R. M., "Water Permeability of Phospholipid Vesicles", J. Memb. Biol., 3, 123-141, (1970).

124. Boroske, E., and Elwenspock, M., and Helfrich, W., "Osmotic Shrinkage of Giant Egg-Lecithin Vesicles", Biophys. J., 34, 95-109, (1981).

125. Fettiplace, R., "The Influence of the Lipid on the Water Permeabiliuty of Artificial Membrane", Biochem. Biophys. Acta, 513, 1-10, (1978).

126. McGrath, J. J., In: "Effects of Temperature on Biological Membranes", eds. G. J. Morris and A Clarke, Academic Press, London, 335-377, (1981).

127. Steponkus, P. L., Wolfe, J., and Dowgert, M. F., In: "Effects of Low Temperature on Biological Membranes", eds, G. J. Morris and A. Clarke, Academic Press, London, 307-322, (1981).

128. Trump, B. F., Young, D. E., Arnold, E. A., and Stowell, R. E. Fed. Proc. 24, 5144-5186, (1965).

129. Pomeroy, M. K. and Siminovitch, D., "Seasonal Cytological Changes in Secondary Parenchyma cells in Robinia Pseudoacacia in Relation to Cold Hardiness", Can. J. Bot., Vol. 49, 787-795,(1971).

130. Steponkus, P. L. and Weist, S. C., In: "Low Temperature Effect in Crop Plants. The Role of Membranes", ed. J. M. Lyons, D. Graham and J. Raison, Academic Press, New York, 231-254, (1979).

131. Grout, B. W. and Fuller, B. J., "Hepatocyte Plasma

Membrane Response to Hypertonic Stress and Related Cell Viability", Cryo-Letters, Vol. 3, 51-56, (1982).

132. Zade-Oppen, A. M. M., "Posthypertonic Hemolysis in Sodium Chloride Systems", Acta Physiol. Scand., Vol. 73, 341-364, (1968).

133. Mazur, P. Leibo, S. P., Miller, R. H., "Permeability of the Bovine Red Cell to Glycerol in Hyperosmotic Solutions at various Temperatures", J. Memb. Biol., Vol. 15, 107-136, (1974).

134. Bunnett, J. F., "Kinetics in Solution", in Investigation of Rates and Mechanisms of Reactions, Techniques of Chemistry, Wiley-Interscience, New York, (1974).

135. Levin, S. W., Levin, R. L., and Solomon, A. K., "Improved Stop-Flow Apparatus to Measure Permeability of Human Red Cells and Ghosts", J. Biochem. Biophys. Methods., 3, 255-273, (1980).

136. Jen, J., Studies of the Hemolysis Kinetics of Human Erythrocytes by Using a Stop Flow System, M.S. Thesis, Dept. of Mechanical Engineering, MSU, (1980).

137. Papanek, T. H., "The water permeability of the Human Erythrocyte in Temperature Range +25 C to -10 C", Ph.D. Thesis, Dept. of Mechanical Engineering, M.I.T., (1978).

138. Levin, R. L., "Kinetics of Water Transport in Biomaterials during Freezing", Sc.D. Thesis, Dept. of Mech. Eng. M.I.T., Feb. (1976).

139. McGrath, J. J., "The Kinetics and Thermodynamics of Human Erythrocyte Freez Thaw Damage at Sub-Optimal Cooling Rates", Ph.D. Thesis, Dept. of Mech. Eng., M.I.T., (1974).

140. Scarth, G. W., and Levitt, J., "The Frost-Hardening Mechanism of Plant Cells", Plant Physiol., 12:51-78, (1937)

141. Steponkus, P. L., and S. C. Wiest, "Plasma Membrane Alterations Following Cold Acclimation and Freezing", In: Plant Cold Hardiness and Freezing stress- Mechanism and Crop Implications. P/ H. Li and A. Sakai, editors. Academic Press, Inc., New York. 75-91, (1978).

142. Mazur, P. Rall, W. F., And Rigopaulos, N., "Relative Contributions of the Fraction of Unfrozen Water and of Salt Concentration to the Survival of Slowly Frozen Human Erythrocytes", Biophys. J., Vol. 36, 653-675, (1981).

143. Leibo, S. P., McGrath, J. J., and Cravalho, E. G.,

"Microscopic observation of Intracellular Ice Formation in Unfertilized Mouse Ova as a Function of Colling Rate", Cryobiology, Vol. 15, 257-271, (1978).

144. Acel, D. and L. Lorber, Biochem.Z., Vol. 147, 557, (1924).

145. Soderstrom, N., "Hemolysis by Hypertonic Solutions of Neutral Salts", Acta Physiol. Scand., 7, 56-68, (1944).

146. Lovelock, J. E., Br. J. Haemat., I, 117-129, (1955).

147. Mazur, P., Miller, R. H. and Leibo, S. P., "Survival of Frozen-Thawed Bovine Red Cells as a Function of the Permeation of Glycerol and Sucrose", J. Membr. Biol., Vol. 15, 137-158, (1974).

148. McIver, D. J. L., Physiol. Chem. Phys., 11, 289-302, (1980)

149. Brandts, J. F., "Thermodynamics of Protein Denaturation", J. Am. Chem. Soc., 86 4291-4314, (1975).

150. Brandts, J. F., In: "Structure and Stability of Biological Macromolecules", 213-290. ed. Timascheff, S. N., and Fasman, G. D. New York. Dekker.

151. Williams, R. J., "Freezing Tolerance in Mytilus Edulis", Comp. Biochem. Physiol., Vol. 35, 145, (1970).

152. Williams, R. J., and Meryman, H. T., "A Calorimetric Method for Measuring Ice in Frozen Solutions", Cryobiology, Vol. 1, 317, (1965).

153. Deuticke, B., "Transformation and Restoration of Biconcave Shape of Human Erythrocytes Induced by Amphiphilic Agents and Changes of Ionic Environment", Biochim. Biophys. Acta, Vol. 163, 494-500, (1968).

154. Chailley, B., Weed. R. I., Leblond, P. F., and Maigne, J. Nouv. Rev. Fr. Hematol, Vol. 13, 71-88, (1973).

155. Lutz, H. U., Liu, S. C., and Palek, J. , "Release of Spectrin-Free Vesicles from Human Erythrocytes During ATP Depletion", J. Cell. Biol., Vol. 73, 548-560, (1977).

156. Birchmeier, W., Lanz. J. H., Winterhalter, K. H., and Conrad, M. J., "ATP-Induced Endocytosis in Human Erythrocytes Ghosts", J. Biol. Chem., Vol. 254, 9298-9304, (1979).

157. Williams, R. J., and Shaw, S. K., "The Relationship

Between Cell Injury and Osmotic Volume Reduction. II. Red Cell Lysis Correlates With Cell Volume Rather Than Intracellular Salt Concentration", Cryobiology, Vol. 17, 530-539, (1981).

158. Williams, R. J. and Meryman, H. T., "Freezing Injury and Resistance in Spinach Chloroplast Grana", Plant Physiol., Vol. 45, 752, (1970).

159. Williams, R. J. and Takashahi, T., "Evidence for Injurious Surface Pressures Developing in the Membranes of Osmotically Stressed Sea Urchin Eggs", Cryobiology, 15, 688, (1978).

160. Gusta, L. V., Burke, M. J., and Kapoor, A. C., "Determination of Unfrozen Water in Winter Cereals at Subfreezing Temperatures", Plant Physiol. 56, 707, (1975).

161. Langmuir, I., and Waugh, J. F., "The Adsorption of Proteins at Oil-Water Interfaces and Artificial Protein-Lipoid Membranes", J. Gen. Physiol. 21, 745, (1938).

162. Wolfe, J., Ph.D. Thesis, The Australian National Unive., Canberra, (1979).

163. Nei, T., "Mechanism of Freezing Injury to Erythrocytes: Effect of Initial Cell Concentration on the Post-Thaw Hemolysis", Cryobiology, 18, 229-237, (1981).

164. Moore, J. W., and Pearson, R. G., Kinetics and Mechanism, John Wiley and sons, (1981).

Interfaces and Artificial Protein-Lipoid Membranes", J. Gen. Physiol. 21, 745, (1938).

162. Wolfe, J., Ph.D. Thesis, The Australian National Unive., Canberra, (1979).

163. Nei, T., "Mechanism of Freezing Injury to Erythrocytes: Effect of Initial Cell Concentration on the Post-Thaw Hemolysis", Cryobiology, 18, 229-237, (1981).

164. Moore, J. W., and Pearson, R. G., Kinetics and Mechanism, John Wiley and sons, (1981).

169. Coldman, M. F., and Good, W., "The Kinetics of MalnoamideInduced Hemolysis of Mammalian Erythrocytes", Biochem. Biophys. Acta, 150, 206-213 , (1968)

170. Banks, B. E. C.,Damjanovic, V., and Vernon, C. A., "The So-Called Thermodynamic Compensation Law and Thermal Death", Nature, 240, 17, 147, (1972).

171. Jacobs, M.H., Glassman, H. N., and Parpart, A. K., "Temperature Coefficient of Hemolysis", J.Cell and Comp. Phys., 7, 197-225, (1935).

172. Davis, J., and Rideal, E., Interfacial Phenomena, Academic Press,N.Y., (1963).

173. Boys, C. V., Soap Bubbles, Doubleday, Garden City, N. Y., (1959).

174. Meryman, H. T., Williams, R. J., and St. J. Douglas, M., "Freezing Injury from "Solution Effects" and its Prevention by Natural or Artificial Cryoprotection", Cryobiology, 14, 287-302, (1977).

175. Jones, M. N., Biological Interfaces, Elsevier, Amsterdam, (1975).

APPENDIX

APPENDIX

DATA FITTING PROCEDURE

The hemolysis history data presented in this work are for the exposure times ranging from few seconds to few minutes. However, to arrive at the reaction constant, K_p^*, only the short exposure time data were used (the reason for this is discussed in the text). The early response portion of the data for each perturbation level considered here is fitted into the 1st and 2nd order reaction rate laws. It was found that the so-called characteristic initial response portion of the hemolysis kinetic of the red blood cells is a function of the perturbation level. Therefore for a given temperature and NaCl concentration several initial time intervals were examined (the time intervals start at zero second). The reaction constant for the interval with highest coefficient of determination (r^2) were then used to calculate the activation parameters. The rate constant and the coefficient of determibation for different conditions are tabulated in Table 1 (1st order reaction rate law) and Table 2(2nd order reaction rate law).

TABLE 1

1st Order Rate Law

2.5m

T(K)	298				283				278				273			268		
Exposure Time(sec)	60	90	180	240	120	150	180	240	180	240	300	90	120	150				
A_e	1.04	1.02	1.03	1.02	1.03	1.03	1.03	1.03	1.03	1.04	1.04	1.01	1.02	1.02				
K_p^*	.19	.14	.07	.06	.06	.06	.06	.06	.04	.05	.05	.05	.06	.07				
r	.987	.954	.998	.992	.999	.997	.999	.997	.996	.996	.997	.983	.992	.983				

3.0m

T(K)	298				283				278				273			268		
Exposure Time(sec)	30	40	60	40	60	90	60	90	120	150	90	60	90	120				
A_e	1.13	1.11	1.05	1.05	1.07	1.10	1.04	1.05	1.06	1.07	1.06	1.07	1.08	1.08				
K_p^*	.92	.84	.62	.31	.34	.45	.22	.23	.26	.27	.26	.35	.38	.38				
r	.995	.994	.963	.988	.988	.990	.997	.997	.994	.995	.999	.961	.988	.995				

3.5m

T(K)	298				283				278				273			268		
Exposure Time(sec)	40	60	60	90	40	60	90	60	90	120	150	180	90	120				
A_e	1.18	1.08	1.25	1.27	1.09	1.14	1.20	1.14	1.17	1.19	1.18	1.16	1.24	1.23				
K_p^*	2.40	1.98	1.79	1.84	.88	1.10	1.31	.96	1.04	1.10	1.09	1.04	1.31	1.27				
r	.978	.967	.981	.993	.983	.978	.981	.993	.995	.996	.997	.996	.990	.995				

4.0m

T(K)	298				283					273			268		
Exposure Time(sec)	25	30	40	60	25	30	40	60	90	30	40	60	60	90	
A_e	1.41	1.43	1.35	1.10	1.16	1.22	1.36	1.51	1.42	1.15	1.21	1.32	1.63	1.48	
K_p^*	5.19	5.30	4.90	3.76	2.28	2.20	3.51	4.10	3.80	1.51	1.80	2.23	3.01	2.65	
r	.964	.979	.981	.933	.959	.952	.936	.968	.982	.977	.974	.976	.988	.987	

$$A = A_e EXP(-K_p^* t/100) \qquad \text{where} \qquad A = 1 - \%H/100$$

TABLE 2

2nd Order Rate Law

2.5m

T(K)	298			283			278			273			268		
Exposure Time(sec)	60	90	150	180	240	150	180	240	150	180	240	90	120	150	
A_o	.961	.971	.973	.971	.973	.968	.965	.969	.972	.968	.961	.986	.983	.977	
K_p^*	.190	.160	.061	.062	.061	.065	.068	.065	.048	.047	.052	.054	.060	.069	
r	.996	.985	.999	.999	.999	.996	.996	.996	.998	.995	.993	.998	.991	.981	

3.0m

T(K)	298			283			278			273			268		
Exposure Time(sec)	40	60	40	60	90	40	60	60	90	120	60	90	120	150	
A_o	.875	.927	.945	.918	.884	.945	.955	.939	.935	.928	.927	.903	.893	.871	
K_p^*	.96	.74	.33	.43	.54	.25	.23	.28	.29	.31	.38	.44	.47	.52	
r	.996	.966	.986	.984	.981	1.00	.998	.996	.999	.997	.969	.986	.993	.989	

3.5m

T(K)	298			283			278			273			268		
Exposure Time(sec)	30	40	60	30	40	60	30	40	60	25	30	40	25	30	
A_o	.630	.671	.810	.920	.897	.850	.920	.893	.799	.928	.920	.897	.938	.923	
K_p^*	3.88	3.65	2.97	0.79	0.92	1.14	0.87	1.02	1.47	0.73	0.79	0.92	0.64	0.71	
r	.995	.994	.972	.986	.981	.976	.975	.976	.950	.978	.986	.981	.994	.989	

4.0m

T(K)	298			283			278			273			268		
Exposure Time(sec)	40	60	90	20	30	20	30	40	20	25	30	90	120	150	
A_o	-.013	.041	.394	.874	.694	.907	.821	.714	.858	.805	.747	-.64	-.97	-.95	
K_p^*	11.6	11.3	9.61	2.15	3.79	1.20	1.80	2.42	1.79	2.15	2.57	7.83	8.87	8.80	
r	.963	.984	.974	.939	.907	.997	.962	.945	.987	.975	.970	.972	.981	.990	

$$1/[RBC] = A_o + K_p^* * t$$

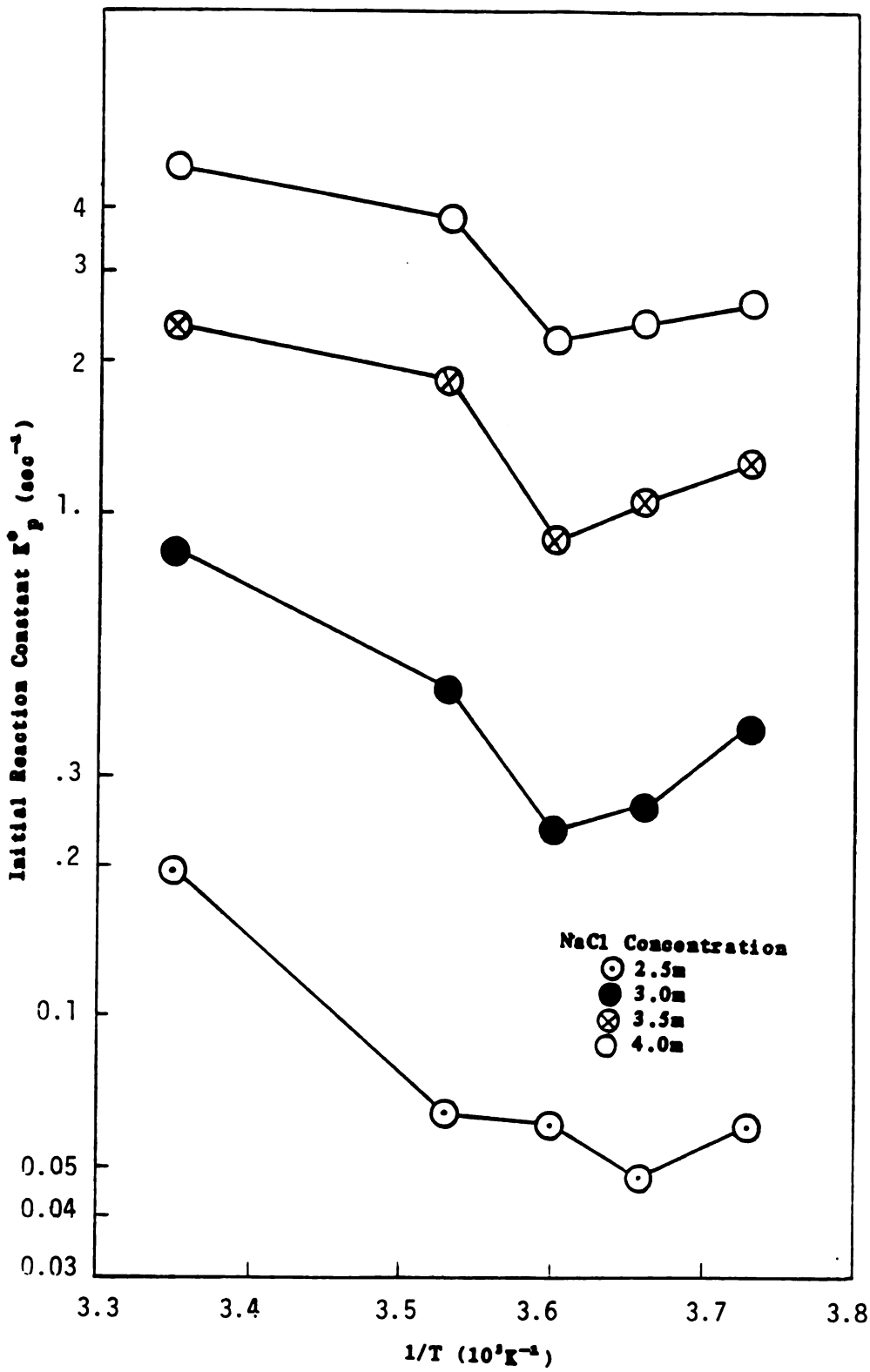

FIGURE 1: Initial Hemolysis Rate at Different NaCl Concentrations.